# International Journal of Computer Networks (IJCN)

ISSN : 1985 - 4129

Volume 2 - Issue 1
Number of issues per year: 6

Copyright © 2010 Computer Science Journals. All rights reserved.

**Editor in Chief Associate Professor Min Song**

# International Journal of Computer Network (IJCN)

Book: 2010 Volume 2, Issue 1
Publishing Date: 31-03-2010
Proceedings
ISSN (Online): 1985-4129

This work is subjected to copyright. All rights are reserved whether the whole or part of the material is concerned, specifically the rights of translation, reprinting, re-use of illusions, recitation, broadcasting, reproduction on microfilms or in any other way, and storage in data banks. Duplication of this publication of parts thereof is permitted only under the provision of the copyright law 1965, in its current version, and permission of use must always be obtained from CSC Publishers. Violations are liable to prosecution under the copyright law.

IJCN Journal is a part of CSC Publishers
http://www.cscjournals.org

© IJCN Journal
Published in Malaysia

Typesetting: Camera-ready by author, data conversation by CSC Publishing Services – CSC Journals, Malaysia

**CSC Publishers**

# Table of Contents

Volume 2, Issue 1, March 2010.

## Pages

# Reducing Packet Transmission Delay in Vehicular Ad Hoc Networks using Edge Node Based Greedy Routing

**K.Prasanth** prasanthkaliannan@gmail.com
*Research Scholar, Department of IT*
*K.S.Rangasamy College of Technology*
*Tiruchengode-637215, Tamilnadu, India*

**Dr.K.Duraiswamy** drkduraiswamy@yahoo.com
*Dean Academic, Department of CSE*
*K.S.Rangasamy College of Technology*
*Tiruchengode-637215, Tamilnadu, India*

**K.Jayasudha** jayasudhakaliannan@yahoo.com
*Research Scholar, Department of MCA*
*K.S.R College of Engineering*
*Tiruchengode-637215, Tamilnadu, India*

**Dr.C.Chandrasekar** ccsekar@gmail.com
*Reader, Department of MCA*
*Periyar University*
*Salem, Tamilnadu, India*

**Abstract**

VANETs (Vehicular Ad hoc Networks) are highly mobile wireless ad hoc networks and will play an important role in public safety communications and commercial applications. Routing of data in VANETs is a challenging task due to rapidly changing topology and high speed mobility of vehicles. Conventional routing protocols in MANETs (Mobile Ad hoc Networks) are unable to fully address the unique characteristics in vehicular networks. In this paper, we propose a potential EBGR (Edge Node Based Greedy Routing), a greedy position based routing approach to forward packets to the node present in the edge of the transmission range of source/forwarding node. The most suitable next hop is selected based on potential score of neighbor node. We propose Revival Mobility model (RMM) to evaluate the performance of our routing technique. This paper presents a detailed description of our approach and simulation results using ns2.27 show that end to end delay in packet transmission is minimized considerably compared to current routing protocols of VANET.

**Keywords:** Vehicular Ad hoc Networks, Greedy Position Based Routing, Potential EBGR, Revival Mobility Model, End to End delay.

.

## 1. INTRODUCTION

Vehicular Ad hoc Networks (VANETs) are based on short range wireless communications (e.g., IEEE 802.11) for the use in road safety and many other commercial applications. The Federal

Communications Commission (FCC) has allocated 75 MHz in 5.9 GHz band for licensed Dedicated Short Range Communication (DSRC) for vehicle-to-vehicle and vehicle to infrastructure communications. The radio range of VANETs is several hundred meters, typically between 250 and 300 meters. It is expected that more vehicles would be equipped with computing and wireless communication devices in the near future. We assume that vehicles should be equipped with wireless communication devices, GPS, digital maps, and optional sensors for reporting vehicle conditions. Vehicles exchange information with other vehicles as well as road-side infrastructures within their radio ranges. A vehicular network is a mobile ad hoc network and its characteristics can be summarized as high dynamics, mobility constraints, predicable mobility, large scale and energy constraints are not that high as every vehicle has a large enough battery capacity**.**

## 2. RELATED WORK

In this section, we briefly summarize the characteristics of VANETs related to routing and also we will survey the existing routing schemes in both MANETs and VANETs in vehicular environments.

### 2.1. VANETs Characteristics

In the following, we only summarize the uniqueness related to routing of VANETs compared with MANETs.

**Unlimited transmission power:** Mobile device power issues are not a significant constraint in vehicular Networks. Since the vehicle itself can provide continuous power to computing and communication devices.
**High computational capability:** Operating vehicles can afford significant computing, communication and sensing capabilities.
**Highly dynamic topology:** Vehicular network scenarios are very different from classic ad hoc networks. In VANETs, vehicles can move fast. It can join and leave the network much more frequently than MANETs. Since the radio range is small compared with the high speed of vehicles (typically, the radio range is only 250 meters while the speed for vehicles in freeway will be 30m/s). This indicates the topology in VANETs changes much more frequently.
**Predicable Mobility:** Unlike classic mobile ad hoc networks, where it is hard to predict the nodes' mobility, vehicles tend to have very predictable movements that are (usually) limited to roadways. The movement of nodes in VANETs is constrained by the layout of roads. Roadway information is often available from positioning systems and map based technologies such as GPS. Each pair of nodes can communicate directly when they are within the radio range.
**Potentially large scale:** Unlike most ad hoc networks studied in the literature that usually assume a limited network size, vehicular networks can in principle extend over the entire road network and so include many participants.
**Partitioned network:** Vehicular networks will be frequently partitioned. The dynamic nature of traffic may result in large inter vehicle gaps in sparsely populated scenarios and hence in several isolated clusters of nodes.
**Network connectivity:** The degree to which the network is connected is highly dependent on two factors: the range of wireless links and the fraction of participant vehicles, where only a fraction of vehicles on the road could be equipped with wireless interfaces.

### 2.2 Routing protocols in MANET

The routing protocols in MANETs can be classified by their properties. On one hand, they can be classified into two categories, proactive and reactive.

**Proactive algorithms** employ classical routing strategies such as distance-vector routing (e.g., DSDV [1]) or link-state routing (e.g., OLSR [2] and TBRPF [3]). They maintain routing information about the available paths in the network even if these paths are not currently used. The main drawback of these approaches is that the maintenance of unused paths may occupy a significant

part of the available bandwidth if the topology of the network changes frequently [4]. Since a network between cars is extremely dynamic we did not further investigate proactive approaches.

**Reactive routing protocols** such as DSR [5], TORA [6], and AODV [7] maintain only the routes that are currently in use, thereby reducing the burden on the network when only a small subset of all available routes is in use at any time. It can be expected that communication between cars will only use a very limited number of routes, therefore reactive routing seems to fit this application scenario. As a representative of the reactive approaches we have chosen DSR, since it has been shown to be superior to many other existing reactive ad-hoc routing protocols in [8].

**Position-based routing** algorithms require that information about the physical position of the participating nodes be available. This position is made available to the direct neighbours in form periodically transmitted beacons. A sender can request the position of a receiver by means of a location service. The routing decision at each node is then based on the destination's position contained in the packet and the position of the forwarding node's neighbours. Position-based routing does thus not require the establishment or maintenance of routes. Examples for position-based routing algorithms are face-2 [9], GPSR [10], DREAM [11] and terminodes routing [12]. As a representative of the position based algorithms we have selected GPSR, (which is algorithmically identical to face-2), since it seems to be scalable and well suited for very dynamic networks.

### 2.3. Routing protocols in VANET

Following are a summary of representative VANETs routing algorithms

.

**GSR (Geographic Source Routing):** Lochert et al. in [13] proposed GSR, a position-based routing with topological information. This approach employs greedy forwarding along a pre-selected shortest path. The simulation results show that GSR outperforms topology based approaches (AODV and DSR) with respect to packet delivery ratio and latency by using realistic vehicular traffic. But this approach neglects the case that there are not enough nodes for forwarding packets when the traffic density is low. Low traffic density will make it difficult to find an end-to-end connection along the pre-selected path.

**GPCR (Greedy Perimeter Coordinator Routing):** To deal with the challenges of city scenarios, Lochert et al. designed GPCR in [14]. This protocol employs a restricted greedy forwarding procedure along a preselected path. When choosing the next hop, a coordinator (the node on a junction) is preferred to a non coordinator node, even if it is not the geographical closest node to destination. Similar to GSR, GPCR neglects the case of low traffic density as well.

**A-STAR (Anchor-based Street and Traffic Aware Routing):** To guarantee an end-to-end connection even in a vehicular network with low traffic density, Seet et al. proposed A-STAR [15]. A-STAR uses information on city bus routes to identify an anchor path with high connectivity for packet delivery. By using an anchor path, A-STAR guarantees to find an end-to-end connection even in the case of low traffic density. This position-based scheme also employs a route recovery strategy when the packets are routed to a local optimum by computing a new anchor path from local maximum to which the packet is routed. The simulation results show A-STAR achieves obvious network performance improvement compared with GSR and GPSR. But the routing path may not be optimal because it is along the anchor path. It results in large delay.

**MDDV (Mobility-Centric Data Dissemination Algorithm for Vehicular Networks):** To achieve reliable and efficient routing, Wu et al. proposed MDDV [16] that combines opportunistic forwarding, geographical forwarding, and trajectory-based forwarding. MDDV takes into account the traffic density. A forwarding trajectory is specified extending from the source to the destination (trajectory-based forwarding), along which a message will be moved geographically closer to the destination (geographical forwarding). The selection of forwarding trajectory uses the geographical knowledge and traffic density. MDDV assumes the traffic density is static.

Messages are forwarded along the forwarding trajectory through intermediate nodes which store and forward messages opportunistically. This approach is focusing on reliable routing. The trajectory-based forwarding will lead to large delay if the traffic density varies by time.

**VADD (Vehicle-Assisted Data Delivery)**
To guarantee an end-to-end connection in a sparse network with tolerable delay, Zhao and Cao proposed VADD [17] based on the idea of carry and forward by using predicable mobility specific to the sparse networks. Instead of routing along a pre-select path, VADD chooses next hop based on the highest pre-defined direction priority by selecting the closest one to the destination. The simulation results show VADD outperforms GPSR in terms of packet delivery ratio, data packet delay, and traffic overhead. This approach predicts the directions of vehicles movement. But it doesn't predict the environment change in the future.

**DGRP (Directional Greedy Routing Protocol)**
DGRP is a position based greedy routing protocol [18], which uses the location, speed and direction of motion of their neighbors to select the most appropriate next forwarding node. Like GPSR [9] it uses the two forwarding strategies greedy and perimeter. It predicts the position of nodes within the beacon interval whenever it needs to forward a data packet. This prediction can be done using previous known position, speed, and direction of motion of node. If link stability between the forwarding node and its neighbor node is weak, possibility of packet loss is high in DGRP and also prediction of position information is not reliable at all instances. In highly mobile network, inaccurate position information leads to low throughput and high overhead.

**PDGR (Predictive Directional Greedy Routing)**
Jiayu Gong proposed PDGR [19], in which the weighted score is calculated for current neighbors and possible future neighbors of packet carrier. With Predictive DGR the weighted scores of immediate nodes 2-hops away are also calculated beforehand. Here next hop selection is done on prediction and it is not reliable at all situations. It doesn't guarantee the delivery of packet to the node present in the edge of the transmission range of forwarding node, which is considered as most suitable next hop, due to high dynamics of vehicles. This will lead to low packet delivery ratio, high end to end delay and increased packet drops. The various routing protocols of MANET and VANET are analyzed and drawbacks of those routing protocols are described in the Table 1.

| Routing Protocols | Drawbacks |
|---|---|
| GPSR | Frequent network disconnection.<br>Routing loops.<br>Too many hops.<br>Routing in wrong direction. |
| GSR | End to end connection is difficult in low traffic density. |
| GPCR | End to end connection is difficult in low traffic density. |
| A-STAR | Routing paths are not optimal and results in large delay of packet transmission |
| MDDV | Large delay if the traffic density varies by time. |
| VADD | Large delay due to varying topology and varying traffic density. |
| DGR | Large Delay if the traffic density is high.<br>Low Packet delivery ratio.<br>Frequent network disconnection. |
| PDGR | Too many hops.<br>Large Delay if the traffic density is high.<br>Low Packet delivery ratio.<br>Frequent network disconnection |

**TABLE 1**: Drawbacks of Routing Protocols in MANET and VANET

## 3. PROPOSED ROUTING ALGORITHM

### 3.1 Edge Node Based Greedy Routing Algorithm (EBGR)

EBGR is a reliable greedy position base routing algorithm designed for sending messages from any node to any other node (unicast) or from one node to all other nodes (broadcast/multicast) in a vehicular ad hoc network. The general design goals of the EBGR algorithm are to optimize the packet behavior for ad hoc networks with high mobility and to deliver messages with high reliability. The EBGR algorithm has six basic functional units. First is Neighbor Node Identification (NNI), second is Distance Calculation (DC), third is Direction of Motion Identification (DMI), fourth is Reckoning Link Stability (RLS), fifth is Potential score calculation (PS) and sixth is Edge Node Selection (ENS). The NNI is responsible for collection of information of all neighbor nodes present within the transmission range of source/forwarder node at any time. The DC is responsible for calculating the closeness of next hop using distance information from the GPS. DMI is responsible to identify the direction of motion of neighbor nodes which is moving towards the direction of destination. The RLS is responsible for identifying link stability between the source/forwarder node and its neighbor nodes. The PS is responsible to calculate potential score and identifies the neighbor node having higher potential for further forwarding of a particular packet to destination. The ENS is responsible to select an edge node having higher potential score in different levels of transmission range. In the following section, the general assumptions of EBGR algorithm are briefly discussed and then functional units of EBGR algorithm are discussed in detail.

### 3.2 Assumptions

The algorithm design is based on the following assumptions: All nodes are equipped with GPS receivers, digital maps, optional sensors and On Board Units (OBU). Location information of all vehicles/nodes can be identified with the help of GPS receivers. The only communications paths available are via the ad-hoc network and there is no other communication infrastructure. Node power is not the limiting factor for the design. Communications are message oriented. The Maximum Transmission Range (MTR) of each node in the environment is 250m.

### 3.3. Neighbor Node Identification (NNI)

Neighbor node identification is the process whereby a vehicle/node identifies its current neighbors within its transmission range. For a particular vehicle, any other vehicle that is within its radio transmission range is called a neighbor. All vehicles consist of neighbor set which holds details of its neighbor vehicles. Since all nodes might be moving, the neighbors for a particular mobile node are always changing. The neighbor set is dynamic and needs to be updated frequently. Generally, neighbor node identification is realized by using periodic beacon messages. The beacon message consists of node ID, node location and timestamp. Each node informs other nodes of its existence by sending out beacon message periodically. All nodes within the transmission range of source/packet forwarding node will intimate its presence by sending a beacon message every $\mu$ second. After the reception of a beacon, each node will update its neighbor set table. If a node position is changed, then it will update its position to all neighbors by sending beacon signal. If a known neighbor, times out after $\alpha * \mu$ seconds without having received a beacon ($\alpha$ is the number of beacons that a node is allowed to miss) and it will be removed from the neighbor set table.

### 3.4. Distance calculation (DC)

The location and distance information of all vehicles/nodes can be identified with the help of GPS receivers. It can be communicated to neighbor vehicles using periodic beacon messages. The neighbor node which is closer to the destination node is calculated. The closeness of next hop is identified by the mathematical model [18] and it is shown in Fig.1.

$$DC = \left(1 - \frac{D_i}{D_c}\right)$$

*Here,*
$D_i$ : *Shortest distance from edge node i to destination D.*
$D_c$ : *Shortest distance from packet forwarding node c to destination D.*
$\frac{D_i}{D_c}$ : *Closeness of nexthop.*

**Figure 1:** Distance Calculation in EBGR

### 3.5. Direction of Motion Identification (DMI)

The appropriate neighbor node which is moving towards the direction of destination node is identified using the mathematical model [18] and it is shown in Fig.2. The cosine value of vector for velocity of edge node i and vector for location of edge node i to the location of destination node D is measured. A large cosine value implies a vehicle/node can still approach the destination closer and closer along its current direction.

$$DMI = \cos\left(\vec{v}_i, \vec{l}_{i,d}\right)$$

*Here,*
$\vec{v}_i$ : *Vector for velocity of edge node i .*
$\vec{l}_{i,d}$: *Vector for the location of edge node i to the location of destination node D .*
$\cos\left(\vec{v}_i, \vec{l}_{i,d}\right)$ : *Cosine value of angle made by these vectors*

**Figure 2:** Direction of Movement Identification in EBGR

### 3.6 Reckoning Link Stability (RLS)

$$D_1^2 = \left((X_{i0} + Vx_i\Delta t) - (X_{j0} + Vx_j\Delta t)\right) + \left((Y_{i0} + Vy_i\Delta t) - (Y_{j0} + Vy_j\Delta t)\right)^2$$
$$D_1^2 = A\Delta t^2 + B\Delta t + C$$
$$A = (Vx_i - Vx_j)^2 + (Vy_i - Vy_j)^2$$
$$B = 2[(X_i0 - X_j0)(Vx_i - Vx_j) + (X_i0 - X_j0)(Vy_i - Vy_j)]$$
$$C = (X_{i0} - X_{j0})^2 + (Y_{i0} - Y_{j0})^2$$

*Solving the equation:*
$A\Delta t^2 + B\Delta t + C - R^2 = 0$
*we can find* $\Delta t$.
$LifeTime[i,j] = \Delta t$

$$LS[i,j] = \frac{LifeTime[i,j]}{\sigma}$$

*Here,*
$LS[i,j] = 1$ *when* $LifeTime[i,j] \geq \sigma$
$LS_{i,j}$ : *Link stability between two nodes i and j.*

**Figure 3:** Reckoning Link Stability in EBGR

Each vehicle estimates the Link Stability (LS) for each neighboring vehicle before selecting the next hop for the data forwarding/sending. The LS is a relation between the link communication lifetime and a constant value (say: σ) which represents in general cases the routing route validity time, and it depends on the used routing protocol. Fig.3 shows how link lifetimes are estimated [19] based on neighbors' movement information. The lifetime of the link (i, j) $LifeTime[i,j]$ corresponds to the estimated time $\Delta t = t_1 - t_0$ with $t_1$ is the time when $D_1$ becomes equal or bigger than the communication range R (i.e. the time when j goes out of the communication range of i). $D_1$ and $\Delta t$ are estimated using the initial positions of i and j ($(X_{i0}, Y_{i0})$ and $(X_{j0}, Y_{j0})$ and their initial speeds $\vec{V_i}$ and $\vec{V_j}$ respectively).Once LS is calculated for each neighboring vehicle, EBGR selects the node corresponding to the highest LS (corresponding to the most stable neighboring link) as next hop for data forwarding. This approach should help as well in minimizing the risk of broken links and in reducing packet loss.

### 3.7 Potential Score Calculation (PS)

The potential score (PS) of all nodes present within the different levels of transmission range of source/packet forwarding node is calculated. The potential score (PS) is calculated to identify the closeness of next hop to destination, direction of motion of nodes and reliability of neighbor nodes. The appropriate edge node with largest potential score will be considered as having higher potential to reach the destination node and that particular node can be chosen as next hop to forward the packet to the destination node. Potential score is calculated by addition of DC, DMI and LS and that mathematical model represented in Fig.4.

$$PS_i = \rho \times DC + \omega \times DMI + \lambda \times LS$$

$$PS_i = \rho \times \left(1 - \frac{D_i}{D_c}\right) + \omega \times \cos\left(\vec{v}_i, \vec{l}_{i,d}\right) + \lambda \times LS_{c,i}$$

*Here,*

$PS_i$ : *Potential score of node i*

$\rho, \omega, \lambda$ : *Potential factors*

*Let* $\rho + \omega + \lambda = 1$ ; $\lambda > \rho$ *and* $\lambda > \omega$

$D_i$ : *Shortest distance from edge node i to destination D.*

$D_c$ : *Shortest distance from packet forwarding node c to destination D.*

$\frac{D_i}{D_c}$ : *Closeness of nexthop.*

$\vec{v}_i$ : *Vector for velocity of edge node i .*

$\vec{l}_{i,d}$: *Vector for the location of edge node i to the location of destination node D*

$\cos\left(\vec{v}_i, \vec{l}_{i,d}\right)$ : *Cosine value of angle made by these vectors*

$LS_{c,i}$: *Link stability between packet forwarding node c to edge node i.*

**Figure 4:** Potential Score Calculation in EBGR

## 3.8. Edge Node Selection (ENS)

In the Edge Node Selection, edge nodes are selected for packet forwarding event. An edge node is a node which has shortest distance to the destination D compared to all other nodes within the different levels of transmission range of source/packet forwarding node.

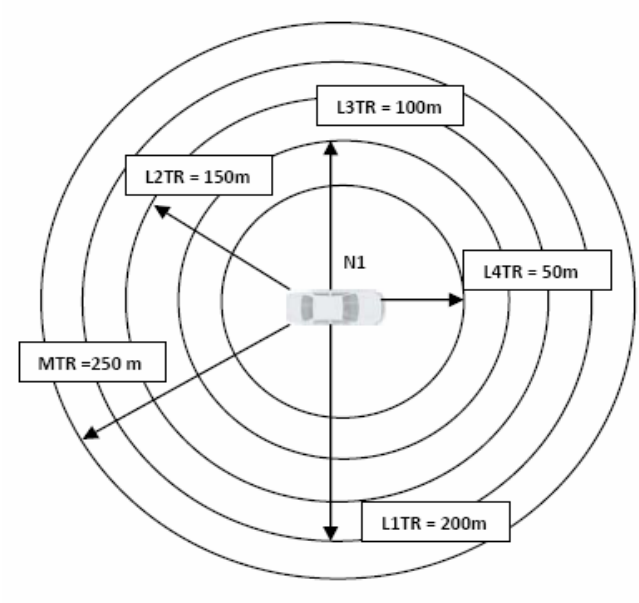


**Figure 5:** Different Levels of Transmission Range in EBGR

The different levels of transmission range are considered to avoid packet loss due to high speed mobility of vehicles. An edge node has the responsibility of saving received data packets in forwarding table and transfers it later when those nodes meet new neighbors. The overall objective of the algorithm is to forward the packet as soon as possible to increase packet delivery ratio, minimize the end to end delay and avoid packet loss. The MTR of a vehicle/node is 250m.The other levels of transmission range is considerably less than MTR. The different levels of transmission range is shown in Fig.5 which includes, Maximum Transmission Range (i.e. MTR=250m),Level1 transmission range (i.e.L1TR=200m),Level2 transmission range (i.e.L2TR=150m),Level3 transmission range (i.e.L3TR=100m) and Level4 transmission range (i.e.L4TR=50m).

$MTR$: Maximum Transmission Range $= 250m$
$L1TR$: Level1 Transmission Range $= 200m$
$L2TR$: Level2 Transmission Range $= 150m$
$L3TR$: Level3 Transmission Range $= 100m$
$L4TR$: Level4 Transmission Range $= 50m$
$currentnode$: the current packet carrier
$loc_c$: the location of current node
$\overrightarrow{v_c}$: speed vector for current node
$dest$: destination of the packet
$loc_d$: the location for destination
$nextHop$: the node selected as next hop
$neigh_i$: the ith neighbor
$loc_i$: the location of the ith neighbor
$\overrightarrow{v_i}$: the speed vector of the ith neighbor

1. $loc_c \leftarrow getLocation(currentnode)$
2. $\overrightarrow{v_c} \leftarrow getSpeed(currentnode)$
3. $loc_d \leftarrow getLocation(dest)$
4. $D_c = distance\ (loc_c, loc_d)$

In

5. $\overrightarrow{l_{c,d}} = loc_d - loc_c$
6. $PS = \omega \times \cos\left(\overrightarrow{v_c}, \overrightarrow{l_{c,d}}\right)$

7. $nextHop = currentnode$
8. **for all** $neighbors\ of\ currentnode$ **do**
9. $loc_i \leftarrow getLocation(neigh_i)$
10. $\vec{v}_i \leftarrow getSpeed(neigh_i)$
11. $D_i = distance(loc_d, loc_i)$
12. $D_{ci} = distance(loc_c, loc_i)$
13. **for all** $neighbors\ of\ currentnode\ with\ D_{ci}$ **do**
14. **if** $(D_{ci} < MTR \ \&\& \ D_{ci} > L1TR)$
15. $\vec{l}_{i,d} = loc_d - loc_i$
16. $PS_i = \rho \times \left(1 - \frac{D_i}{D_c}\right) + \omega \times \cos\left(\vec{v}_i, \vec{l}_{i,d}\right) + \lambda \times LS_{ci}$
17. **for** $neigh_i$ **with greater** $PS_i$ **do**
18. $PS = PS_i$
19. $nextHop = neigh_i$
20. **end for**
21. **else if** $(D_{ci} < L1TR \ \&\& \ D_{ci} > L2TR)$
22. $\vec{l}_{i,d} = loc_d - loc_i$
23. $PS_i = \rho \times \left(1 - \frac{D_i}{D_c}\right) + \omega \times \cos\left(\vec{v}_i, \vec{l}_{i,d}\right) + \lambda \times LS_{ci}$
24. **for** $neigh_i$ **with greater** $PS_i$ **do**
25. $PS = PS_i$
26. $nextHop = neigh_i$
27. **end for**
28. **else if** $(D_{ci} < L2TR \ \&\& \ D_{ci} > L3TR)$
29. $\vec{l}_{i,d} = loc_d - loc_i$
30. $PS_i = \rho \times \left(1 - \frac{D_i}{D_c}\right) + \omega \times \cos\left(\vec{v}_i, \vec{l}_{i,d}\right) + \lambda \times LS_{ci}$
31. **for** $neigh_i$ **with greater** $PS_i$ **do**
32. $PS = PS_i$
33. $nextHop = neigh_i$
34. **end for**
35. **else if** $(D_{ci} < L3TR \ \&\& \ D_{ci} > L4TR)$
36. $\vec{l}_{i,d} = loc_d - loc_i$
37. $PS_i = \rho \times \left(1 - \frac{D_i}{D_c}\right) + \omega \times \cos\left(\vec{v}_i, \vec{l}_{i,d}\right) + \lambda \times LS_{ci}$
38. **for** $neigh_i$ **with greater** $PS_i$ **do**
39. $PS = PS_i$
40. $nextHop = neigh_i$
41. **end for**
42. **else if** $(D_{ci} < L4TR)$
43. $\vec{l}_{i,d} = loc_d - loc_i$
44. $PS_i = \rho \times \left(1 - \frac{D_i}{D_c}\right) + \omega \times \cos\left(\vec{v}_i, \vec{l}_{i,d}\right) + \lambda \times LS_{ci}$
45. **for** $neigh_i$ **with greater** $PS_i$ **do**
46. $PS = PS_i$

```
47. nextHop = neigh_i
48. end for
49. else
50. carry the packet with currentnode
51. end if
52. end for
53. end for
```

**Figure 6:** Pseudo code of Potential EBGR Algorithm

***Step1****:* Neighbor nodes having distance between 250m and 200m from the current node falls between MTR and L1TR. The potential score of all nodes present between the transmission range of MTR and L1TR are calculated. The node which is having higher potential score is considered as edge node of the MTR. So the packet from the current node is forwarded to that particular edge node. If no node present between MTR and L1TR, then L1TR and L2TR are considered.

***Step2****:* Neighbor nodes having distance between 200m and 150m from the current node falls between L1TR and L2TR. The potential score of all nodes present between the transmission range of L1TR and L2TR are calculated. The node which is having higher potential score is considered as edge node of the L1TR.So the packet from the current node is forwarded to that particular edge node. If no node present between L1TR and L2TR, then L2TR and L3TR are considered.

***Step3:*** Neighbor nodes having distance between 150m and 100m from the current node falls between L2TR and L3TR. The potential score of all nodes present between the transmission range of L2TR and L3TR are calculated. The node which is having higher potential score is considered as edge node of the L2TR.So the packet from the current node is forwarded to that particular edge node. If no node present between L2TR and L3TR, L3TR and L4TR are considered.

***Step4:*** Neighbor nodes having distance between 100m and 50m from the current node falls between L3TR and L4TR. The potential score of all nodes present between the transmission range of L3TR and L4TR are calculated. The node which is having higher potential score is considered as edge node of the L3TR.So the packet from the current node is forwarded to that particular edge node. If no node present between L3TR and L4TR, then L4TR are considered.

***Step5:*** Neighbor nodes having distance within 50m from the current node falls to L4TR. The potential score of all nodes present L4TR are calculated. The node which is having higher potential score is considered as edge node of the L4TR.So the packet from the current node is forwarded to that particular edge node. If no node present in any of the above mentioned range, then the current node store and carry the packet until it find some other node comes within its transmission range. The pseudo code of ENS algorithm is illustrated in Fig.6.

## 4. SIMULATION RESULTS AND ANALYSIS

In this section, we evaluate the performance of routing protocols of vehicular networks in an open environment. So among the routing protocols we aforementioned, we choose GPSR, PDGR and Potential EBGR for comparison.

### 4.1 Revival Mobility model (RMM)

We use Revival Mobility model (RMM) to simulate the movement pattern of moving vehicles on streets or roads defined by maps from the GPS equipped in the vehicles. In Revival Mobility model (RMM), the road comprises of two or more lanes. Vehicles or nodes are randomly distributed with linear node density. Each vehicle can move in different speed. This mobility

model allows the movement of vehicles in two directions. i.e. north/south for the vertical roads and east/west for the horizontal roads. In cross roads, vehicles choose desired direction based on the shortest path. A security distance should be maintained between two subsequent vehicles in a lane. Overtaking mechanism is applicable and one vehicle can able to overtake the preceding vehicle. Packet transmission is possible and can be done by vehicles moving in both directions, which means front hopping and back hopping of data packet is possible as shown in the Fig.7.

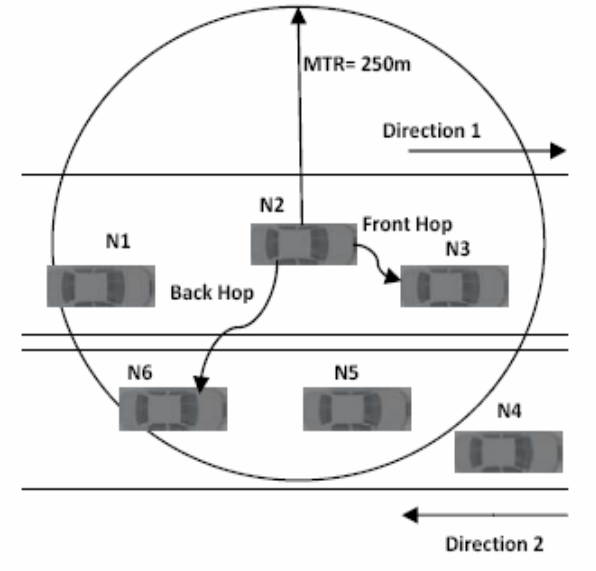


**Figure 7:** Revival Mobility Model

In this mobility, deterministic and instantaneous transmission mechanism in which a message is available for receiving within a certain radius *r=250m* from the sender with certainty, but unavailable further away. Vehicles can unicast and broadcast packets to the neighbour vehicle which is present within its transmission range.

The Simulations were carried out using Network Simulator (NS-2) ([20]). We are simulating the vehicular ad hoc routing protocols using this simulator by varying the number of nodes. The IEEE 802.11 Distributed Coordination Function (DCF) is used as the Medium Access Control Protocol. The packet size was fixed to 512 bytes. The Traffic sources are UDP. Initially the nodes were placed at certain specific locations, and then the nodes move with varying speeds towards new locations. The nodes move with speeds up to 25 meter/sec. For fairness, identical mobility and traffic scenarios were used across the different simulations. The simulation parameters are specified in Table 2

| PARAMETER | VALUE |
|---|---|
| Simulation Area | 1000m * 1000m |
| Number of Vehicles | 0 - 100 |
| Average speed of vehicles(m/s) | 0 - 25 |
| Number of packet Senders | 30 |
| Transmission Range | 250m |
| Constant Bit Rate (Packets/Second) | 2 |
| Packet Size (Bytes) | 512 |
| Vehicle beacon interval (Seconds ) | 0.25,0.50,1.0 |
| MAC Protocol | 802.11 DCF |
| Vehicle mobility model | Revival mobility model |

**TABLE 2:** Simulation Parameters

### 4.2. Performance Metrics to evaluate simulation

In order to evaluate the performance of vehicular ad hoc network routing protocols, the following metric is considered**.**

#### 4.2.1 End-to-End delay

The delay experienced by a packet from the time it was sent by a source till the time it was received at the destination.

### 4.3 Number of Nodes vs. End-to-End Delay

In this part, we compare the end-to-end delay from the source node to the destination. In Figure.5 the number of nodes varies with fixed CBR rate. The end-to-end delay for GPSR increases much faster than others. When no node available, GPSR switches to perimeter mode and it increases delay of packet transmission. PDGR have comparatively small end-to-end delay with GPSR when nodes become more. It is because when there are more nodes present, then it will forward packets easily. But next hop selection is done for future 2 hop neighbors on prediction and it is not reliable at all situations. The end-to-end delay of potential EBGR is comparatively small with PDGR when the vehicle density is high enough (n=100). More nodes in network will provide more opportunities to find some suitable node for efficient forwarding of packet by considering potential score of neighbor nodes. With high node density, the transmission delay is dramatically reduced in potential EBGR compared to PDGR and GPSR.

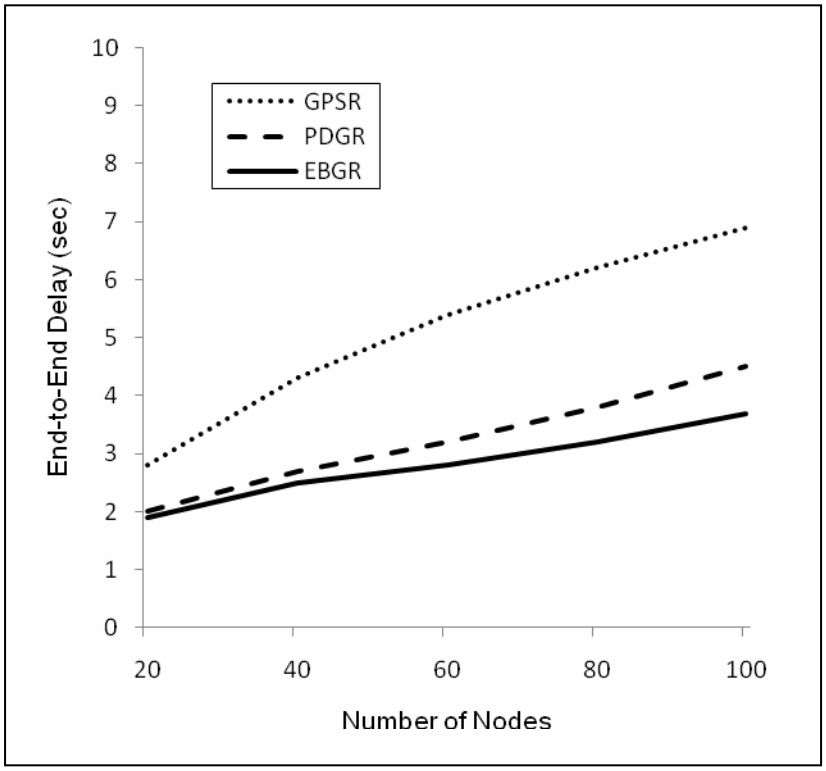


**FIGURE 5:** Number of Nodes vs. End to End Delay

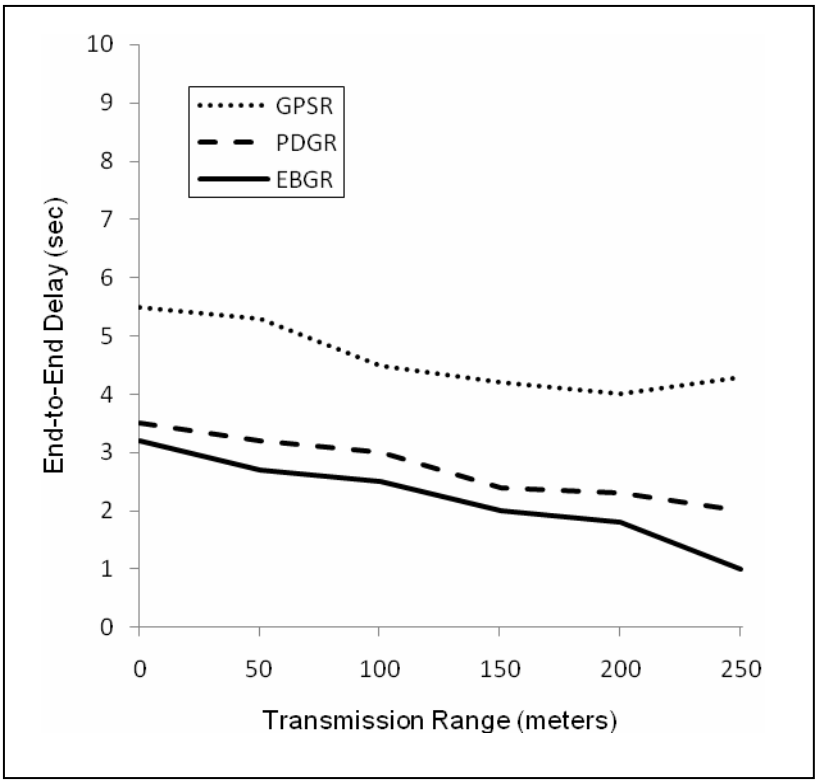


**FIGURE 6:** Transmission range vs. End to End Delay

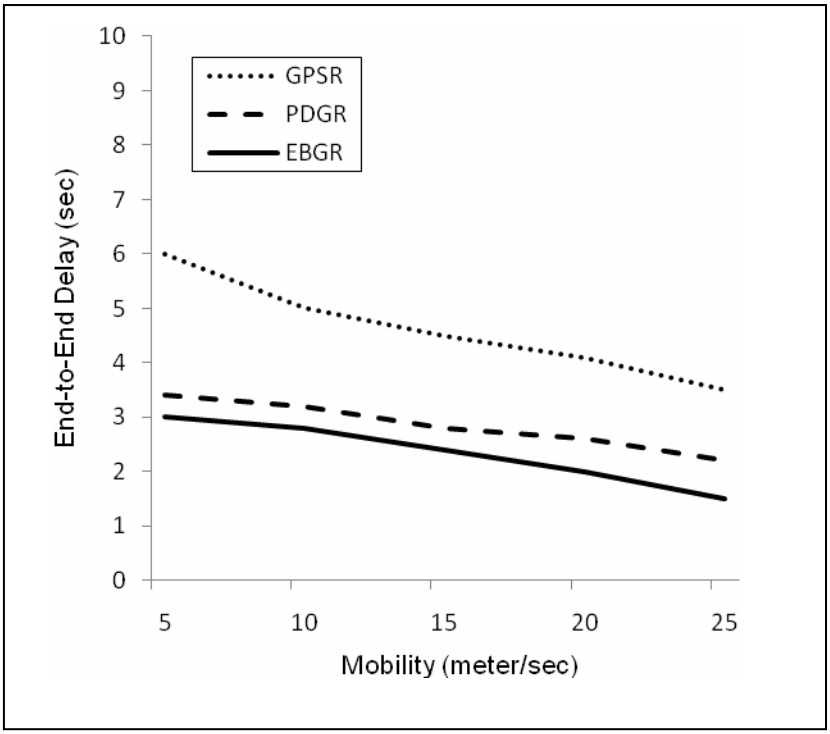


**FIGURE 7:** Mobility vs. End to End Delay

**4.4 Transmission Range vs. End-to-End Delay**

In this part, we compare the end-to-end delay with different levels of transmission range. The GPSR and PDGR always select the immediate neighbor and future 2 hop neighbors respectively to forward the packet. It increases average number of hops to transmit the packet to the destination, which leads to high end to end delay. In potential EBGR, the vehicle always selects the nodes present in LTR (i.e. L1TR, L2TR, L3TR & L4TR) based on the high potential score. The average number of hops is reduced, which results in reduced end to end delay. In the Figure 6, end-to-end delay of potential EBGR is comparatively small with GPSR and PDGR when the transmission range is 200m and 250m.

**4.5 Mobility vs. End-to-End Delay**

In this part, we compare the end-to-end delay with varying mobility of vehicles. When speed of vehicle increases, the end-to-end delay of GPSR and PDGR decreases. Because high speed of vehicles may leads to link failure during packet transmission and results in loss of packets. Figure 7 shows that end to end delay for potential EBGR is comparatively reduced from GPSR and PDGR as the speed of vehicles increases.

## 5. CONCLUSION

In this paper we have investigated routing aspects of VANETs. We have identified the properties of VANETs and previous studies on routing in MANETs and VANETs. We have commented on their contributions, and limitations. By using the uniqueness of VANETs, we have proposed a new position based greedy routing approach potential EBGR. Our simulation results have shows potential EBGR outperform GPSR and PDGR significantly in the terms of minimizing end to end delay. In the future, our approach requires modifications by taking into account the city environment characteristics and different mobility models with obstacles. Comparison of

proposed EBGR approach with other existing approach shows that our routing algorithm is considerably better than other routing protocols in reducing end to end delay in packet transmission.

## REFERENCES


[1]. Charles E. Perkins and Pravin Bhagwat, "Highly dynamic destination-sequenced distance-vector routing (DSDV)," in *Proceedings of ACM SIGCOMM'94 Conference on Communications Architectures, Protocols and Applications*, 1994.

[2]. T. H. Clausen and P. Jacquet. "Optimized Link State Routing (OLSR)", RFC 3626, 2003.

[3]. Richard G. Ogier , Fred L. Templin , Bhargav Bellur , and Mark G. Lewis , "Topology broadcast based on reverse-path forwarding (tbrpf)," Internet Draft, draft-ietf-manet-tbrpf-03.txt, work in progress, November 2001.

[4]. S. R. Das, R. Castaneda, and J. Yan, "Simulation based performance evaluation of mobile, ad hoc network routing protocols," *ACM/Baltzer Mobile Networks and Applications (MONET) Journal*, pp. 179–189, July 2000.

[5]. David B. Johnson and David A. Maltz, "Dynamic Source routing in ad hoc wireless networks," in *Mobile Computing*, Tomasz Imielinske and Hank Korth, Eds., vol. 353. Kluwer Academic Publishers, 1996.

[6]. Vincent D. Park and M. Scott Corson, "A highly adaptive distributed routing algorithm for mobile wireless networks," in *Proceedings of IEEE INFOCOMM*,1997, pp. 1405–1413.

[7]. Charles E. Perkins and Elizabeth M. Royer, "Adhoc on-demand distance vector routing," in *Proceedings of the 2nd IEEE Workshop on Mobile Computing Systems and Applications*, February 1999, pp. 1405–1413.

[8]. Josh Broch , David A. Maltz , David B. Johnson , Yih-Chun Hu , and Jorjeta Jetcheva , "A performance comparison of multi-hop wireless ad hoc network routing protocols," in *Proceedings of the Fourth Annual ACM/IEEE International Conference on Mobile Computing and Networking (MobiCom '98)*, Dallas, Texas, U.S.A., October 1998, pp. 85 – 97.

[9]. P. Bose, P. Morin, I. Stojmenovic, and J. Urrutia, "Routing with guaranteed delivery in ad hoc wireless networks," in *Proc. of 3rd ACM Intl. Workshop on Discrete Algorithms and Methods for Mobile Computing and Communications DIAL M99*, 1999, pp. 48–55.

[10]. Brad Karp and H. T. Kung, "GPSR: Greedy perimeter stateless routing for wireless networks," in *Proceedings of the 6th Annual ACM/IEEE International Conference on Mobile Computing and Networking (MobiCom 2000)*, Boston, MA, U.S.A., August 2000, pp. 243–254.

[11]. Stefano Basagni, Imrich Chlamtac, Violet R. Syrotiuk, and Barry A.Woodward, "A distance routing effect algorithm for mobility (dream)," in *ACM MOBICOM '98*. ACM, 1998, pp. 76 – 84.

[12]. Ljubica Blazevic , Silvia Giordano , and Jean- Yves Le Boudec , "Self-organizing wide-area routing," in *Proceedings of SCI 2000/ISAS 2000*,Orlando, July 2000.

[13]. C. Lochert, H. Hartenstein, J. Tian, D. Herrmann, H. Fubler, M. Mauve: "A Routing Strategy for Vehicular Ad Hoc Networks in City Environments", IEEE Intelligent Vehicles Symposium (IV2003).

[14]. C. Lochert, M. Mauve, H. Fler, H. Hartenstein. "Geographic Routing in City Scenarios" (poster), MobiCom. 2004, ACM SIGMOBILE Mobile Computing and Communications Review (MC2R) 9 (1), pp. 69–72, 2005.

[15]. B.-C. Seet, G. Liu, B.-S. Lee, C. H. Foh, K. J. Wong, K.-K. Lee. "A-STAR: A Mobile Ad Hoc Routing Strategy for Metropolis Vehicular Communications", NETWORKING 2004.

[16]. H. Wu, R. Fujimoto, R. Guensler and M. Hunter. "MDDV: A Mobility-Centric Data Dissemination Algorithm for Vehicular Networks", ACM VANET 2004.

[17]. J. Zhao and G. Cao. "VADD: Vehicle-Assisted Data Delivery in Vehicular Ad Hoc Networks", InfoCom 2006.

[18]. Rupesh Kumar, S.V.Rao. "Directional Greedy Routing Protocol (DGRP) in Mobile Ad hoc Networks", International Conference on Information Technology,2008.

[19]. Jiayu Gong, Cheng-Zhong Xu and James Holle. "Predictive Directional Greedy Routing in Vehicular Ad hoc Networks", (ICDCSW' 07).

[20]. The Network Simulator: ns2, http: //www.isi.edu/nsnam /ns/."

# Run-Time Adaptive Processor Allocation of Self-Configurable Intel IXP2400 Network Processor

**A.Satheesh** vbsatheesh@yahoo.com
*Department of Computer Science and Engineering*
*Periyar Maniammai University*
*Thanjavur-613 403, Tamil Nadu, India*

**Dr.D.Kumar** kumar_durai@yahoo.com
*Department of Electronics and Communication Engineering*
*Periyar Maniammai University*
*Thanjavur-613 403, Tamil Nadu, India*

**Dr.A.Vincent Jeyakumar** avjeyakumar2004@yahoo.com
*Department of Mathematics*
*Periyar Maniammai University*
*Thanjavur-613 403, Tamil Nadu, India*

**Abstract**

An ideal Network Processor, that is, a programmable multi-processor device must be capable of offering both the flexibility and speed required for packet processing. But current Network Processor systems generally fall short of the above benchmarks due to traffic fluctuations inherent in packet networks, and the resulting workload variation on individual pipeline stage over a period of time ultimately affects the overall performance of even an otherwise sound system. One potential solution would be to change the code running at these stages so as to adapt to the fluctuations; a near robust system with standing traffic fluctuations is the dynamic adaptive processor, reconfiguring the entire system, which we introduce and study to some extent in this paper. We achieve this by using a crucial decision making model, transferring the binary code to the processor through the SOAP protocol.

**Keywords:** Network Processor, Reconfiguration, Runtime adaptation, dynamically adapting processor, Active Network, Self-Configurable, SOAP, IXP2400

## 1. INTRODUCTION

Traditionally most of the network core components have been implemented using Application Specific Integrated Chips (ASICs). We first recapitulate some of the earlier related works. *Kevin Lee and Geoffrey Coulson* in [ 14 ] analyse the exact position that runtime reconfiguration occupies in Network Processor (NP), such as dynamically extendable services, network resource management, configurable network based encryption , offload processing etc. Dynamic deployment of resources to different flows in NPs has been known to Kind, Pletka and Waldvogel (see [ 1 ]). Implementations of NPs as system-on-a chip multiprocessor, involving multiple multithreaded processing engines and on-and-off chip memory, was the contribution of Tilman

Wolf [ 18 ], [ 19 ]. However, these devices lack flexibility and speed and also consume more energy. They therefore require replacement of physical components in the network core whenever there is a protocol change or update. These replacements still need some fine tuning which we provide by the use of programmable processors in the reconfigurable environment. These Neo Network Processors are multiprocessor devices designed for the efficient data-plane and control-plane by processing in networking applications. They are programmed to offer the required flexibility in packet processing and at the same time they appropriately provide the necessary computing resources to meet the speed requirement constraints of the network protocols. Intel's IXA architecture provides the basis of a family of such NPs, of which the IXP2400 Network Processor is being used in this paper for the implementation of run-time adaptive processor allocation of self-configurable systems. An adaptive processor allocation to pipeline stages of a packet processing application at run-time can improve robustness of the system to traffic fluctuations, can reduce processor provisioning requirement of the system and can conserve energy.

## 2. THE SYSTEM ARCHITECTURE

The Intel IXP2400 scores over many other processors due to its high programming flexibility, code reuse, and faster deployment capabilities and many other advantages like supporting a wide variety of LAN and WAN applications. We therefore choose this Network Processor for our study.

### 2.1 Intel IXP2400 Network Processor

The IXP2400 is an integrated Network Processor, comprised of a single X-Scale Core processor, eight Micro engines, standard memory interfaces, and high-speed bus interfaces. It is targeted at networking applications requiring a high degree of flexibility, programmability, scalability, performance, and low power consumption. The unique architecture of the IXP2400 affords the user a highly concurrent packet processing model, while keeping the programming model simple. This is accomplished by providing many features in hardware that simplify the programming model. It allows the designer to implement the software, what was previously implemented in custom ASICs. This flexible, reprogrammable approach makes development time faster, facilitates easy bug-fixing, adds features to products after deployment in the field while conforming to standards that are not yet finalized. The micro engines are custom processors implemented specifically for networking applications. They are especially well suited to high-speed data manipulation and movement. The micro engines being fully programmable processors are able to examine packet contents at all levels of the networking stack. This makes them suitable not only for layer 2 and 3 switching/forwarding, but also for applications that require deeper inspection and manipulation of packet contents. The key features of IXP2400 NP are scrupulously discussed in [ 7 ], [ 15 ], [17] whose standard block diagram of Intel IXP2400 NP architecture as shown in Figure.1. This shows the six functional units, which are traditionally known as Intel X-Scale Core [ 3 ], Micro-engines [ 5 ], control store, contexts, Data path Registers [ 9 ], local memory, SRAM and DRAM controller [ 10 ] , [ 11 ], Media and switch Fabric Interface, PCI controller, X-Scale core Peripheral, Performance monitor [ 8 ], Scratchpad memory and Hash unit.

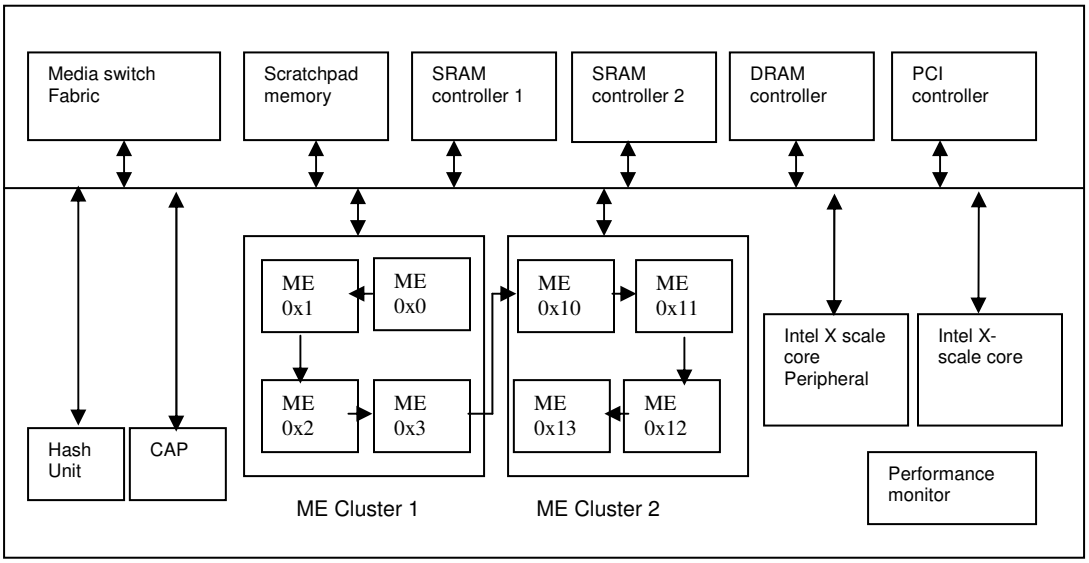


**FIGURE 1**: Simplified block diagram of the IXP2400

### 2.2 Workload Model

Network processing in Intel IXA is essentially a series of tasks that are applied to a constant stream of packet or cell data. With the multi-processor/multi-threaded architecture of the IXP 2400 network processor, these tasks are distributed over several micro-engines, each of which is programmed to perform specific tasks. When a micro-engine completes its tasks, it passes the context to the next micro-engine so that it can continue processing the data.

### 2.3 Performance Metrics

In our analysis, we focus on the following performance metrics, which are key indicators of the performance of a runtime system:

- **Processor utilization (ρ):** This metric is defined as the fraction of time that the processor is busy. Processor utilization indicates the efficiency at which the system operates.
- **Packets in the system K**. This metric indicates the extent to which the queues and processors are utilized in the system. A large value indicates that many packets are queued and that packets experience a large delay when traversing the system.

### 2.4 Organization of the paper

The remainder of this paper is organized as follows: Section 3 discusses related works. The overall methodology is described in Section 4. In Section 5 we draw the state diagram of the proposed system. In Section 6 we describe the model which we propose to introduce. The implementation details will be discussed in section 7. The results will be analyzed in Section 8. We conclude the paper in section 9.

## 3. RELATED WORK

Recently, several studies have been initiated in reconfiguration of network processors. We brief a few here. Xin Huang and Tilman Wolf [ 22 ],[ 23 ] in their work present a methodology for evaluating runtime systems for NPs by defining workload models, queuing discipline and improving existing mapping algorithm . In paper [ 12 ] J. Allen et al have used Hifn PowerNp, wherein they discussed the challenges and demands posed by next generation networks and have described how network processors can address these issues by performing highly sophisticated packet processing at line speed. *Kevin Lee and Geoffrey Coulson* [ 13 ], [ 14 ] in their work demonstrated the importance of the specialized software, to support runtime reconfiguration that exploits the potential of NPs. They have focused mainly on the generic mechanism that can be potentially applied in all areas. They have used Intel IXP 2400 as a representative of the state-of-the-art current generation of NPs. In fact, they discover new approaches that present a runtime component based approach to programming NPs. The approach promotes conceptual uniformity and design portability across a wide variety of NP types while simultaneously exploiting hardware assists that are specific to individual NPs. *Troxel, et al* [ 6 ] have demonstrated the superior performance of enhanced NP over baseline NP for prioritized traffic that is non uniform. In the baseline experiments, the ME pipelines were not reconfigurable. This type of system mimics the behavior of today's NPs. *Ravi kokku, et al* [ 16 ], [ 17 ] have presented a new approach of delay-conscious processor allocation algorithm (PAL) for packet processing systems. And they analyzed the benefits and challenges of adapting allocations of processors to packet types in the above systems and also they demonstrated that, for all the applications and traces considered, run-time adaptation can reduce energy consumption and processor provisioning level. On the other hand, *Vinod Balakrishnan, et al* [ 21 ] concentrate on balancing two requirements in packet-processing applications on multi-core processors. *Arun Raghunath, et al* [ 2 ] present yet another approach to support network processor platforms, which are increasingly required to support a rich set of services. These multi-service systems are also subjected to widely varying and unpredictable traffic. According to them, current network processor systems do not simultaneously deal well with a variety of services and fluctuating workloads. They have implemented an adaptive system that automatically changes the mapping of services to processors, and handles migration of services between different processor core types to match the current workload.

## 4. THE INTEL IXP2400 NP CONFIGURABLE ENVIRONMENT

This section gives the complete high level design details of the Intel IXP2400 NP that is needed in our work, by developing a self-configurable environment that would dynamically reconfigure its resources based on the results of monitoring traffic flows. For this, flow statistic is gathered by runtime-mapping-technique. In contrast, the unused hardware resources such as micro-engines are also quantified. These statistics will be used for choosing the appropriate resources for the services being offered, i.e., dynamic deployment reconfiguration.

The proposed system and its architecture are depicted in Figure.2. This will provide the resources based on the network traffic for the purpose of reconfiguration. The network traffic is analyzed using the monitoring module. The monitoring module will scrutinize the number of packets coming in and getting out of packet processing system, using a counter. Based on the number of packets, the arrival rate and departure rate of the packets can be determined.

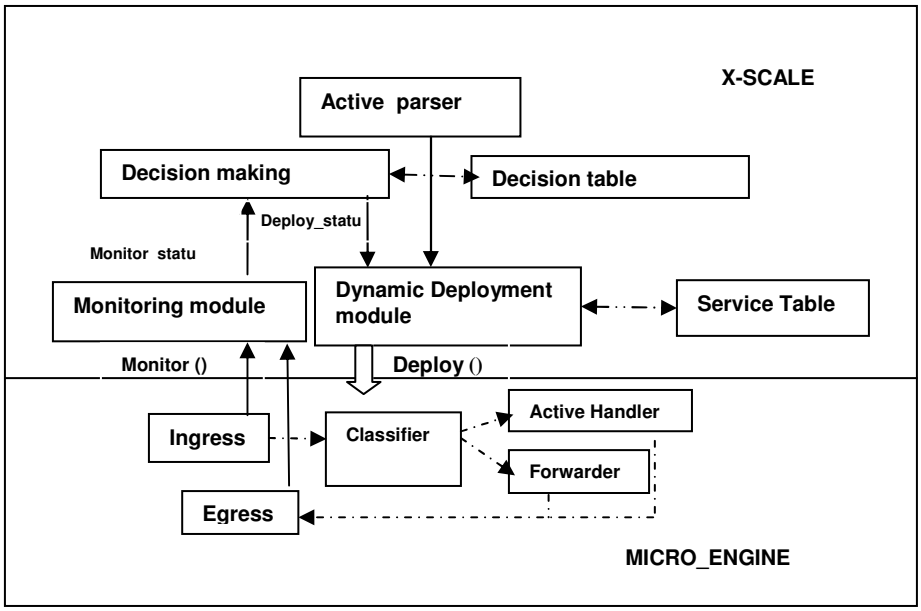


**FIGURE 2:** Functional block diagram of NP reconfiguration

The result of this monitoring module will be used for decision making wherein the need for extra processor is decided. This is done using the decision table and service table (see Table.1 and Table 2) to be explained in section 4.2.

We list below the salient functions of the above reconfigurable diagram,
1. *Monitoring module* monitors the incoming and outgoing packets.
2. *Decision-making module* decides whether to deploy the code or to stop the Micro-engine.
3. *Dynamic deployment module* dynamically deploys the code in the Micro-engine.
4. *Active code transfer module* parses the SOAP packet that comes from administrator. This packet contains the binary file for deployment.

### 4.1 Monitoring Module

The counter is set at the micro-engine level. The counters at ingress will keep track of the incoming packets to the queue. And the last counter, which is at egress, will keep track of the outgoing packets from the packet processing system that is to be processed by the egress. These two counters help to determine the number of packets in the intermediate stage. So, with the help of Arrival and Departure rate from and to the packet processing system, the traffic intensity is determined as shown in Figure 3. Since there is need for accessing the counter by both the processors, the counter values must be maintained in common to both the X-scale processor and Micro-engine for easy access to it.

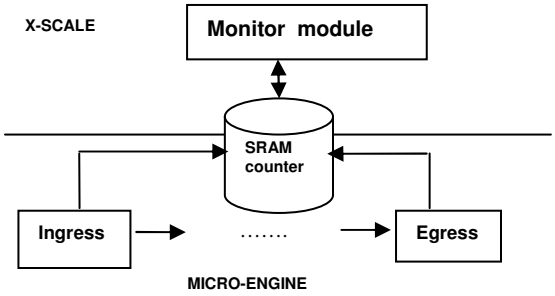


**FIGURE 3:** Role of X scale and ME in the Monitoring Process

In this module the following two functions are performed,

1: Counting of incoming packets to the ingress and
2: Counting of outgoing packets from the egress

We calculate the service rate in this module using the following equation (1),

$$\text{Overall service rate } X(t) = N/t, \quad (1)$$

where $N$ = Number of packets (packet count) transmitted
$t$ = Time interval in seconds.

We also generalize these ideas to $k$ server by iteration process as shown below.

At the initial level, we are assuming the traffic level is low. In this situation the system is used in single micro-engine for packet processing. So the service rate is

$$X_1(t) = \frac{E}{t}. \quad (2)$$

We are assuming in the second level that the system is in moderate traffic, so that it can be provisioned by additional resources. The service rate of the second processor is,

$$X_2(t) = \frac{E - X_1(t)}{t}. \quad (3)$$

And when the system is in heavy traffic, more number of processors can be provisioned. The service rate of additional resource is,

$$X_3(t) = \frac{E - [(X_1(t) + X_2(t)]}{t}. \quad (4)$$

We can generalize the service rate of the $j^{th}$ server as

$$X_j(t) = \frac{E - \sum_{i=1}^{j-1}[X_1(t) + X_2(t) + \cdots + X_{j-1}(t)]}{t} \quad (1 \leq j \leq k). \quad (5)$$

where,

E = total count of egress value.

### 4.2 Decision making module

Before we go into the various parameters of this module, we must explain the most important aspect of this module, which is perhaps the most important concept of this paper itself. The basic idea is to optimize the resources and avoid the packet loss when the activated micro-engines are at full throttle. We fix two parameters $T_{q_1}$ and $T_{q_2}$, for the queue lengths where $T_{q_1} < T_{q_2}$.

The decision making module decides whether to dynamically deploy the code in a Micro-engine or relieve the load on a currently utilized Micro-engine, based on the packet arrival rate ( $\lambda$ ) and the lagging packets in the intermediate queue (k). When the arrival rate is less, we call $T_{q_1}$ the minimum threshold ($T_{min}$) and when the arrival rate is at its peak, we call $T_{q_2}$ the maximum threshold ($T_{max}$) and these threshold values are fixed based on the network trace obtained by monitoring module. This module employs the decision table (Table. 1) and the service table (Table. 2) for dynamic deployment.

| Traffic | Threshold | Processor |
|---|---|---|
| Low | $< T_{q_1}$ | P1 |
| Medium | $T_{q_1} \leq M < T_{q_2}$ | P2 |
| High | $\geq T_{q_2}$ | P3 |

**TABLE 1**: Decision Table

| Processor | Process | Flag | Service |
|---|---|---|---|
| **ME0** | SRAM1.uof | 8107 | Ingress |
| **ME1** | x.uof | 8107 | Dynamic deployment |
| **ME2** | SRAM2.uof | 8107 | Egress |
| **ME3** | x.uof | 8107 | Dynamic deployment |
| **ME4** | - | 8106 | inactive |
| **ME5** | - | 8106 | inactive |
| **ME6** | - | 8106 | inactive |
| **ME7** | - | 8106 | inactive |

**TABLE 2:** An example of Service and Resource table (Moderate Traffic)

where,

Flag value 8106 and 8107 indicate that the micro-engine is inactive and active,
Service – is the functionality of the instance.

The pseudo code for the rules adopted by the decision-making module is given below Algorithm.1 and 2.

Algorithm: 1. ***Allocation Rule***

```
1. int i ← T_min
2. int j ← T_max
3. int q1 ← T_q1
4. int q2 ← T_q2
5. if ( λ > i) and (k >q1) then
6.         deploy_code_for_moderate_traffic
7. if ( λ> j) and (k >q2) then
8.         deploy_code_for_maximum_traffic
```

Algorithm: 2. ***Deallocation Rules***

```
1. int i ← T_min
2. int j ← T_max
3. if  ( λ < i) and current_code == moderate_traffic then
4.                 stop_code_for_moderate_traffic
5. if ( λ< j) and current_code == maximum_traffic then
6.                 stop_code_for_maximum_traffic
```

In case the traffic is low, the threshold value $T_{q_1}$ = $T_{min}$ will be fixed in such a way that the arrival rate is less than $T_{min.}$, the system will activate the first micro-engine S1 (see State diagram S1). $T_{q_1}$ is fixed in such way that arrival rate is above 70% of the service rate of the micro-engine. Incidentally our blanket assumption is that all micro-engines in the system have equal capacity of service rate.

The application code for the moderate traffic occupies four micro-engines (moderate resource provisioned) while that for heavy traffic uses all available resources in order to tolerate the maximum traffic.

### 4.3 Active code Transfer module

In Figure.4, shows the working principle of Active code transfer module. All the packet processing would be carried out in data plane (micro-engine level).Hence when the packet comes in; the packet is classified based on the destination IP and Port by classifier. The active code will be passed on to the active code handler and the other traffic to normal packet handler. The active code handler will check for more flag bit set and fragmentation ID, then extract the packet content and copy an image to SRAM. Later the X-scale will monitor the SRAM for active code and get the content to form a binary file.

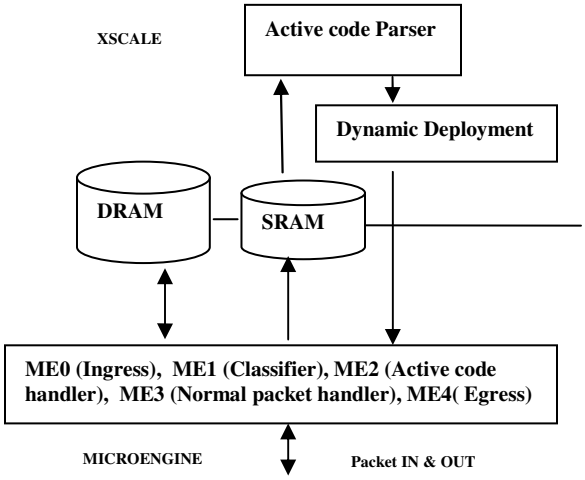


**FIGURE 4**: Functional Block Diagram

The algorithm for identifying and extracting the active packet from the rest of the traffic is shown below,

**Algorithm : 3.** *Identifying and Extracting the Active packet*

```
1.  If (Destination_IP = NP_IP && Destination_port=port)
    //Classifier
    {
            //Active code Handler
2.  Check for More Flag bit set;
3.          Extract Fragmentation ID;
            Extract Total length of the packet;
4.  Set the flag in SRAM with the offset of packet content;
5.          Move the packet content from DRAM to SRAM;
6.  Next SRAM_LOC;
    }
```

### 4.4 Active code Parser module

The XML Code which comes by SOAP as active code will be parsed in this module. SRAM location is monitored in order to check whether the flag is set. If the flag is set, from the offset detail, the packet content is parsed. The header and the binary image are separated from the packet content. The Micro-engine number and file name of the active code can be identified by parsing the content header between the XML tag **<ME></ME>** and <**IMAGE></IMAGE>.b** The Binary UOF file will be extracted by parsing the active code between **–MIME-BOUNDARY**. The Figure 5. shows the X-Scale module function.

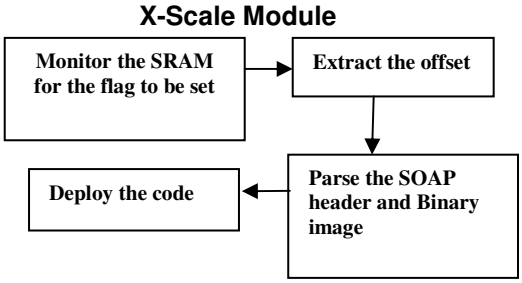


**FIGURE 5:** X Scale module

### 4.5 The SOAP Format for Active code

Simple Object Access Protocol (SOAP) is a way to structure data so that any computer program in any language can read SOAP and send messages in SOAP. SOAP provides the answer to two main requirements. More precisely, XML provides a standard way to represent data, and SOAP provides an extensible message format ("extensible" essentially means you can make up your own tags; for example, HTML is not extensible). So this helps to create an active packet with information of the code by extensible message format (see Figure.6), where the binary file can be carried by the attachment part.

```
--MIME_boundary
Content-Type: text/xml; charset=UTF-8
                        Content-Transfer-Encoding: 8bit
Content-ID: networkprocessor.xml@annauniv.com

<?xml version='1.0'?>
<SOAP-ENV:Envelope xmlns:SOAP-
ENV="http://schemas.xmlsoap.org/soap/envelope/">
                                <SOAP-ENV:Body>
<ME>
<MENO>17</MENO>
<IMAGE>packet5</IMAGE>
 <theAttachment href="cid:packet5.uof@annauniv.com"/>
</ME>
</SOAP-ENV: Body>
</SOAP-ENV: Envelope>

--MIME_boundary
Content-Type: text/plain
Content-Transfer-Encoding:binary
Content-ID: packet5.uof@annauniv.com
Binary Code…….
--MIME_boundary
```

**FIGURE 6**: Format for Active packet

## 5. THE STATE-DIAGRAM

At this stage, we introduce queuing theory as the primary systematic network analysis network delay. The conventional method of taking transmission delay L/C has been improved in the present day contexts to Little's Law $N = \lambda T$ and its infinitesimal modification $N_t = \lambda_t T_t$, which we follow in our situation ( for details see [ 4 ] ).

Let,

$N(t)$ = Number of packets in the queue at time t
$\alpha(t)$ = Number of arrival in the interval (0,t)
$\beta(t)$ = Number of departure in the interval (0,t)

So that,

$$N(t) = \alpha(t) - \beta(t) \qquad (6)$$

Let $t_i$ and $T_i$ be the time of arrival and the time spent in the system respectively, by the $i^{th}$ customer. Using elementary integration theory as a limit of summation, we obtained the following identity:

$$\int_0^t N(\tau)d\tau = \sum_{i=1}^{\beta(t)} T_i + \sum_{i=\beta(t)+1}^{\alpha(t)} (t - t_i) \qquad (7)$$

Dividing throughout by $t$, we obtained the modified Little's Law

$$N_t = \lambda_t T_t,$$

where,

$N_t = \frac{\int_0^t N(\tau)d\tau}{t}$ = Time average of the number of customers in the system in the interval (0,t)

$\lambda_t = \frac{\alpha(t)}{t}$ = Time average of the customer arrival rate in the interval (0,t).

$T_t = \frac{\sum_{i=1}^{\beta(t)} T_i + \sum_{i=\beta(t)+1}^{\alpha(t)} (t-t_i)}{\alpha(t)}$ = Time average of the time a customer spends in the system in the interval (0,t)

We explain the situation in the state-diagram Figure.7. Here $S_1, S_2, \ldots, S_c$ denote the active servers and $S_{c+1}$ and $S_{c+2}$ denote respectively the ingress and egress. Since, the total number of servers = k, we have k = c + 2. Suppose, we use minimum resource (less number of micro-engines) with high traffic flow, we incur packets loss and this can be represented by dotted lines in the state diagram. The $T_{q_1}$ and $T_{q_2}$ are the position of minimum and maximum of queue length. The packets arrive in *Poisson* distribution and service of each server is exponential. The mean arrival rate is $\lambda$ and mean service rate is $\frac{1}{\mu}$. The incoming packets are distributed from the dispatcher in FCFS discipline. The queuing model is *M/M/1/* or in *M/M/c* as a generalized version.

It is surprising to note that the dotted line representing the 'critical line' where the packet loss occurs (before our innovation of resource optimization) resembles the 'critical line' ***Res =*** ½ , where the zeros of the classical Rieman-zeta function $\sum \frac{1}{\zeta^s}$ in complex analysis are conjectured to fall. This emphasis the natural connection between classical mathematics, probability theory and modern computer analysis.

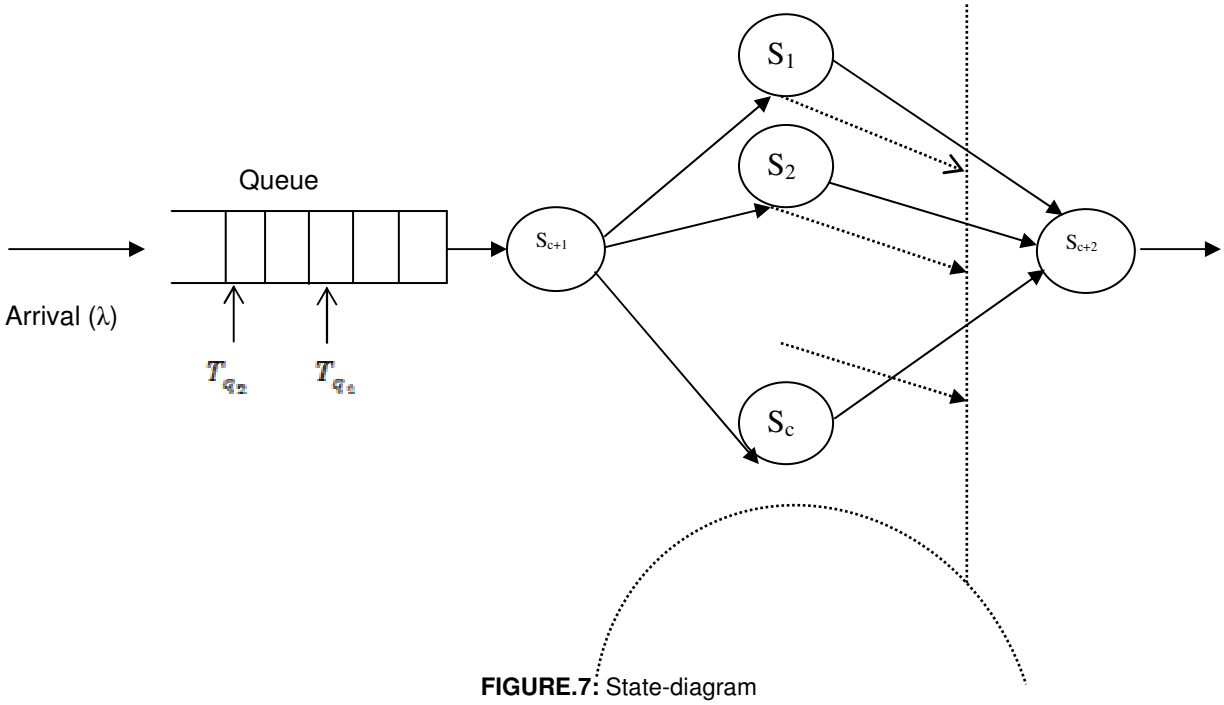


**FIGURE.7:** State-diagram

We now enter into the actual methodology for the proposed system model.

## 6. PROPOSED SYSTEM MODEL

In this proposed system we adopt the principles of Adaptive load balancing model. This application is all about sharing the load directed upon a single server across multiple redundant severs thereby reducing the per head load. The per-head load is reduced by sharing the load equally by all the redundant servers. The scenario is as shown in Figure 8.

### 6.1 Assumptions

It is assumed that the system has only five replicated servers all the time and the service each provides is identified by the respective port number only. If two different redundant servers provide a service in the same port number it is assured that the two services are the same *i.e.* if a client requests for a service providing a port number all redundant servers (if they have such a service) have the same service at that requested port number. All the packets that flow through the NP are assumed to be TCP packets running on IP.

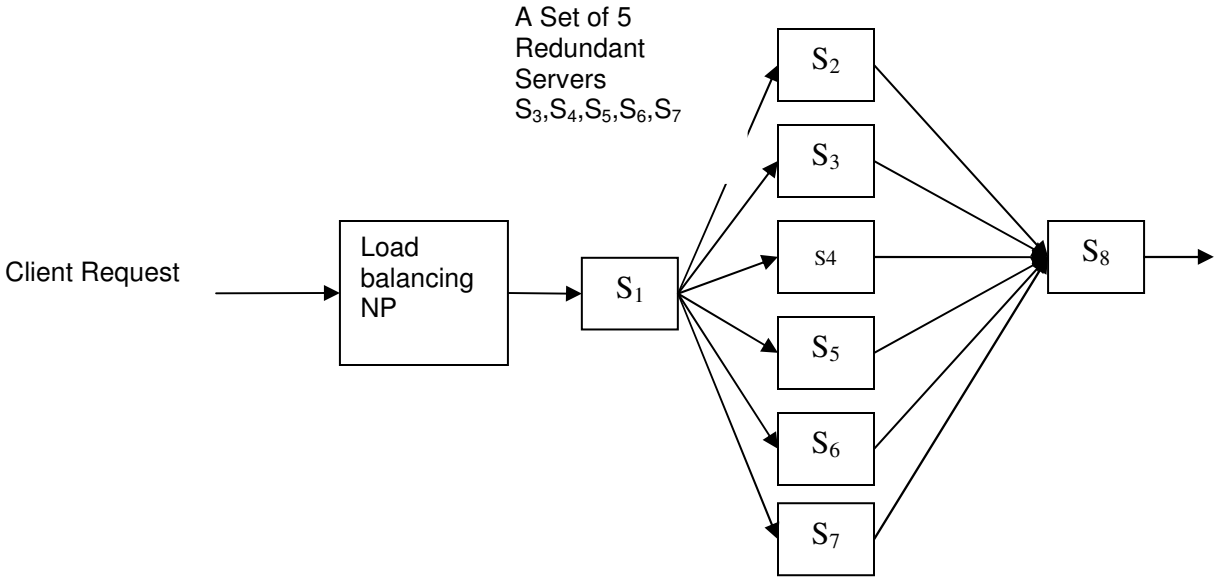


**FIGURE 8:** Adaptive Load Sharing- Context diagram

### 6.2 Runtime Mapping

*6.2.1 Mapping I: Min_service_upon_less_traffic*

First, we consider the minimum traffic in the system. At that time, the system uses only single ALS instance. This is a basic pipeline consisting of Ingress, processing ALS operations (i.e., ALS instance) and egress as shown in Figure 9.

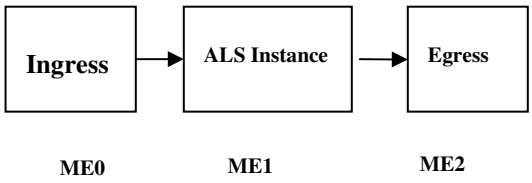


**FIGURE 9:** Base line Configuration

*6.2.2 Mapping II: Min_service_upon_moderate_traffic*

Second, we consider the moderate traffic flow. A copy of the previous instance is replicated in order to accommodate the moderate traffic as shown in Figure 10.

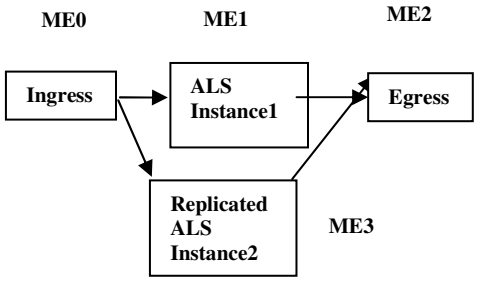


**FIGURE10**. Replication of the same instance

*6.2.3 Mapping III: Max_service_upon_high_traffic*

In order to overcome the heavy traffic, a new 'substituted' instance of the ALS application is deployed (Figure. 11). In the substituted new instance, the ALS function is split to different micro-engines, whereas in the replicated instance all the functions are carried out in a single micro-engine.

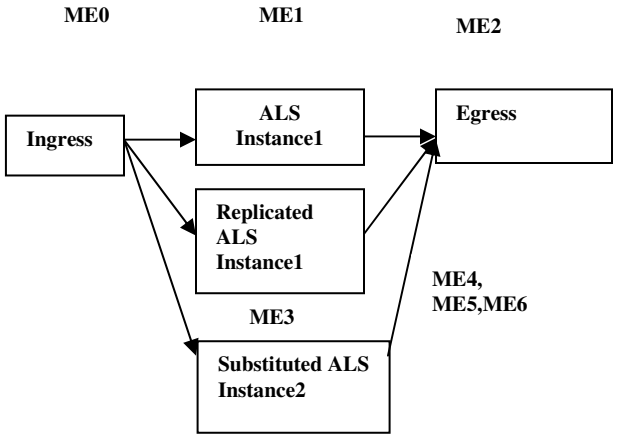


**FIGURE 11**: Substituting new instances

We use the following setup to evaluate the runtime systems

## 7. IMPLEMENTATION - HARDWARE PLATFORM

Our setup contains a PC hosting the Radisys ENP-2611 board with Intel® 600MHZ network processor. IXP2400 contains one XScale™ core and eight micro-engines. Each micro-engine has an instruction store to hold 4K-40 bit instructions that are optimized for fast-path packet processing. In Intel IXP2400 Developers Workbench, Microcode Assembly language is used to implement the system and X-scale implementation incorporated Embedded C programming language for implementation. Intel IXP2400 Developers Workbench in a simulation tool which helps us to execute the micro engine code on it and give the performance measures for the application program. Later the same application is ported onto the hardware. The execution of the code can be traced on an instruction-by-instruction basis using the simulation tool. This helps in debugging the code as well as in providing means to validate the code. There are provisions to watch the runtime values getting stored in various memory storage units like SDRAM, SRAM, Scratch Pad Memory, Local Memory and Micro -engine Registers.

## 8. RESULT ANALYSIS

The following section details the manner in which the baseline configurations (a) and (b) are compared to the dynamic configuration (c) described by us so far.

**a. Traffic from outside Network:**

The Traffic trace taken from the network are classified into low (250 pkts/sec), moderate (450 pkts/sec) and high (950 pkts/sec) and the traffic mixture taken are low, moderate and high. In Figure.12, the traffic mixture with low traffic was maintained for the first 10 seconds and then the traffic was increased to moderate for the next 10 seconds and finally the traffic was increased to high profile.

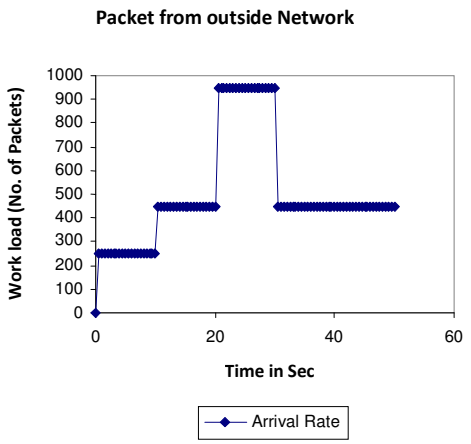


**FIGURE 12:** Snapshot of Traffic from outside network

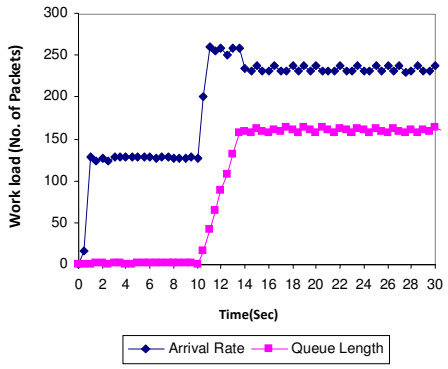


**FIGURE 13:** Arrival rate and lagging packet in Mapping I

### b. NP without Dynamic Reconfiguration:

#### Mapping I

At the initial stage, the system uses minimum resources so that (3 micro-engines) have been provisioned for NP. And the monitoring interval is 0.5 second. In Figure 13., the traffic mixture taken is low, moderate and high. So, when the workload gets increased (moderate traffic), the micro engine will not be able to process all the incoming packets, hence the queue size increases abruptly and queue overflow takes place, because in this mapping-I, the system uses only three micro-engines, which are ingress and egress. Hence the system itself with a single micro-engine, so it will tolerate only moderate traffic.

#### Mapping II

In the second level, the system is in moderate traffic. The Figure.14 shows the mapping of second level. At this moderate traffic, four micro engines have been used. And the monitoring interval is 0.5 second. The traffic mixture taken is low, moderate and high. So when the workload is increased (high traffic), the micro engine will not be able to process all the incoming packets, hence the queue size increases abruptly and as before queue overflow takes place.

#### Mapping III

At the third level, the system is in high traffic; here all the eight micro engines have been provisioned for NP. And the monitoring interval is 0.5 second. The traffic mixture taken is low, moderate and high. So when the workload increases, the micro engine will be able to process all the incoming packets, hence the queue overflow will not take place (see Figure. 15). So, in this mapping-III the system used, maximum capacity in high level traffic.

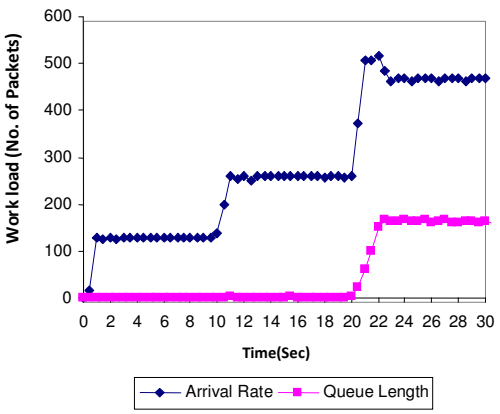


**FIGURE 14:** Arrival rate and lagging packet in Mapping II

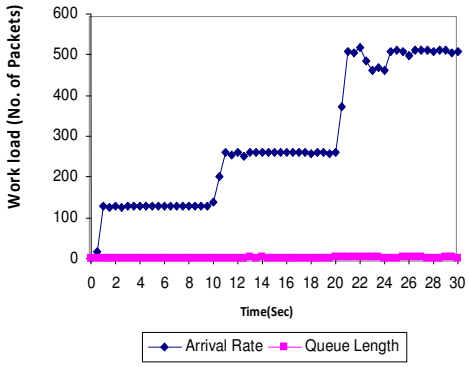


**FIGURE 15:** Arrival rate and lagging packet in Mapping III

### c. NP with Dynamic Reconfiguration

In this dynamic reconfiguration, at initial stage minimum resource will be provisioned for NP. When the traffic get increased from low to medium, the minimum resource will not be able to manage the workload, so the queue length get increases in time for example 10-12 sec and 20-22 sec (see Figure.16) .In this stage, the system will balance this situation to activate additional resources. The monitoring module which monitors the packet rate from X-scale core, deploy the code using runtime environment module in order to tolerate the moderate workload. Once again the heavy traffic is injected into the NP and the maximum resource will be provisioned in order to overcome the network traffic.

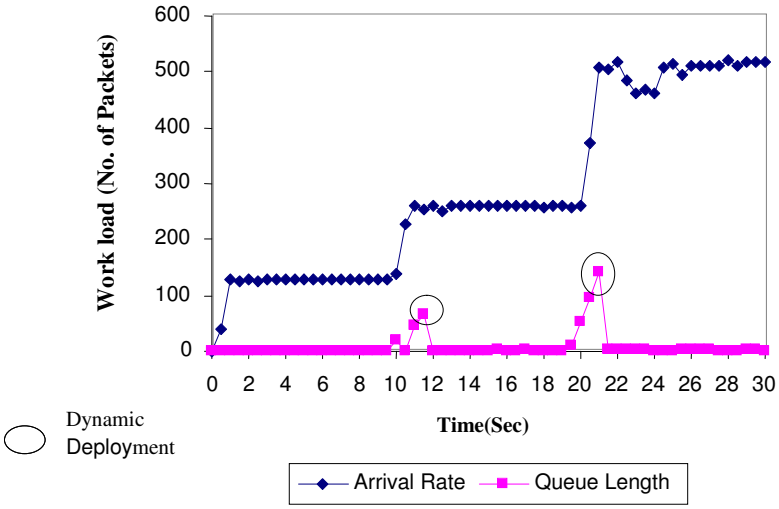


**FIGURE 16:** Arrival rate and lagging packet in Dynamic Reconfiguration

## 9. CONCLUSION AND FUTURE PLAN

To summarize, we have described the design and implementation of a dynamic reconfigurable system for Intel IXP2400 NP that can perform resource allocation at runtime. This allows maximum utilization of resources whenever possible in the steady state. In the baseline experiments (using the three mappings), the Micro-engine pipelines were not reconfigurable. The comparison of the baseline configuration over dynamically reconfigurable NP as described in the earlier sections shows the superior performance of Self-Configurable NPs over baseline NPs. Our future work is to develop an adaptive system for IPV6 services. We propose to implement an adaptive system that automatically changes the mapping of IPV6 services to processors, and handles migration of services between different processor core types to match the needs.

## 10. REFERENCES


1. A.Kind, R.Pletka, and M.Waldvogel *"The role of network processors in active networks"* In Proceedings of IWAN 2003, pages 18-29, Kyoto, Japan, December 2003.

2. Arun Raghunath, Aaron Kunze, Erik J. Johnson, Vinod Balakrishnan *"Framework For Supporting Multi-Service Edge Packet Processing On Network Processors*". Architecture for networking and communications systems. 26-28 Oct. 2005 Page(s):163 – 171.

3. Bill Carlson, "*Intel® Internet Exchange Architecture & Applications A Practical Guide to Intel's Network Processors",* Intel Press.

4. Dimitri Bertsekas, Robert Gallager , "*Data Networks*" , pp.115, PHI-1987.

5. Douglas E. Comer "*Network Systems Design using Network Processors*", Prentice Hall, Jan 2003.

6. A. Troxel, A. D. George, S. Oral, "*Design and Analysis of a Dynamically Reconfigurable Network Processor*," 27th Annual IEEE International Conference on Local Computer Networks (LCN'02), 2002, pp.0483.

7. Intel IXP2400/IXP2800 Network Processors, *"Intel XScale Core Support Libraries Reference Manual"* November 2003.

8. Intel® IXP2400 and IXP2800, Network Processor Programmer's Reference Manual, July 2005.

9. "*IXP2400 Hardware Reference Manual",* June 2001, Intel Corporation,

10. "IXP 2400 Development Tools User's Guide", June 2001, Intel Corporation.

11. J. Allen, B. Bass, C.Basso, R. Boivi, J.Calvignac, G.Davis, L.Frelechoux, M.Hedds, A. Herkersdorf, A.Kind, J.Logan, M.Peyravian, M.Rinaldi, R.Sabhikhi, M.Siegel, and M. Waldvogel, *"IBM PowerNP Network processor: Hardware, software, and applications", IBM* Journal of Research and Development , Volume (47), nos. 2/3 , pp.177-194,2003.

12. Kevin Lee, Geoff Coulson, Gordon Blair, Ackbar Joolia, Jo Ueyama *"Towards a Generic Programming Model for Network Processors*" In Proc IEEE International Conference on Networks (ICON04), Singapore, November 2004.

13. Kevin Lee, Geoffrey Coulson *"Supporting Runtime Reconfiguration on Network Processors",* Proceedings of the 20th International IEEE Conference on Advanced Information Networking and Applications (AINA'06) Volume 1, 18-20 April 2006 Page(s): 721 – 726.

14. L.Thiele, S.Chakraborty, M.Gries, and S.K¨unzli, *"Design Space Exploration of Network Processor Architectures"*, Proc. First Network Processor Workshop/Eighth IEEE Int'l symp. High Performance Computer Architecture (NP/HPCA'02), pp.30-41, Feb.2002.

15. Ravi Kokku, T.Rich´e, A. Kunze , J.Mudigonda , J.Jason and H.Vin, *"A Case for Run-time Adaptation in Packet Processing Systems"* Proc.Second Workshop Hot Topics in Networks (HOTNETS'03), Nov.2003.

16. Ravi Kokku, Upendra Shevade, Nishit Shah, Harrick M. Vin, Mike Dahlin *"Adaptive Processor Allocation in Packet Processing Systems"* University of Texas at Austin Technical Report # TR04-04.

17. A.Satheesh**,** S.Krishnaveni, S.Ponkarthick *"Self-Configurable Environment for the Intel IXP 2400 Network Processor"* International Journal of Computers and Applications, 31(4):268-273, 2009.

18. Tilman Wolf, *"Network Processors - Flexibility and Performance for Next-Generation Networks"*, ACM SIGCOMM Computer Communication Review, Volume 32 , Issue 1 (January 2002) Pages: 65.

19. T.Wolf and M.Franklin, *"Performance Models for Network Processor Design", IEEE Trans. on Parallel and Distributed Systems*, vol. 17, no.6, Pages: 548 – 561, June 2006.

20. Tilman Wolf, Ning Weng, Chia-Hui Tai, *"Runtime Support for Multicore packet processing systems"*, IEEE Network, Page(s).29-37, July/August-2007.

21. Vinod Balakrishnan, Ravi Kokku, Aaron Kunze, Harrick Vin, Erik J. Johnson *"Supporting Run-Time Adaptation in Packet Processing System"* Intel Research and Development University of Texas at Austin 2004, Technical Report.

22. Xin Huang, Tilman Wolf, *"A Methodology for Evaluating Runtime Support in Network Processors"*, Architecture for Networking and Communications systems, ACM/IEEE Symposium on Volume , Issue , 3-5 Dec. 2006 Page(s):113 – 122.

23. Xin Huang, Tilman Wolf, *"Evaluating Dynamic Task Mapping in Network Processor Runtime Systems"* IEEE Transactions on Parallel and Distributed systems, vol. 19, no. 8, August 2008, Page(s).1086-1098.

# An Efficient Wireless Backhaul Utilizing MIMO Transmission and IPT Forwarding

**Ehab Mahmoud Mohamed** ehab@mobcom.is.kyushu-u.ac.jp
*Faculty of Engineering*
*Advanced Information Technology Dept*
*Wireless Communication Section*
*Kyushu University*
*Motooka 744, Nishi-ku,*
*Fukuoka-city 819-0395, Japan*

**Daisuke Kinoshita** kinoshita@mobcom.is.kyushu-u.ac.jp
*Faculty of Engineering*
*Advanced Information Technology Dept*
*Wireless Communication Section*
*Kyushu University*
*Motooka 744, Nishi-ku,*
*Fukuoka-city 819-0395, Japan*

**Kei Mitsunaga** mitsunaga@mobcom.is.kyushu-u.ac.jp
*Faculty of Engineering*
*Advanced Information Technology Dept*
*Wireless Communication Section*
*Kyushu University*
*Motooka 744, Nishi-ku,*
*Fukuoka-city 819-0395, Japan*

**Y.Higa** higa@mobcom.is.kyushu-u.ac.jp
*Faculty of Engineering*
*Advanced Information Technology Dept*
*Wireless Communication Section*
*Kyushu University*
*Motooka 744, Nishi-ku,*
*Fukuoka-city 819-0395, Japan*

**Hiroshi Furukawa** furuhiro@is.kyushu-u.ac.jp

*Faculty of Engineering/*
*Advanced Information Technology Dept/*
*Wireless Communication Section/Kyushu University*
*Motooka 744, Nishi-ku, Fukuoka-city 819-0395, Japan*
*Phone +81-92-802-3573, Fax +81-92-802-3572,*

**Abstract**

Wireless backhaul has been received much attention as an enabler of future broadband mobile communication systems because it can reduce deployment cost of pico-cells, an essential part of high capacity system. A high performance network, high throughput, low average delay and low packet loss rate, is highly

appreciated to sustain the increasing proliferation in multimedia transmissions. The critical issue reducing the performance of wireless backhaul is the interference occurred in the network due to simultaneous nodes transmissions. In this research, we propose a high performance wireless backhaul using the low interference sensitivity MIMO based nodes. MIMO transmission has a better BER performance over SISO one even with the same transmission rate and bandwidth, which means that MIMO can operate at lower SINR values than SISO and give the same performance. This MIMO robust performance against interference gives us a greater benefit when adopted as a wireless interface in wireless backhaul than SISO. These facts motivated us to use the IEEE 802.11n the current MIMO standard to design a MIMO based wireless backhaul. In addition and to justify our assumptions, we investigate the effect of MIMO channels correlation, a major drawback in MIMO transmission, upon the system performance, and prove the robustness of the scheme under different MIMO channels correlation values.

After proving the effectiveness of MIMO as a wireless interface for wireless backhaul, we further improve the performance of this MIMO-backhaul using the high efficient Intermittent Periodic Transmit (IPT) forwarding protocol. IPT is a reduced interference packet forwarding protocol with a more efficient relay performance than conventional method in which packets are transmitted continuously form the source nodes. By using these two techniques (IEEE 802.11n (MIMO) + IPT), wireless backhaul nodes can meet more demanding communication requirements such as higher throughput, lower average delay, and lower packet dropping rate than those achieved by simply applying IEEE 802.11n to conventionally relayed backhaul.

The proposed wireless backhaul will accelerate introduction of picocell based mobile communication systems.

**Keywords:** Wireless Backhaul Networks, IEEE 802.11n, MIMO-OFDM, IPT forwarding.

## 1. INTRODUCTION

Wireless backhaul is a wireless multihop network in which base nodes are linked wirelessly [1] [2]. Wireless backhaul has been received much attention as an enabler of future broadband mobile communication systems because it can reduce deployment cost of pico-cells, an essential part of high capacity system. A high throughput with a minimum delay network is highly appreciated to sustain the increasing proliferation in multimedia transmissions. In wireless backhaul, base nodes have capability of relaying packets, and a few of them called core nodes serve as gateways connecting the wireless multihop network and the outside network (i.e. the Internet) by cables. Although wireless backhaul has many attractive features over wired backhaul networks like ATM, T1 or DSL line, it is still lack for high throughput design [3]. Recently, researchers in the field of wireless multihop try to improve its performance using MIMO [4-7].

One of the advanced wireless standards driven by MIMO technology is IEEE 802.11n (Dot11n) [8]. Dot11n is an amendment, proposed by a group in IEEE802.11 committee called TGn group,

over the previous OFDM based 802.11 standards (802.11a/g) with PHY and MAC enhancements [8]. Using different space time code structures, the Dot11n's MIMO-OFDM PHY layer can support data ranges up to 600 Mbps which is higher than IEEE 802.11a/g (Dot11a/g) data rate (54 Mbps at maximum). In order to take the full advantage of Dot11n PHY layer enhancements, TGn also enhances the MAC layer by introducing new frame structures that can be used to aggregate multiple subframes to improve throughput.

Because Dot11n is in small age, an adoption of the interface to wireless multihop is in its infancy [5] [6]. Some studies concerned about investigating more efficient MIMO-based MAC protocol than the Dot11n's one so as to be suitable for Ad-Hoc and Wireless Mesh Networks [6] [7]. Others concerned about improving IEEE 802.11s performance, an IEEE 802.11 standard for Wireless Mesh Networks (WMN), by using Dot11n [5]. To do that, the authors in [5] first utilize the variable transmission rate of Dot11n to find the best PHY data rate related to instantaneous channel quality. By using this data rate, they find the best MAC aggregation number that guarantees low packet dropping rate. At last, they use theses two settings (PHY rate + MAC aggregation number) to optimally allocate bandwidth to each type of traffic [5].

According to the knowledge of the authors, most of the studies that adopt Dot11n utilize its MAC and PHY enhancements to improve the performance of Wireless Mesh Networks (WMN) and Ad-Hoc networks, whereas no proposals concerned about adopting the standard to wireless backhaul. Even though all the three networks can be categorized as a wireless multihop network, wireless backhaul is the only one that can adopt a static tree topology routing. This is because all the nodes are fixed in their positions and all uplink and downlink packets are distributed to entire backhaul network via core nodes. On the other hand, dynamic mesh routings are preferred for WMN and Ad-Hoc because of the specific structure of these networks, i.e. multi-point to multi-point connections among all neighboring nodes and dynamic changes of node positions. Difference of the two routings is shown in Fig. 1.

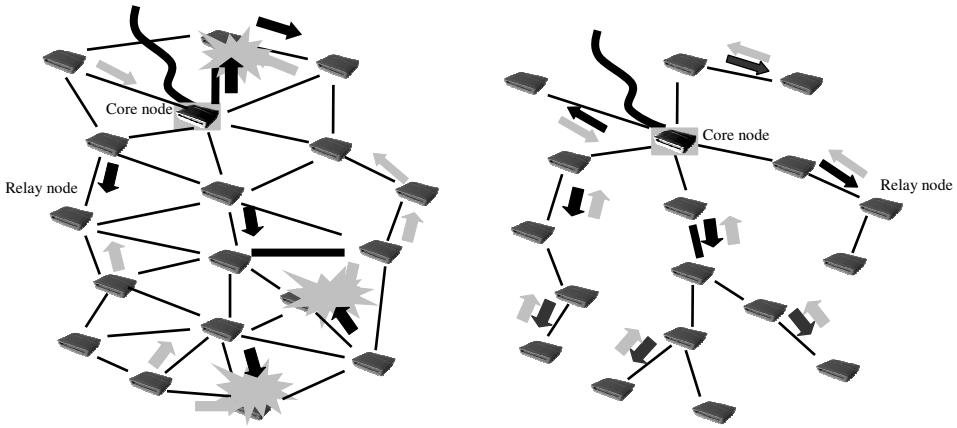


**Figure 1:** WMN and Ad Hoc Routings versus Wireless Backhaul Routing

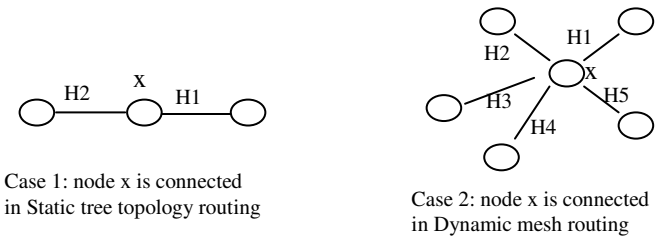


**Figure 2:** WMN and Ad Hoc Routings versus Wireless Backhaul Routing example.

In wireless backhaul with a static tree topology routing, since we can reduce the number of intersections on its routes as shown in Fig. 1, each node can maintain fewer number of connecting nodes, which will contribute to reduce complexity in necessary processes relating to MIMO signal detection such as synchronization, channel state acquisition and so on. To deeply understand this point, consider the two cases in Fig. 2. In case 1, node x has only two intersection connections, and in case 2 node x has many intersection connections (5 connections in this example). Let us suppose immobile scenario which is the static tree topology case for both cases, so in case 1, it is required from node x to make only two MIMO channel matrices estimation (H1 and H2) procedures and only two MIMO synchronization procedures and save these data (channels estimation and synchronization) for other MIMO detections which saves time and computation , but in case 2, it is required from node x to make five (for this example) channel matrices estimation and synchronization procedures and save these data for other detection procedures. In addition, and if we assume mobile scenario which can only happen for case 2 (the WMN and Ad Hoc routing topology case), then node x will always need to make MIMO channel matrices estimation and synchronization for every transmission which extremely increases the complexity and time delay required to detect MIMO signal. So we can conclude that; the static tree topology routing has a lower complexity and time delay than the dynamic mesh one when adapted to MIMO transmissions. This will deliver us a larger benefit of MIMO adoption to wireless backhaul compared with other wireless multihop networks.

This paper considers an application of Dot11n as a MIMO wireless interface to wireless backhaul with a static tree topology routing in order to enhance throughput and spectrum efficiency of its relay network. To cope with this issue, we first adopt Dot11n for conventionally relayed wireless backhaul in which packets are transmitted continuously from source nodes, and compare its performance with the currently used Dot11a (SISO) under the same conditions of evaluation (transmission rate, bandwidth, evaluation site….,etc). Although we compare the two performances using the same conditions of evaluations, Dot11n (MIMO)-backhaul show a significantly improved performance, this is because MIMO based relay nodes have a lower interference sensitivity (a vital demand for high performance wireless backhaul) than SISO based ones. This MIMO's low interference sensitivity comes from MIMO's much better BER (Bit Error Rate) characteristics compared to SISO, which gets MIMO operates under lower SINR (Signal to Interference Ratio) conditions. This MIMO low interference sensitivity gives us a higher performance backhaul over SISO based one.

One of the major drawbacks degrading the BER performance of Dot11n and MIMO transmission in general is MIMO channels correlation. MIMO transmission has an optimal BER performance under completely uncorrelated MIMO channels, and this performance is degraded as the correlation increased. In order to investigate the effect of MIMO channels correlation on system performance, we test the performance of the proposed Dot11n-conventional backhaul under different channels correlation coefficient values. We show the robustness of the scheme under different channels correlations, which further supports the idea of adopting Dot11n (MIMO in general) as a cost effective way in realizing a high performance wireless backhaul.

After proving the effectiveness of Dot11n as a wireless interface for wireless backhaul, we further improve the relay efficiency of this Dot11n based network through the utilization of Intermittent Periodic Transmit forwarding protocol (IPT) [9]. IPT is a provably efficient relaying protocol in which, a source node sends source packets intermittently and periodically with a controllable transmit period. By suitably adjust this period, we can eliminate packet interference occurred in conventional method and maximize the relay efficiency [10]. Obtained results show the effectiveness of IPT based Dot11n wireless backhaul over conventionally based one.

The rest of the paper is organized as follows. Section 2 describes IPT protocol in more details. The simulation scenarios and performance metrics are given in section 3. Section 4 gives a

comparison between Dot11a and Dot11n conventionally based backhauls. Section 5 shows the Impact of MIMO channel correlations upon system performance. Further performance improvements using the advanced packet forwarding technique (IPT forwarding) is given in section 6 followed by the conclusion in section 7.

## 2. Intermittent Periodic Transmit (IPT) Forwarding Protocol

Intermittent periodic transmit (IPT) forwarding is a highly efficient packet relay method for wireless multihop networks in general and backhaul in especial [9] [10]. In this method, a source node intermittently sends source packets with some transmit period, and intermediate nodes forward each incoming packet immediately after the reception of it. Figure 3 shows packet relays carried out by IPT in which two transmit periods, P_1 and P_2 are given. If the transmit period is greater than a certain threshold (critical limit), packet collisions due to interference are removed, hence collision free wireless multihop relay is realized. Ascertaining the reception states at the intermediate and destination nodes in Fig.3, throughput measured by the respective nodes is constant irrespective of hop counts which completely changed the old thought: the throughput is decreased as the hop nodes numbers is increased [11]. An adaptive transmit period adjustment protocol has been proposed in [10] in order to optimally eliminate the interference and maximize the throughput.

After proving the efficiency of IPT over the conventional method of relaying in which packets are transmitted continuously with minimum path loss routing, The authors proposes a new routing method, called spiral mesh routing, to enable the IPT in 2-dimentional base nodes layout. With the spiral mesh routing, neighboring nodes are linked together in a point to point fashion so as to make a spiral-shaped route and multiple spiral routes are folded assigning each of them a different channel. This technique removes intersections on respective routes and reduces interference in the direction toward or apart from the central node, which enables the IPT for 2D.
Further developing researches are conducted to increase the efficiency of IPT forwarding for different scenarios and prove its efficiency over the conventional method of relaying [12] [13].
In this paper, we will only use the basic idea of IPT as shown in fig.3.

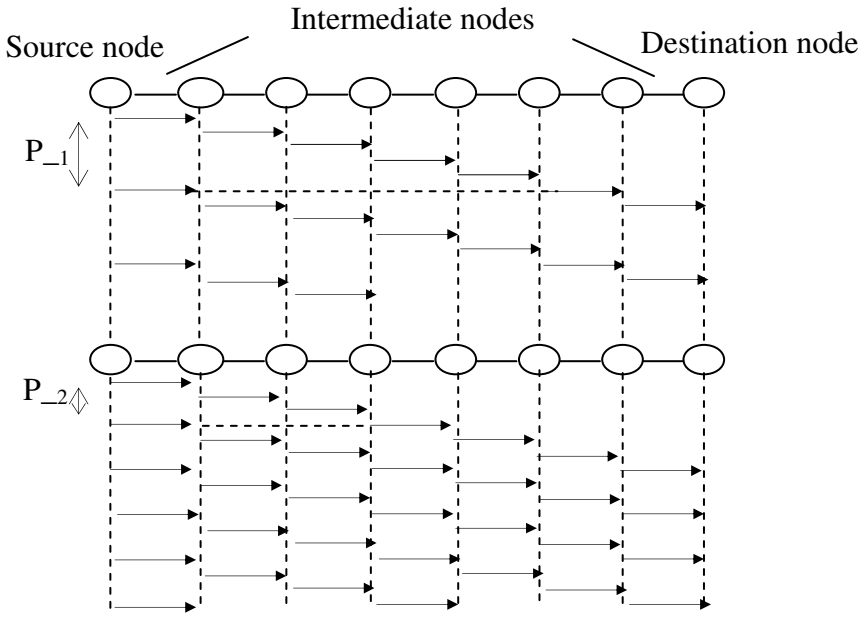


**Figure 3:** Packet relays by the IPT forwarding

## 3. Simulation Scenarios and Performance Metrics

To evaluate the performance of the suggested MIMO wireless backhaul network and prove its efficiency, we link the MATLAB program with our original network simulator. The MATLAB program is used to evaluate the PHY layer performance, and the network simulator is used to evaluate the whole system performance using the PHY performance data obtained by MATLAB.

### 3.1 Simulation Scenarios and Parameters

#### 3.1.1 PHY Layer

In order to prove the efficiency of MIMO wireless backhaul over SISO based one, we compare the performance of two PHY layers

- IEEE 802.11n (MIMO standard)
- The currently used IEEE 802.11a (SISO standard)

For fair comparison, the evaluation was done under the same conditions, .i.e. transmission bandwidth, transmission rates….etc,
We evaluate Dot11n and Dot11a PHY performances under two transmission rates 36Mbps and 48Mbps.

Table 1 shows Dot11n and Dot11a PHY layers simulation parameters:

| Parameter | Dot11n | Dot11a |
|---|---|---|
| Bandwidth | 20 MHz | 20 MHz |
| Number of Data Subcarrier | 48 | 48 |
| IFFT Size | 64 | 64 |
| Cyclic Prefix length | 16 | 16 |
| Pilot Subcarriers per Symbol | 4 | 4 |
| QAM mapping | QPSK-16QAM | 16-64 QAM |
| Transmiter antennas | 2 | 1 |
| Receiver antennas | 2 | 1 |
| FEC Rate | ¾, 1/2 | ¾, 2/3 |
| Raw Data Rates | 36, 48 Mbps | 36, 48 Mbps |
| MIMO Detector /channel equalizer | SOMLD (Soft Output Maximum Likelihood) | |
| Channel Estimation | Perfect | |
| Synchronization | Perfect | |
| Quasi-Static Channel model<br>Rayleigh fading (NLOS) with exponential PDP (Power Delay Profile) indoor or outdoor (large open space) case<br>Tmax(MAX delay spread)=300ns,<br>Trms (RMS delay spread)=150ns | | |

**TABLE 1:** PHY layers parameters

#### 3.1.2 MAC Layer

For MAC operation, the operation mode of CSMA/CA, the MAC standardized by IEEE 802.11, dynamically changes in between the Basic and RTS/CTS modes depending on message transmit method and IPT activation: when IPT forwarding is carried out, the Basic mode is applied otherwise the RTS/CTS mode is chosen.

### 3.1.3 Traffic Model

Downlink traffic directed to terminals that stay under base nodes is all generated at a core node and forwarded to each base node. Uplink traffic caused by terminals is gathered at the base node in which the terminals stay and forwarded to a core node. The Poisson origination is employed as a traffic model. The number of data packets per session is randomly determined by the log-normal distribution, the mean of which is 20 for downlink and 3 for uplink. The ratio of the total offered load of downlink to uplink is 10:1 [14].

### 3.1.4 Packet forwarding methods

In order to prove the efficiency of MIMO- IPT wireless backhaul over MIMO – conventional based one, we compare the two-method with the same forwarding path shown in Fig 4.

- **Conventional method**- packets are transmitted continuously with minimum path loss with RTS/CTS MAC mode for all transport sessions.
- **IPT protocol**- IPT protocol is used with basic MAC mode.

### 3.1.5 Evaluation Site

We chose the floor of our department building as a test site Fig 4. In order to handle a complex interference situation as correctly as possible, we use a simple deterministic radio propagation model such as a path loss coefficient of 2 dB until 5m and 3.5 dB beyond this distance [15], 12 dB penetration loss of the wall [16]. 23 base nodes are placed on the floor and a core node is placed on stairs area of the floor Fig 4. A forwarding path is formed in advance and fixed during simulation Fig 4. Spectrum assigned to the wireless repeater network is assumed to be different from one assigned to wireless communication links between mobile terminals and base station (access network) so interference between access network and repeater network can be excluded.

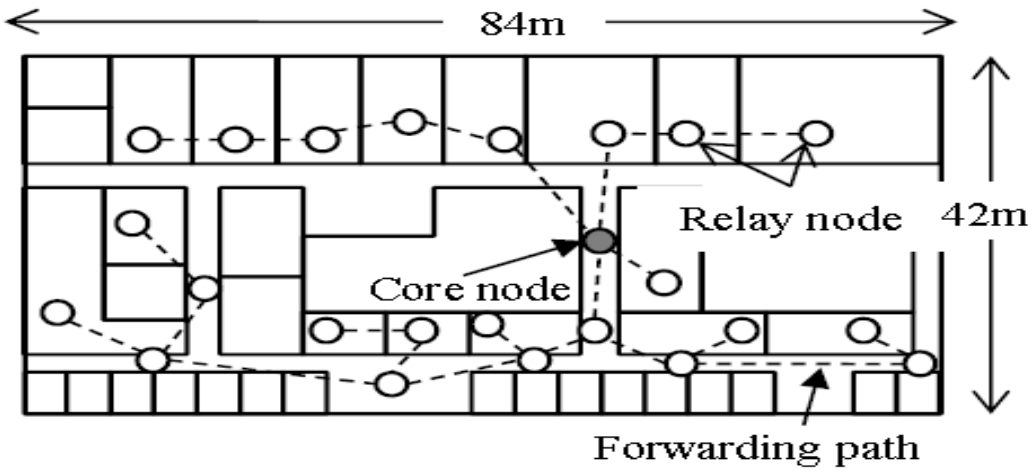


**Figure 4:** Floor plan and node layout for evaluations

## 3.2 Performance Metrics

### 3.2.1 PHY layer simulator

We evaluate the BER (Bit Error Rate) performance of each tested PHY layer, i.e., Dot11a 36, Dot11a 48, Dot11n 36, and Dot11n 48 Mbps.

### 3.2.2 System level simulator

Three system level performance metrics are used: Aggregated end-to-end throughput, Average delay, and packet loss rate.

a. *Aggregated end-to-end throughput* is defined as sum of throughputs for all sessions each of which successfully delivered to a destination.
b. *Average delay* is defined as an average time period from the instant when a packet occurs at a source node to the instant when the destination node completes reception of the packet.
c. *Packet loss rate* is defined as follows:
   Packet loss rate [%] =*ND*100 / (NS +ND).*
   Where *NS* denotes the number of packets received successfully by destination nodes.
   *ND* denotes the number of discarded packets due to exceeding a retry limit

Each simulation is carried out for 200 sec; this simulation period has been ensured to achieve a good convergence. Also, we assume UDP traffic.

## 4. Comparison between Dot11a and Uncorrelated Channels Dot11n based Backhauls

Mont carol simulations are carried out for evaluating the comparison between Dot11a and Dot11n based wireless backhauls.

## 4.1 PHY Layer Simulator

Figure 5 shows the BER performance of the compared PHY layers (Dot11a 36, 48 Mbps and Dot11n 36, 48 Mbps). Although we compare the same transmission rates for both PHY layers, Dot11n shows better BER performance than Dot11a. This Dot11n better BER performance comes from using multiple antennas at both transmitter and receiver (MIMO) which is not the case for Dot11a. By using MIMO, Dot11n uses lower MCS (Modulation Coding Scheme) than Dot11a to obtain the same transmission rate under the same bandwidth. For example, in order to obtain a transmission rate of 36 Mbps for both Dot11a and Dot11n under the same bandwidth of 20 MHz, Dot11a uses 16-QAM with FEC=3/4, but 2*2 MIMO Dot11n uses QPSK with FEC=3/4. This Dot11n's MCS reduction resulting from using MIMO greatly enhances its BER performance.

## 4.2 System Level Simulator

Using the BER performances of Dot11a and the uncorrelated channels Dot11n evaluated in section 4.1, we compare their system level performances using conventional method of relaying. Figures 6-8 show the system level performances of Dot11a and Dot11n, these figures show the highly efficient Dot11n performance compared with Dot11a under the same transmission rates. This Dot11n high performance comes from its better BER performance as explained in section 4.1. Better BER performance means that for a certain required PER (Packet Error Rate) performance value, MIMO operates at a lower SINR (Signal to Interference Ratio) value than SISO, which gives MIMO robust characteristics against interference, i.e., MIMO has a lower sensitivity to interference than SISO. This important MIMO phenomenon has a great impact on system performance in which interference causes a significant degradation in performance. These facts are reflected on the system level performance in terms of higher throughput, lower delay and lower packet loss rate of Dot11n based backhaul than those achieved by Dot11a

based one as revealed by figures. These simulations provide evidence the idea of enhancing wireless backhaul performance using MIMO-based nodes.

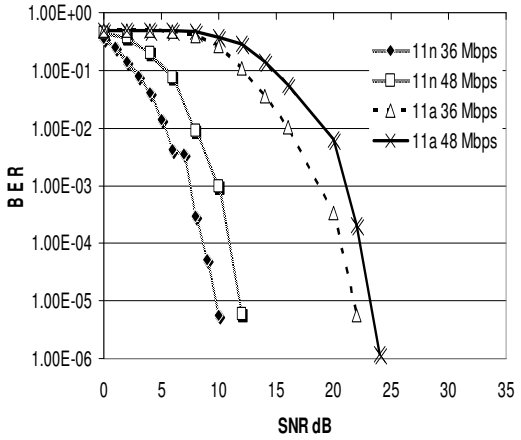


**Figure 5:** BER performance of Dot11n and Dot11a

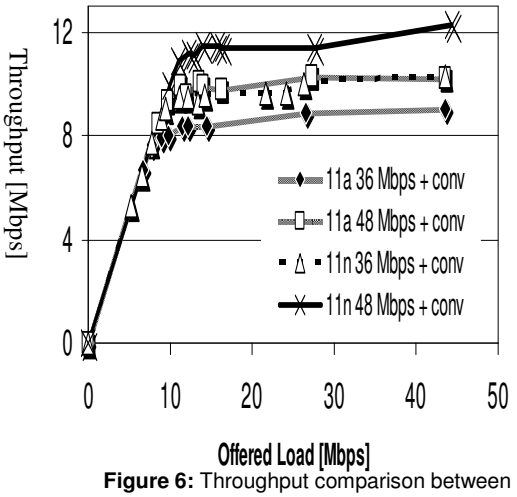


**Figure 6:** Throughput comparison between Dot11a and Dot11n with conventional method

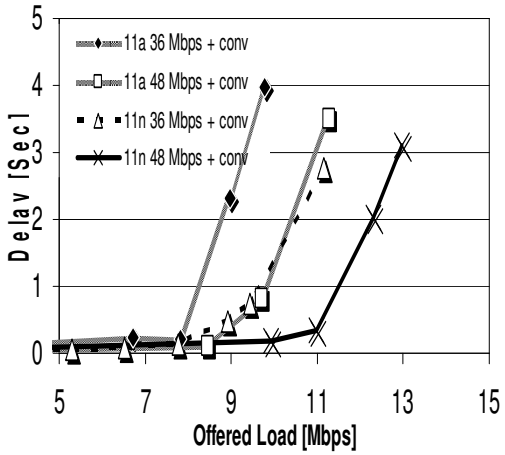


**Figure 7:** Delay comparison between Dot11a and Dot11n with conventional method

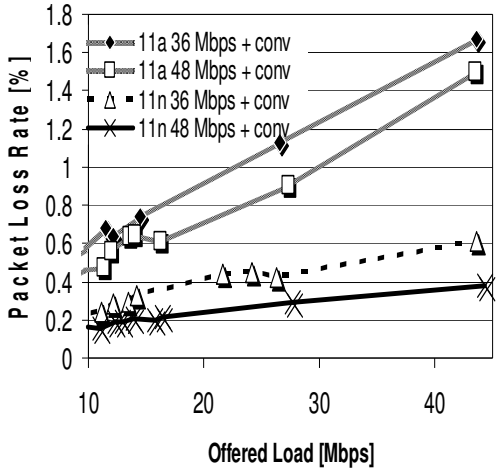


**Figure 8:** Packet Loss Rate comparison between Dot11a and Dot11n with conventional method

## 5. The Impact of MIMO Channels Correlation upon System Performance

Mont carol simulations are carried out for evaluating the effect of MIMO channels correlation upon the system performance.

### 5.1 PHY Layer Simulator

In this simulation, we evaluate Dot11n 48Mbps performance under different MIMO channels correlation coefficient values 0, 0.5, and 0.75; figure 9 shows the resulting BER performance. From this figure, we can conclude that; as the MIMO channels correlation increased the BER performance degraded, and the optimum BER performance is obtained when the MIMO channels are uncorrelated (Corrcof = 0). Although of Dot11n BER degradation due MIMO channels correlation, it still shows a better BER performance than Dot11a even with a high correlation value of 0.75.

### 5.2 System Level Simulator

Using the BER performances of Dot11n 48 Mbps under different MIMO channels correlation coefficient values (0, 0.5, and 0.75) evaluated in section 5.1, we measure the system level performance using these values with conventional method of relaying. Figures 10-12 show the system performance under each correlation value. From these figures, we can observe the neglected effect of channels correlation on throughput and delay performances, but the packet loss rate performance is little bit affected by this correlation, this is because packet loss rate is highly sensitive to PHY BER performance. Theses neglected effects come from the little changed Dot11n's BER due to channels correlation. All these results show the robustness of Dot11n and MIMO in general as a wireless backhaul interface even in a highly correlated MIMO channels.

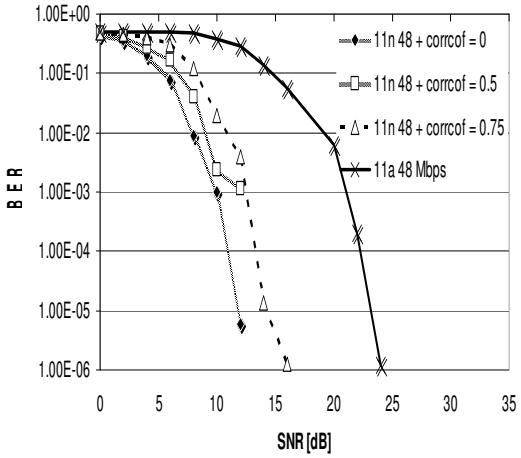


**Figure 9:** BER performance of correlated channels
Dot11n 48 Mbps.

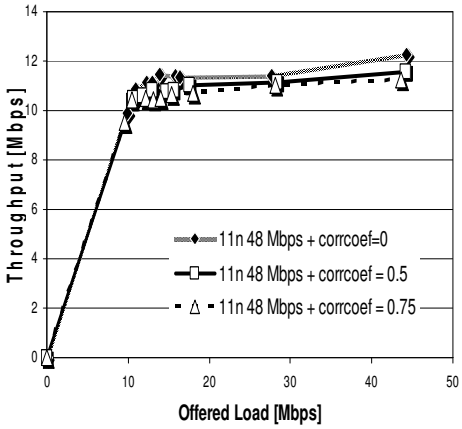


**Figure 10:** Throughput performance of Dot11n 48 Mbps+ conventional method for different MIMO channels correlation

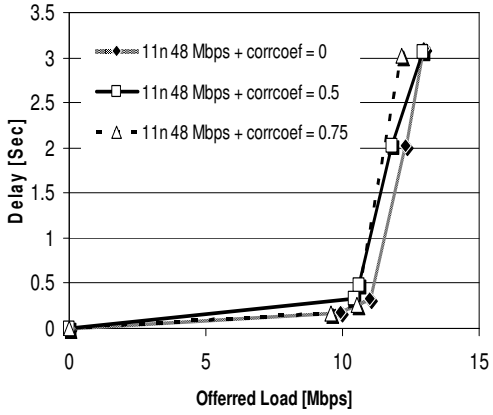


**Figure 11:** Delay performance of Dot11n 48 Mbps + conventional method
for different MIMO channels correlation

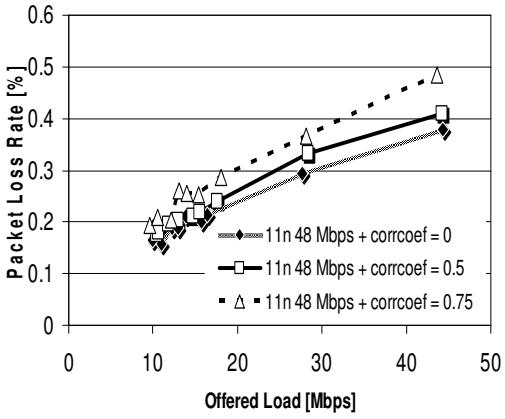


**Figure 12:** Packet Loss Rate performance of Dot11n 48 Mbps + conventional method
for different MIMO channels correlation

## 6. Further Performance Improvements using Advanced Packet Forwarding Technique (IPT forwarding)

In this section, we introduce the Intermittent Periodic Transmit (IPT) forwarding protocol as an advanced packet forwarding technique, previously proposed by the authors [9], to enhance the relay efficiency of the suggested MIMO – wireless backhaul instead of the conventional method of relaying.

### 6.1 IPT Based Wireless Backhaul Performance

Mont carol simulations are carried out for evaluating the system performance using IPT forwarding

### 6.1.1 Dot11a versus Dot11n in IPT Environment

By using the BER performance of Dot11a and uncorrelated channels Dot11n evaluated in section 4.1, we compare Dot11a and Dot11n system performance using IPT protocol, figures 13-15 show system throughput, average delay, and packet loss rate in IPT environment. Also, in these simulations, Dot11n shows a much better performance than Dot11a from the system point of view.

### 6.1.2 Comparison between Dot11n-IPT and Dot11n-Conventional Backhauls

In these simulations, we compare the system level performance of Dot11n 48 Mbps IPT based and Dot11n 48 Mbps conventionally based backhauls. Figures 16-18 show the system level performances of these two backhauls. Simulation results ensure better performance of the IPT based network over conventionally based one. This enhanced IPT performance comes from the interference rejection resulting from the intermittent packet transmission introduced by IPT. These results verify the effectiveness of the MIMO-IPT based wireless backhaul as a key enabler for the next wireless mobile communication generation.

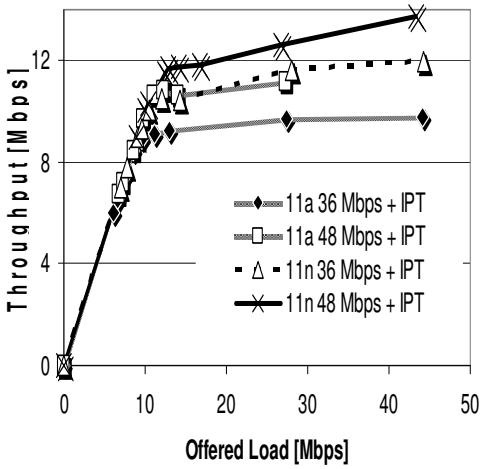


**Figure 13:** Throughput comparison between Dot11a and Dot11n with IPT

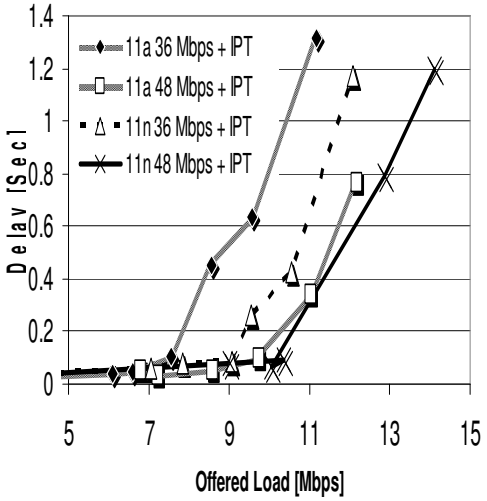


**Figure 14:** Delay comparison between Dot11a and Dot11n with IPT

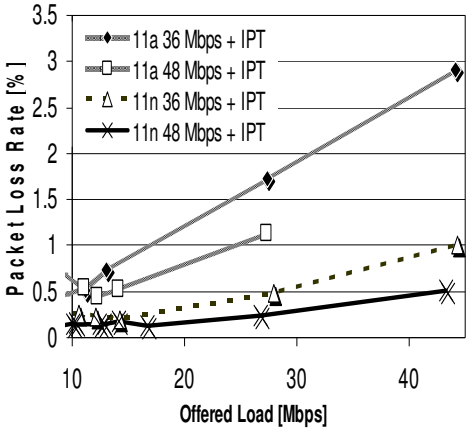


**Figure 15**: Packet Loss Rate comparison between Dot11a and Dot11n with IPT

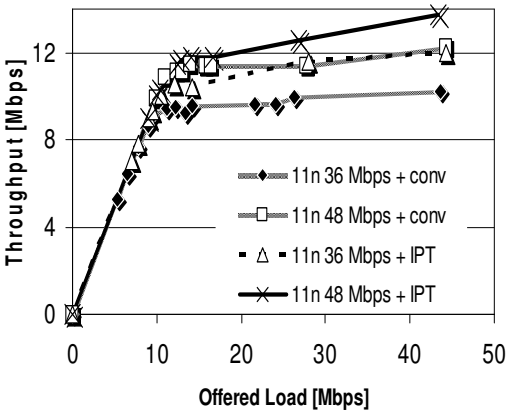


**Figure 16:** Throughput comparison between conventional method and IPT with Dot11n

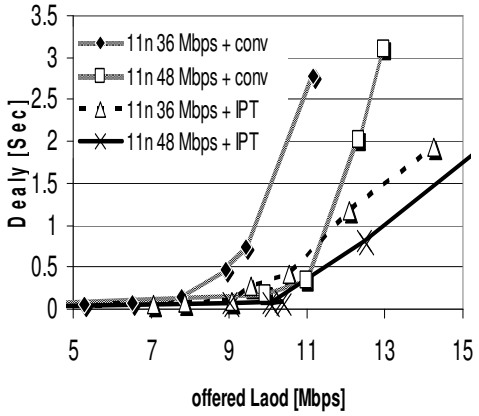


**Figure 17:** Delay comparison between conventional method and IPT with Dot11n

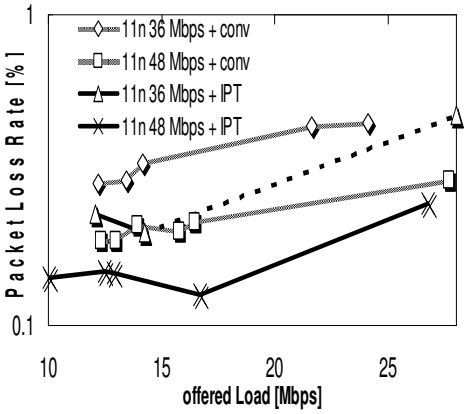


**Figure 18:** Packet Loss Rate comparison between conventional method and IPT with Dot11n

## 7. CONSLUSION & FUTURE WORK

In this paper, we investigate the application of Dot11n (MIMO standard) as a low interference sensitivity wireless interface, with a good BER performance, to improve the performance of the current Dot11a (SISO) based wireless backhaul networks. We show the effectiveness of applying MIMO in terms of backhaul system performance. MIMO based wireless backhaul has a higher throughput, lower average delay, and lower packet loss rate than SISO based one. In addition, we study the effect of MIMO channels correlation on the proposed wireless backhaul performance, and we prove the robustness of the scheme against different correlation values.

At the end of this research, we consider the application of Intermittent Transmit Periodic (IPT) forwarding as a packet forwarding protocol in order to improve the relay efficiency of the MIMO based wireless backhaul. MIMO–IPT wireless backhaul outperforms the MIMO-conventional based one, which provides evidence the application of MIMO-IPT wireless backhaul as a key enabler for the next wireless backhaul generation.

For future work, we will modify the IPT protocol, like multi-channel IPT, to be more suitable for MIMO transmissions and obtain a further improved wireless backhaul.

## 8. REFERENCES


[1] S. Romasszko, C. Blondia, “Cross layer PHY-MAC protocol for wireless static and mobile Ad Hoc networks,” in Eurasip Journal on Advances in Signal Processing 2009, art. No. 278041, 2009.

[2] R. Pabst et al, “Relay based deployment concepts for wireless and mobile broadband radio,” IEEE Com. Mag, pp.80-89, Sep. 2004.

[3] G. Narlikar, G. Wilfong, L. Zhang, “Designing Multihop Wireless Backhaul Networks with Delay Guarantees.”, in proc INFOCOM 2006. 25th IEEE International Conference on Computer Communications, pp.1-12, 2006.

[4] Mohinder Jankiraman, “Space-Time Codes and MIMO Systems”, book, Cambridge university press.

[5] A. Ashtaiwi. H. Hassanein, “Utilizing IEEE 802.11n to enhance QoS support in wireless mesh networks”, in Local Computer Networks LCN 2008. 33rd IEEE Conference, pp. 689-696, Oct. 2008.

[6] A. Ashtaiwi, A. Hassanein, H.S, “Rate Splitting MIMO-based MAC Protocol,” in Proc Local Computer Networks, 2007. LCN 2007.

[7] K. Sundaresan, R. Sivakumar, Ingram, M.A, and Tae-Young Chang. “Medium access control in ad hoc networks with MIMO links: optimization considerations and algorithms,” Mobile Computing, IEEE Transactions, Vol.3, pp. 350-365, 2004

[8] T. K. Paul, T. Ogunfunmi, “Wireless LAN Comes of Age: Understanding the IEEE 802.11n Amendment”, in Circuits and Systems Magazine, IEEE, pp28 -54, First Quarter 2008.

[9] H. Furukawa, “Hop Counts Independent Throughput Realization by a New Wireless Multihop Relay,” in Proc. VTC’04-Fall, Sep. 2004.

[10] Y. Higa and H. Furukawa,”Time Interval Adjustment Protocol for the New Wireless Multihop Relay with Intermittent Periodic Transmit,” national conference of IEICE, pp. 514, Sep.2004 (in Japanese)

[11] S. Bansal, R. Gupta, R. Shorey, I. Ali, A. Razdan and A. Misra, “Energy efficiency and throughput for TCP traffic in multi-hp wireless networks,” Proc INFOCOM2002, 23-27, pp. 210-219, 2002.

[12] K. Maruta, Y. Tohzaka, Y. Higa, H. Furukawa, “Bidirectional Traffic Handlings in Wireless Multihop Networks Incorporating Intermittent Periodic Transmit and Packet Forwarding Path Reservation”, in Proc. IEEE APWCS 2007, 2007.

[13] K. Mitsunaga, K. Maruta, Y. Higa, H. Furukawa, “Application of directional antenna to wireless multihop network enabled by IPT forwarding” proc. ICSCS, December, 2008.

[14] K.Fukuda, K.Cho, and H.Esaki, "The Impact of Residential Broadband Traffic on Japanese ISP Backbones," Computer Communication Review, vol.35, no.1, pp.15-22, 2005.

[15] TGn Indoor MIMO WLAN Channel Models, IEEE 802 11-03/161r2, 2004.

[16] ITU-R WP3K, “Draft revision of recommendation ITU-R P.1238; Propagation data and prediction models for the planning of indoor radio communication systems and radio local area networks in the frequency range 900MHz to 100GHz,” ITU-R Document 3/53,1999.

# Inter-operator Dynamic Spectrum Sharing (Analysis, Cost and Implications)

**Gbenga Salami** g.salami@surrey.ac.uk
*Center for Communication Systems Research*
*University of Surrey,*
*Guildford, GU2 7XH, United Kingdom*

**Rahim Tafazolli** r.tafazolli@surrey.ac.uk
*Center for Communication Systems Research*
*University of Surrey,*
*Guildford, GU2 7XH, United Kingdom*

**Abstract**

This paper addresses Dynamic Spectrum Sharing (DSS) between two wireless operators. The Universal Mobile Telecommunication System (UMTS) network is used as a case study. The proposed protocol is evaluated under the uniform and non-uniform traffic conditions. The underlying principles of the algorithm can be deployed in the UMTS extension Band (2500MHz-2690MHz) which is yet to be allocated or the re-farmed GSM spectrum (900MHz/1800MHz). The simulation results for the proposed protocol shows that significant spectrum sharing gains can be obtained. However such spectrum efficiency gain need to be carefully balanced with the complexity in terms of latency (delays) and additional overhead it brings to the network. The results show that significant spectrum sharing gain of 4.0 % and 2.0 % can be obtained under uniform and non-uniform traffic conditions.

**Keywords:** Dynamic spectrum sharing, fixed spectrum allocation, call setup, queuing.

## 1. INTRODUCTION

Several measurement studies have indicated that the finite spectrum resource is not efficiently utilized [1] [2]. When the scarce spectrum resource is viewed dynamically as a function of time (temporal variations) and space (spatial variation) or a combination of both, there exists “spectrum opportunities or holes” that require more efficient techniques in order to be exploited. The traditional spectrum management method is known as Fixed Spectrum Allocation (FSA). FSA is simple and effectively controls interference through the use of a guard band. However, it has three main deficiencies; it is static, inefficient and it limits innovation or rapid deployment of new technologies [3]. This is because spectrum licenses and hence chunks of spectrum blocks are issued in an exclusive manner to the network provider/operator. Therefore a new network provider/operator is not allowed to use this spectrum during the idle or less busy periods.

The future/next generation wireless network will consist of a plethora of heterogeneous networks. In order to satisfy the service demands of these complex networks, Dynamic Spectrum Access (DSA) provides a very promising solution to address the problem of spectrum underutilization [4] [5]. The DSA solutions can be centralized [6] [7], distributed [8] or a combination of both. A

classification of these solutions according to the intelligent decision maker together with the advantages and disadvantages of each approach is presented in [9].

The successful realization of DSA schemes will depend on the elimination of a number of technical, economic and regulatory barriers. These barriers are highlighted in [5]. A detailed survey on the challenges to be addressed within the context of opportunistic spectrum access is presented in [4] [5] [10]. These papers have outlined the key requirements involved in the design of DSA schemes for next generation wireless systems. The requirements include: architectural design requirements, techniques to effectively identify reuse opportunities (spectrum sensing), efficient exploitation of detected opportunities through adaptive transmission and modulation waveforms, reconfigurability, the release of the resource once communication has ended (spectrum mobility) and interference mitigation mechanisms [10]. A framework for hierarchical spectrum management in a heterogeneous network is presented in [11]. The successful management of DSA networks involves specialized “protocols” and “policies”. An example of such a policy is discussed in [12]. The goals of these spectrum sharing protocols are usually multi-objective in nature. The protocols should ensure efficient and fair use of the spectrum in a stable manner by allowing secondary users into the white spaces, while at the same time minimizing harmful interference to the licensed primary users of the spectrum.

The main contributions of this paper are as follows; the paper describes a spectrum access framework for the evaluation of spectrum sharing algorithms. The proposed protocol takes into account the fact that although the peak period may coincide, the differential loading during the peak hour between two operator’s traffic pattern provides sufficient gain which can be exploited to improve system capacity and hence spectrum efficiency gain. The characterization depicted here represents the lower bound conditions (worst case scenario). It has been shown in [22] that the spectrum efficiency gain increases significantly in un-correlated traffic situations. The simulated performance takes into account soft handover and Inter-operator interference in the form of Adjacent Channel Interference (ACI). The impact of ACI is particularly important if the operator base stations are non-co-located and displaced by distance *(d)*. This effect serves to reduce the achievable capacity gain for DSS, since in the real world base stations belonging to different operators are more likely to be displaced.
Secondly, the paper has evaluated the call setup latency associated with the proposed algorithm, since longer call setup times will be expected if the User Equipment (UE) is unable to seek connection on its initial network. Furthermore the overhead cost in the form of call setup messages is also presented. The overall aim is to provide a guideline for wireless operators in the selection of an appropriate scheme, taking into account the spectrum efficiency gains and the associated penalty or complexity resulting from the use of such DSS schemes.
Similarly, the algorithm takes into account uniform and non-uniform traffic cases. In the non-uniform traffic case, hotspots cell areas have been included in the model. Hotspots are areas of temporarily high call volume occurring statically or dynamically, due to specific events such as campaign rallies, sporting events, airports etc.
The work presented in this paper addresses a case study involving two UMTS operators sharing spectrum and may be deployed in any band as stated earlier. Furthermore, this paper proposes the architecture for enabling co-operative spectrum sharing between two UMTS operators. A major component of any DSA scheme is the signaling cost and control information overhead associated with it. Therefore central to the implementation of any spectrum sharing algorithm is the determination of the cross-over point at which spectrum sharing may be detrimental to the network. This paper gives an insight into the signaling overhead (call setup delays) involved in the proposed schemes.
The remainder of this paper is structured as follows. Section II introduces the spectrum access framework and the cases investigated. Section III and Section IV gives the details of the system model and algorithm description respectively. Section V analyses the call setup delays. The simulation metrics and DSA performance results are presented in Section VI. This section also gives a discussion of the results. The conclusions and future work plans are outlined in Section VII.

## 2. RELATED WORK

DARPA Next Generation (XG) [13] has initially investigated dynamic spectrum access with the aim of developing new technologies and system concepts (including new waveforms) to intelligently redistribute the spectrum through opportunistic access. Since the early 1990s, DSA has been formerly studied under the heading of Dynamic Channel Allocation (DCA) [14]. In 2000, the European projects such as the DRIVE [15] and its successor OVERDRIVE [16] have proposed network centric algorithms such as contiguous and fragmented schemes for addressing dynamic spectrum access. This investigation quantifies the spectrum efficiency gain in UMTS-DVB-T sharing scenario to be about twenty nine percent. More recently in 2008, the work in [17] under the $E^2R$ II (End to End Reconfigurability) project applies genetic algorithm to solve the optimization problem involved in cell-by-cell DSA. This work reported a spectrum efficiency gain of 38 % and 41 % respectively under uniform and non-uniform traffic conditions. Reconfigurability is an important practical enabler of DSA systems. The European project $E^2R$ project, and its follow up $E^2RII$ [18], have focused on different aspects of radio reconfigurability, spectrum sharing, and CR implementation in a test-bed. In [18], the factors for achieving this are captured in three-dimensional spaces: technical, economic and regulatory. The technical requirements (radio segment and network segment) can further be broken into a multi-dimensional space composed of service *(s),* time *(t),* space *(sp)* (i.e. location), frequency *(f),* and RAT dimensions. In 2009, the End to End Efficiency ($E^3$) project [19] funded by the European Union aims to address the integration of Cognitive Wireless networks into beyond 3G network. A further manifestation of the intense interest within the research community in this area is demonstrated by the numerous publications in the IEEE conferences DySPAN [20], CROWNCOM [21].

### 2.1 Spectrum Access Framework

In order to adequately develop a Spectrum Access Framework, it is important to understand the variety of spectrum sharing models available in literature. The authors in [4] [23] have provided a detailed classification of the different types of sharing options. This paper focuses on a centralized mechanism for spectrum sharing between two operators using the same technology. The traffic demand of Network Operator A is given by ($D_{1A}$, $D_{2A}$, $D_{3A}$, .....,$D_{NA}$) at time intervals ($t_1$, $t_2$, $t_3$, $t_4$....., $t_n$), similarly for Network Operator B, the traffic demand is given by ($D_{1B}$, $D_{2B}$, $D_{3B}$,.....,$D_{NB}$) at time intervals ($t_1$, $t_2$, $t_3$, $t_4$,....., $t_n$). It can be seen that although the operator may have the same peak hour periods, this does not necessarily mean that the two operators have exactly the same peak load.

The traffic profile for the two operators is exactly the same. The peaks coincide as shown in Fig.1. A realistic traffic model inspired by [1] [24] is used in this paper. Fig. 1 shows the normalized traffic profile of the two operators (initially measured in calls/cell/hour), with similar peak periods occurring at 8-10 am (morning) and 4-6 pm (evening).

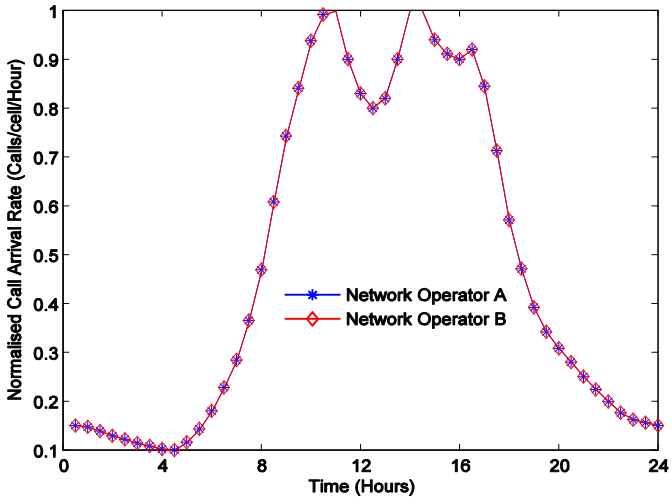


**FIGURE 1:** Showing normalized traffic profile for two networks

A closer look at the Fig. 1 indicate that although the peaks coincide there are instantaneous opportunities that could be exploited during the peak hour due to statistical multiplexing of call arrivals. This represents the worst case scenario and it gives the lower bound on the spectrum efficiency gain. These instantaneous fluctuations are captured in Fig. 2.

.

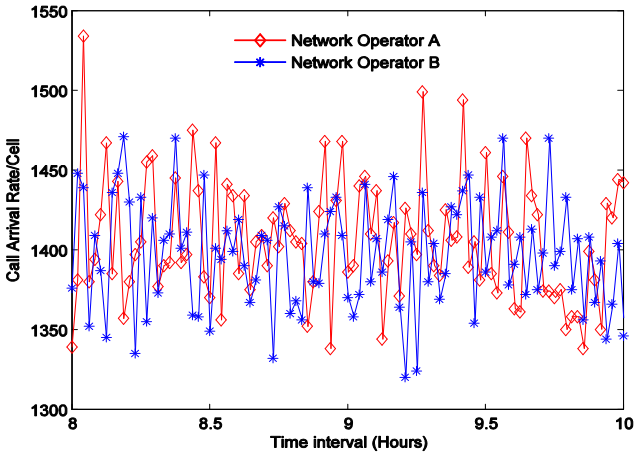


**FIGURE 2:** Instantaneous variation in peak hour load for two networks with similar traffic profile.

In order to properly address spectrum sharing, the papers in [8], [17] have proposed a hierarchical solution. Fig. 3 presents an architectural enabler to facilitate spectrum sharing between two operators. The Spectrum Management Entity (SME) controls all spectrum related activity such as user migration between networks, carrier allocation and release. The architecture allows resource optimization to occur at different levels from intra-network to inter-network.

.

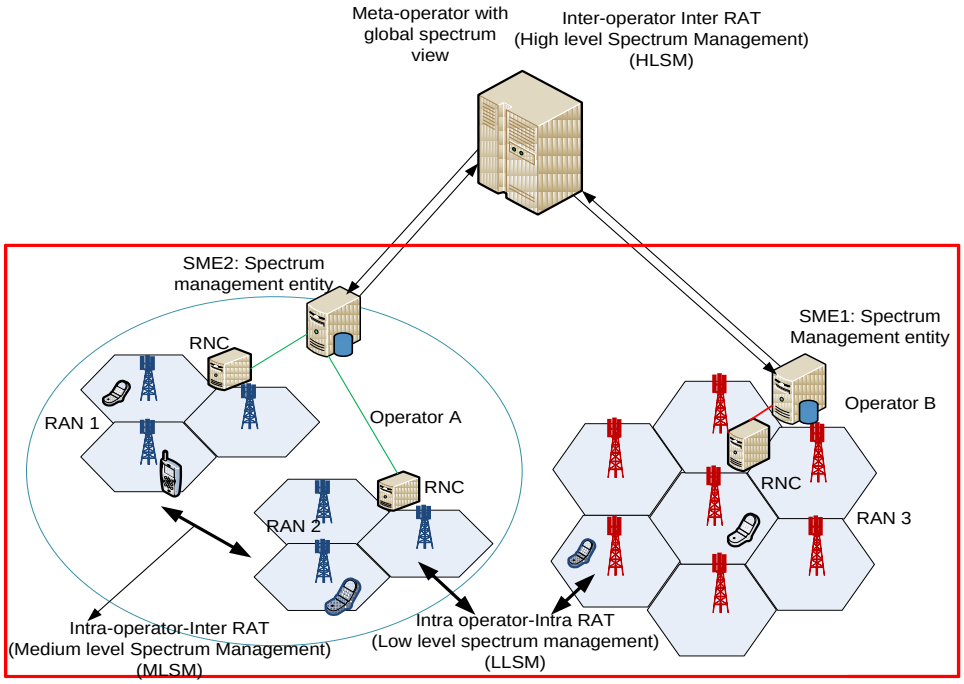


**FIGURE 3:** Architectural enabler for UMTS spectrum sharing showing interfaces and network elements.

This paper presents an algorithm description of the component required at the different levels of the spectrum access framework. It is important to note that at each level, resource optimization is required using a combination of legacy and new techniques (power control, call admission control, load balancing and inter-operator resource scheduling etc) in order to achieve the desired overall spectrum efficiency gain.

Based on Fig. 4, a resource allocation request in the network triggers the low level spectrum management functionality (LLSM). The specific techniques at this level will encompass intra-operator intra-RAT resource management strategies. The time scale for this operation is also considered to be of the order of milliseconds. If the resource optimization criteria can be met at this level no further interaction with the MLSM entity is necessary and the resource is granted to the user. The inability of the system to satisfy the UE at the lower level triggers the Medium Level Spectrum Management (MLSM) subsystem. This subsystem includes a number of intra-operator inter-RAT resource management techniques. The time scale for the MLSM operation is longer compared to the LLSM but shorter compared to the HLSM. This will be of the order of few minutes. The failure of MLSM to address the spectrum needs of the user triggers the HLSM functionality.

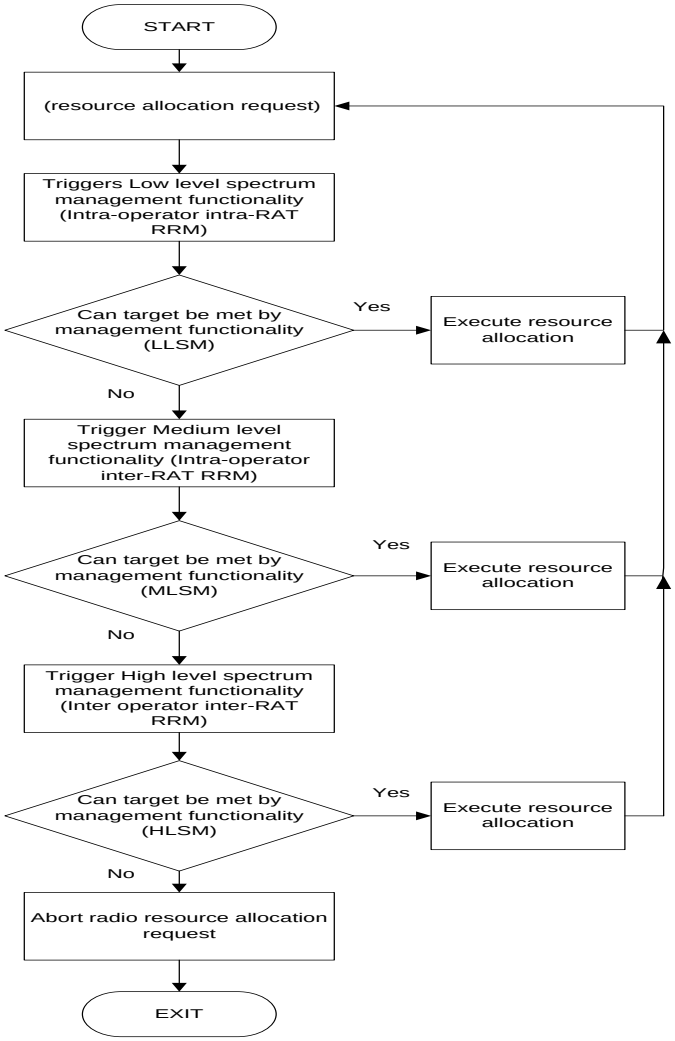


**FIGURE 4:** Flowchart description of the UMTS spectrum management framework

### 2.2 System Model

Consider the following model, in which two operators share the spectrum. The traffic profile of the two networks ($T_a$ and $T_b$) is as described in Fig. 2. Two cases have been identified. In the first case, whole carriers may be exchanged by the operator depending on their traffic and hence carrier requirement. In the second case, the users from one operator may be migrated to another operator's network based on pre-establishment agreement between the two operators. The second is more likely in the case of Wideband Code Division Multiple Access (WCDMA) system where the release of whole carrier is highly unlikely due to the wideband nature of CDMA.

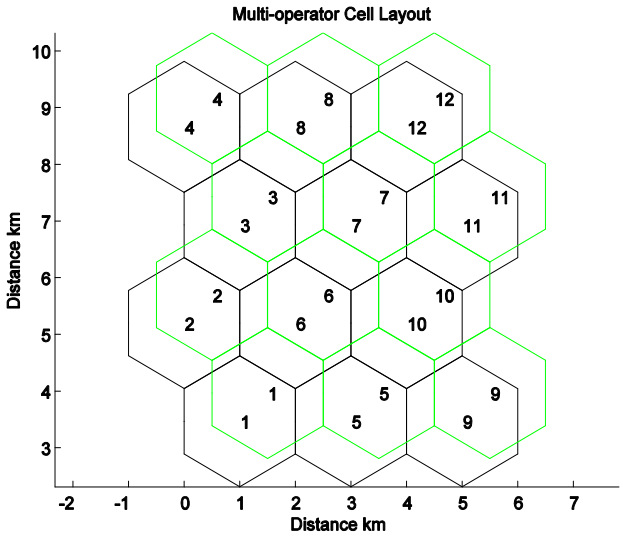


**FIGURE 5:** Cell deployment for two operators covering same geographic area with displaced BS

In the model, the operators are assumed to have the cell grid deployment shown in Fig. 5 with wraparound mobility to maintain constant user density. It is an important assumption that both operators cover the same geographical area and the cell radius is 1km. The displaced cell model means the impact of ACI needs to be taken into account. ACI primarily due to imperfection in transmit and receive filter characteristics, is modeled as a reduction in the network capacity [25]. Soft handover gain is modeled according to [26] [27]. Perfect power control is also assumed. Two traffic models are used in the simulation. The first is the uniform traffic case in which the average cell load in all the different cells is approximately the same. In the non-uniform traffic case, three hotspots cells with 10% higher call volume are included. According to [28], the same cell interference ($I_{sc}$) is given in (1) for mobiles in the same cell as;

$$\mathrm{I_{sc}} = (\mathrm{M}-1)\times \mathrm{S}\times \alpha_{\mathrm{r}} \qquad (1)$$

Where $S$ is the power of each mobile at the receiver, $\alpha_r$ is the average reverse link voice activity factor. The other cell interference ($I_{oc}$) is given in (2) as

$$\mathrm{I_{oc}} = (\mathrm{M}\times \alpha_{\mathrm{r}} \times \mathrm{S})\times \xi \qquad (2)$$

Where $\zeta$ is the reuse fraction given by;

$$\xi = \frac{\text{total other cell received power}}{\text{total same cell received power}} = \text{reuse fraction}$$

The UMTS capacity equation used in the simulation is given in [29-30] by (3)

$$M = 1 + \frac{1}{\alpha_r}\left(\frac{B_w}{R_b}\right)\left(\frac{N_o}{E_b}\right) \times \frac{1}{1+i} \qquad (3)$$

Where "*i*" is the ratio of other cell to own cell interference.

### 2.3 Algorithm Description

In the algorithm description, there is a primary and secondary operator. The primary operator (PO) is defined as the operator which has instantaneous spare capacity to support the secondary operator (SO) during a capacity crisis. The secondary operator suffers capacity problems and requires additional resources from another network for a given period of time. It is important to note that the process is dynamic in time (i.e op A and op B may interchangeably be PO or SO) based on traffic demand. In FSA, the operators maintain their carrier allocations and no spectrum sharing takes place. In Fig. 6, no further effort is made to admit dropped calls and the right hand side of the flow chart is ignored.

In DSA, the operators are able to support their user requests on another network. Furthermore, queuing is introduced to minimize inter-network signaling. The priority is to support the connection request of the users on its own network initially. If the users are unable to find a free channel, then the calls are queued for a short period of time (2 - 3 seconds) respectively. The connection request times due to queuing introduces increased spectrum efficiency gain at the expense of delays. This process termed "DSA with queuing" helps to minimize the inter-network signaling overhead involved in the process. This is because the user is initially queued on its home network before inter-network signaling occurs. A flow chart of the DSA algorithm is shown in Fig. 6.

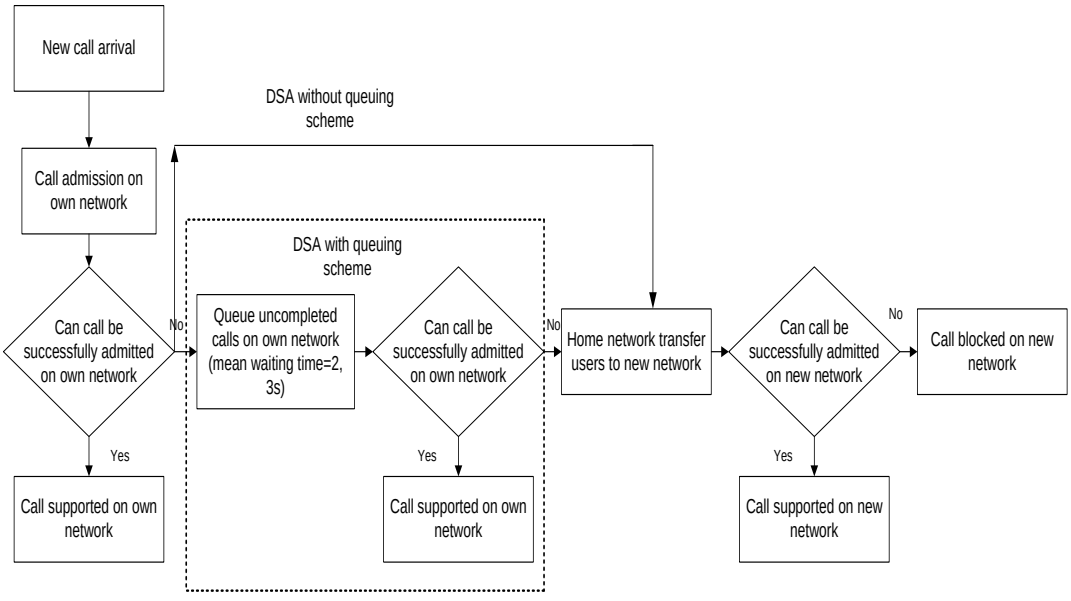


**FIGURE 6:** Flowchart of the FSA and DSA spectrum admission procedure

## 3. Call Setup Analysis

The process of establishing a call involves a number of procedures before the resource is assigned to the user equipment (UE). In this section the call setup involved in FSA and DSA is analyzed. Three cases have been identified.

### 3.1 FSA or Non-shared mode

This refers to the mode when no spectrum sharing occurs. Hence, users are only admitted in their home networks. In the FSA mode, the call setup phase includes the Radio Resource Connection (RRC) establishment, security handshake, radio bearer setup, alerting, connect acknowledge, etc. The recommended one way end to end delay for conversational voice service according to [33] is less than 150ms and the limit should be no more than 400ms. All call requests are assumed to be originated from the UE [31].

Neglecting practical constraints such as the actual radio channel condition, the estimate shown in [31] assumes the best case scenario. However, it has been shown in [25] that the typical delay budget is usually between 6-8 seconds under practical conditions. In [31], the UE is assumed to be in the idle mode initially. The reason for the different UE states (idle and connected) as defined in [25] is for terminal power efficiency and network resource maximization. The main components introducing delays in the FSA call setup is the RRC connection establishment and the radio bearer setup**.**

### 3.2 DSA Mode with shared RNC

In the shared Radio Network Controller (RNC) mode, the operators share the same RNC. An agent in the RNC proactively monitors the base station loading of the two operators. In this case, the delay budget will be similar to that described for FSA in [31]. Since the information is contained in the network, capacity can be served directly to the users without additional delays.

### 3.3 DSA Mode without shared RNC

In the non-shared RNC mode, additional delay is incurred in granting resources on the foreign network. It is an assumption that the Common Pilot Channel (CPICH) of both operators can be decoded by the terminal. The paper [34] has presented the call flow procedure for FSA and DSA. We further analyze the impact of queuing and call setup latency on the spectrum sharing gain in this work.

In addition to the modes mentioned above based on the infrastructure, the connection requests can be queued on the home network. This measure aims to reduce the connection signaling overhead associated with inter-network transfers. For the FSA mode, two main methods are identified. These are; the FSA with queuing, and FSA without queuing modes. In FSA with queuing the calls are queued but not transferred to the foreign network. In the FSA without queuing, calls are either blocked or dropped and no queuing is implemented.

Similarly for the DSA schemes, two modes are identified. These are; the DSA with queuing and the DSA without queuing modes. In the DSA with queuing, the calls are queued for 2-3 seconds respectively as shown in Fig. 7. After this period, the calls are transferred to the foreign network. In the DSA without queuing scheme, the connection requests that cannot be completed on the home network are transferred to the new operator without further queuing on the home network. The main focus of this work is on the DSA schemes and hence simulation results presented in section VI focus on the latter scenarios.

## 4 Simulation Results

A simulation tool described in [32] has been developed to evaluate the performance of the DSA algorithms. The main simulation parameters used in this work is shown in Table I. The call arrivals are modeled using the Poisson distribution, while the call holding times are exponentially distributed with a mean of 120 seconds.

| Parameters | Values |
|---|---|
| Service type | Speech traffic |
| Data rate | 12.2 Kbps |
| Call Duration | Mean = 120 seconds ( Exponential ) |
| $E_b/N_o$ | 7 dB |
| Adjacent Channel Interference | 2 % |
| Soft handover Gain | 3 dB |
| Cell radius | 1 Km |
| Voice Activity Factor | 0.67 |
| UMTS carrier bandwidth | 5 MHz |
| Chip rate | 3.84 MCps |
| Simulation borders | Wraparound mobility of MS at simulation borders |
| Propagation Model | Path loss model with 4$^{th}$ order power exponent |
| User distribution | Uniform and Non-Uniform (3 Hotspots ) |
| Frequency re-use factor | 1 |
| Handover | Based on geometric cell boundaries |
| Total Number of cells | 12 ( with interference modeling ) |
| Carrier distribution | Primary ( 3 carriers ), secondary ( 3 carrier) |
| Cell layout | Hexagonal with omni-directional antenna Deployment |
| Connection queuing times | 1 second, 2 seconds |

**Table I:** Simulation Parameters

To evaluate the spectrum efficiency gain, the FSA scenario when no spectrum sharing takes place is compared with the DSA scenario with and without queuing. The gain is measured in terms of the capacity improvement at 98 % Satisfaction Ratio (*SR*). The *SR* is defined in (4). This value is considered sufficient to give the desired level of Quality of Service *(QoS)* in an operator's network.

$$SR = 1 - (P_B - (10 \times P_D)) \qquad (4)$$

$P_B$ is the call blocking probability and $P_D$ is the call dropping probability. The dropped calls are given a higher weighting since there are less tolerable than blocked calls. The spectrum efficiency gain (Δη) is defined in (5) as

$$\Delta\eta = \frac{\text{Load}_{\text{DSA},98\%} - \text{Load}_{\text{FSA},98\%}}{\text{Load}_{\text{FSA},98\%}} \qquad (5)$$

$Load_{DSA,98\%}$ is the Users/Cell/Hour for DSA at 98% Satisfaction ratio, $Load_{FSA,98\%}$ is the Users/Cell/Hour for FSA at 98% Satisfaction ratio.

### 4.1 Dynamic spectrum sharing system level protocol performance and analysis

The simulation results are presented in this section. Fig. 7 and Fig. 8 show the FSA and DSA performance curves for network 1 and 2 respectively for the uniform traffic case. According to the figure, the satisfaction ratio decreases as the traffic offered (Mobile Subscribers/Cell/Hour) increases. Similarly, the results show that the DSA without queuing provides a least spectrum efficiency gain compared to the other two techniques. This is due to the fact that in the DSA scheme without queuing, no further measures are taken to account the call if the operator is unable to accommodate the call it is either blocked or dropped.

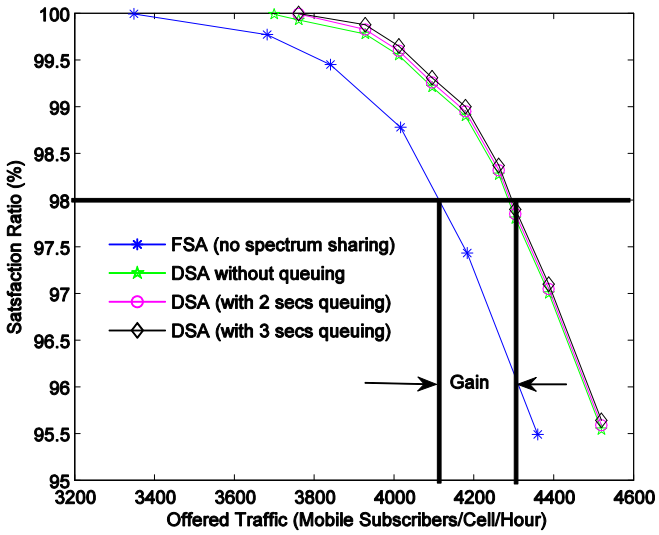


**FIGURE 7:** Performance comparison between FSA and DSA with and without queuing for network operator 1 (Uniform traffic).

Similarly, the results show that queuing improves the gain at low and medium load (offered traffic). It also shows that queuing is not effective at high load. This is because the probability of both operators being able to accommodate more users on their network during heavy traffic period is very low. Furthermore, the performance of DSA with 3 seconds queuing is slightly better than DSA with 2 seconds because further delays on home network results increases the probability of a service connection at low to medium load. In all the cases investigated, the call setup delay is transparent to the end user. The gain for the three schemes is 4.6 %, 4.3 % and 4.2 % respectively at 98 % satisfaction ratio on network 1. Similarly, the spectrum efficiency gain on network 2 is 4.1 %, 4.0 %, 3.9 %. These figures are obtained by substituting the values on the horizontal axis of Fig. 7 and Fig. 8 into (9).

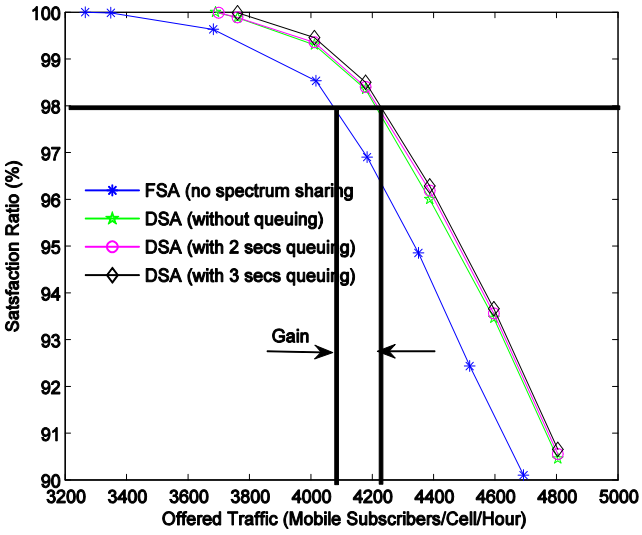


**FIGURE 8:** Performance comparison between FSA and DSA with and without queuing for network operator 2 (Uniform traffic)

Fig. 9 and Fig. 10 show the performance for FSA and DSA with and without queuing for the three schemes investigated in the non-uniform traffic case. Three (3) hotspots which represent areas of temporarily high traffic have been included in the simulation area. The trend in performance for the three schemes is similar to that discussed previously. However, the main difference is that the carriers in the non-uniform traffic case approaches saturation faster due to higher call volumes. It is important to note that the spectrum efficiency gain for all the three schemes is similar at 98% satisfaction ratio regardless of queuing. This fact is more visible at high load due to congestion. It is also observed that the performance of the DSA algorithm approaches that of FSA at high load due to the inclusion of the hotspot.

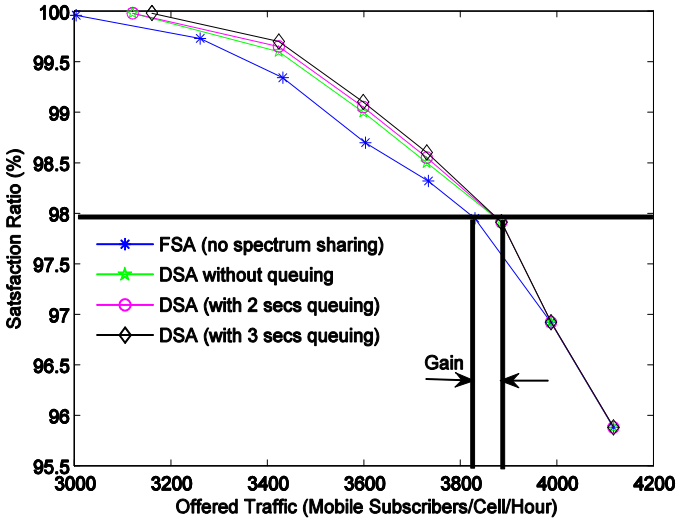


**FIGURE 9:** Performance comparison between FSA and DSA with and without queuing for network operator 1 (Non-Uniform traffic)

Based on the graphs plotted above for both scenarios, the spectrum efficiency gain for the non-uniform traffic scenario for the three DSA schemes for network 1 and 2 is 2.2 % and 2.0 % indicating a reduction in gain compared to first scenario. There is also no significant benefit due to queuing at 98 % SR.

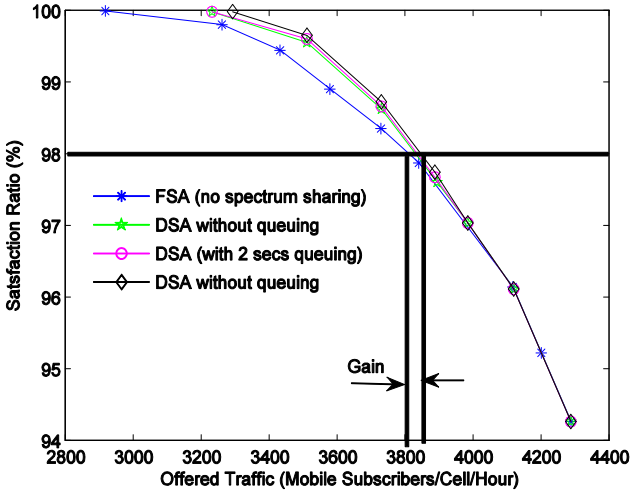


**Figure 10:** Performance comparison between FSA and DSA with and without queuing for network operator 2 (Non- Uniform traffic).

### 4.2 Call setup messages and latency

The detailed description of the call setup sequence is presented in [34]. Here we provide the simulation results in terms of total call setup messages for the two operators at a particular satisfaction ratio. According to Fig. 11 and Fig. 12, the total setup message for the non-uniform traffic (Fig. 12) case is generally higher than Uniform case (Fig. 11). A high number of subscribers results in a higher number of signaling messages. Similarly, it is shown that DSA results in a higher number of signaling messages compared to FSA for all the 3 schemes considered.

It is observed that DSA without queuing has the higher signaling messages since users are directly migrated to the foreign network without any attempt to support them on their home network. The other two schemes minimize the inter-network signaling by trying to support the calls on their home network. DSA with 2 seconds queuing performs better than DSA with 3 seconds queuing since it accommodates less subscribers compared to the latter.

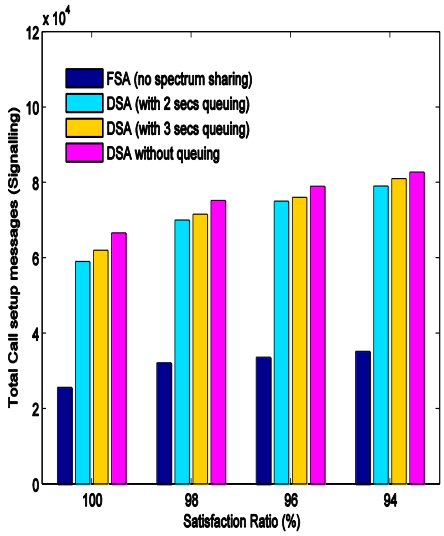


**Fig. 11a.** Total call setup messages versus SR for the DSA schemes (uniform traffic) network 1.

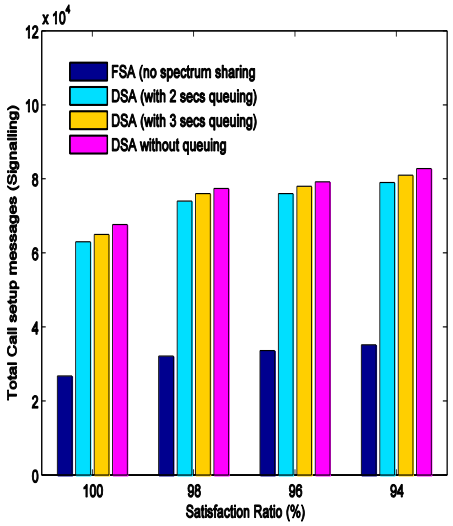


**Fig. 11b**. Total call setup messages versus SR for the DSA schemes (uniform traffic) network 2.

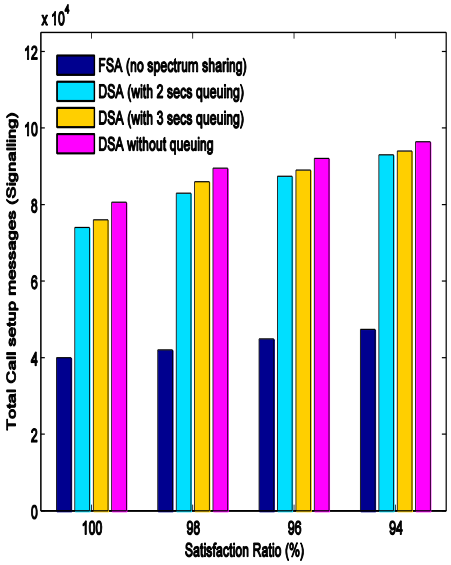


**Fig. 12a.** Total call setup messages versus SR for the DSA schemes (non-uniform traffic) network 1.

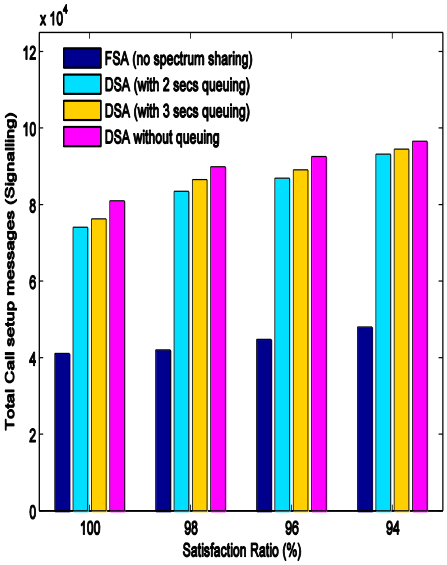


**Fig. 12b.** Total call setup messages versus SR for the DSA schemes (non-uniform traffic) network 2.

To adequately serve users, it is necessary to avoid long call setup delays [25]. Connection request delays should be transparent and imperceptible to the end user. The mean queuing times of 2-3 seconds chosen in the work is considered adequate to reflect these issues. The main implications are that operators will need to carefully weigh the trade-offs between not accommodating a subscriber and hence loss of revenue, to queuing of subscriber for short periods after which they can be served as soon as capacity becomes available. It is also important to note that additional latency is introduced due to spectrum sharing, so that the maximum tolerable delay need to be matched with the service requirements.

## 5 Conclusions and Future Work

This paper has presented a spectrum access framework for dynamic spectrum sharing between operators using the UMTS network as a case study. Three schemes to address UMTS spectrum sharing have been presented. The simulation results show that significant spectrum efficiency gain can be obtained in the low and medium traffic regions for the uniform and non-uniform cases. For the scenarios considered spectrum sharing gain above 4.0 % and 2.0 % was obtained for the uniform and non-uniform traffic at 98 % satisfaction ratio. The DSS gains are primarily due to the statistical multiplexing of call arrivals. The decrease in the gain in the latter scenario was due to the significantly higher call volumes associated with hotspots. The results also show that queuing does not significant improve the spectrum sharing gain under heavy traffic conditions.
The paper has also investigated the trade-off associated with spectrum sharing taking into account the call setup signaling and delay. It is important to note that DSA with queuing schemes provide a more practical approach to increase the gain while minimizing the inter-network signaling overhead. Furthermore, it was shown that the non-uniform traffic scenario presents challenges in terms of signaling for network operators in all the DSS cases. Future work will address operator networks with heterogeneous services and packet level simulations to determine if further gains are possible due to statistical multiplexing of packet transmission.

## ACKNOWLEDGEMENT

This work has been supported, in part, by the European ICT Project QoSMOS.

## REFERENCES

1. D. Willkomm, S. Machiraju, J. Bolot, A. Wolisz. "*Primary Users in Cellular Networks: A Large-scale Measurement study"*. In Proceedings of the 3rd IEEE Symposium on Dynamic Spectrum Access Networks. Chicago, IL, USA, 2008.
2. Shared spectrum company website, Available online: http://www.sharedspectrum.com/measurements/recent.html, [Accessed online December 2008
3. FCC 04-167, "Promoting efficient use of spectrum through elimination of barriers to the development of secondary markets," Jan. 2004.
4. Q. Zhao, B. M. Sadler. "*A Survey of Dynamic Spectrum Access*". IEEE Signal Processing Magazine, 24(3), pp. 79-89, 2007.
5. I. F. Akyildiz, W. Y. Lee, M. C. Vuran, S. Mohanty. *"A survey on spectrum management in cognitive radio networks (Cognitive radio and communication networks)".* IEEE Communications Magazine, 46: 40-48, 2008.
6. P. Leaves. *"Dynamic Spectrum Allocation between Cellular and Broadcast systems",* PhD Thesis, Dept. of Electronic Eng., University of Surrey, Guildford, United Kingdom, January 2004.
7. M. Buddhikot, K. Ryan. *"Spectrum Management in Coordinated Dynamic Spectrum Access Based Cellular Networks".* In Proceedings of the IEEE Symposium on Dynamic Spectrum Access Networks ( DySPAN 05), Baltimore, MD, USA.
8. S. Haykin. *"Cognitive radio: brain-empowered wireless communications".* IEEE Journal of Selected Areas in Communication, 23, pp. 201-220, 2005.
9. G. Salami, O. Durowoju, A. Attar, O. Holland, H. Aghvami, R. Tafazolli. *"A Comparison between the centralized and distributed approaches for spectrum management".* Accepted in IEEE Communications Surveys and Tutorial, Second quarter 2011.
10. A. Attar, S. A. Ghorashi, M. Sooriyabandara, A. H. Aghvami. "Challenges of Real-Time Secondary Usage of Spectrum". *Journal of Computer Networks (Elsevier)*, Special Issue on Cognitive Wireless Networks, 52(4), pp. 816-830, 2008.
11. A. Attar, A. H. Aghvami. "*A Framework for Unified Spectrum Management (USM) in Heterogeneous Wireless Networks"*. IEEE Communications Magazine, 45, pp.44-51, 2007.

12. L. Berlemann, S. Mangold, G.R. Hiertz, B. Walke. *"Policy Defined Spectrum Sharing and medium Access for Cognitive Radios".* Journal of Communication (Academy Publisher), 1, pp. 1-12, 2006.
13. DARPA XG Program Website, Available online: http://www.darpa.mil/ATO/programs/XG/index.htm , [Accessed online: 5th March 2009].
14. I. Katzela, M. Naghshineh. Channel assignment schemes for cellular mobile telecommunication systems: a comprehensive survey. *IEE Personal Communications*, 3, pp. 10-31, 1996.
15. IST DRiVE Project Website, Available online: http://www.ist-drive.org/index2.html , [Accessed online: 18th May 2007].
16. IST Over-DRiVE Project Website, Available online: http://www.comnets.rwth-aachen.de/~o_drive/ [Accessed online: 16th May 2007.
17. D. Thilakawardana, K. Moessner, R. Tafazolli. *"Darwinian approach for dynamic spectrum allocation in next generation systems"*, IET Journal of Communication, 2, pp. 827-836, 2008.
18. IST FP6 E2R2 Project Website, Available online: http://e2r2.motlabs.com/ [Accessed online: 15th February 2009].
19. IST FP7 End to End Efficiency Project Website, Available online: https://ict-e3.eu/project/, [Accessed online: 30th January 2009].
20. IEEE Symposium on New Frontiers in Dynamic Spectrum Access Networks, Available online: http://www.ieee-dyspan.org/2008/, [Accessed online: 30th March 2009].
21. Third International Conference on Cognitive radio Oriented Wireless Networks and Communication, Available: http://www.crowncom.org/2008/, [Accessed online: 31st March 2009.
22. G. Salami, R. Tafazolli. *"On the Performance evaluation of spectrum sharing algorithms between two UMTS operators".* In Proceeding of IEEE International Conference on Telecommunications (ICT), Marrakech, Morocco, 2009.
23. J. M. Peha. Approaches to spectrum sharing. *IEEE Communication Magazine*, 43, pp. 10-12, 2005.
24. J. Guo, F. Liu, Z. Zhu. *"Estimate the Call Duration Parameters in GSM System Based on K-L Divergence Method".* In Proceeding of the International Conference on Wireless Communications, Networking and Mobile Computing, *WiCom*, pp. 2988-2991, 2007.
25. H. Holma, A. Toskala. "*WCDMA for UMTS-HSPA Evolution and LTE"*, Fourth Edition, John Wiley & Sons, 2007.
26. S,-P. Chung, M.T. Li. *"Performance Evaluation of Hierarchical Cellular CDMA networks With Soft Handoff Queuing",* IEEE Trans. Vehicular Technology, 54(2), pp. 652-672, 2005.
27. W. H. Tranter, K. S. Shanmugan, T. S. Rappaport, K. L. Kosbar. *"Principles of Communication Systems Simulation with Wireless Applications"*, Pearson Education, 2004.
28. J. S. Lee, L. E. Miller. *"CDMA Systems Engineering Handbook*". Artech House Publishers, pp. 1013-1017(1998).
29. A. M. Viterbi, A. J. Viterbi. Erlang Capacity of a Power controlled CDMA System. *IEEE Journal on Selected Areas in Communications*, 11, pp. 892-900, 1993.
30. K. I. Kim. "CDMA Cellular Engineering Issues". *IEEE Transaction on Vehicular Technology*, 42(3), pp. 345-350, 1993.
31. Third Generation Partnership Project, Technical Specification Group RAN; TR 25.815 v7.0.0, Signaling enhancements for Circuit-Switched (CS) and Packet-Switched (PS) Connections (Release 7), Sept. 2006.
32. G. Salami, A. Quddus, D. Thilakawardana, R. Tafazolli. *"Non-pool based spectrum sharing for two UMTS operators in the UMTS extension Band"*, *In Proceedings of 19th IEEE International Symposium on Personal Indoor and Mobile Radio Communications (PIMRC)*, pp. 1-5, 2008.
33. Third Generation Partnership Project, Technical Specification 25.853. Delay Budget within the Access Stratum, 2003.
34. G. Salami, S. Thilakawardana, R. Tafazolli. *"Dynamic Spectrum sharing between two UMTS operators in the UMTS Extension Band".* In Proceedings of the IEEE International Conference on Communication Workshops, Dresden, Germany, 2009.

# Performance of Modeling wireless networks in realistic environment

**Mohammad Siraj** siraj@ksu.edu.sa
*Department of Computer Engineering*
*College of Computer and Information Sciences)*
*Riyadh-11543,SA*

**Soumen Kanrar** soumen_kanrar@yahoo.co.in
*Department of Computer Engineering*
*College of Computer and Information Sciences)*
*Riyadh-11543,SA*

**Abstract:**

A wireless network is realized by mobile devices which communicate over radio channels. Since, experiments of real life problem with real devices are very difficult, simulation is used very often. Among many other important properties that have to be defined for simulative experiments, the mobility model and the radio propagation model have to be selected carefully. Both have strong impact on the performance of mobile wireless networks, e.g., the performance of routing protocols varies with these models. There are many mobility and radio propagation models proposed in literature. Each of them was developed with different objectives and is not suited for every physical scenario. The radio propagation models used in common wireless network simulators, in general researcher consider simple radio propagation models and neglect obstacles in the propagation environment. In this paper, we study the performance of wireless networks simulation by consider different Radio propagation models with considering obstacles in the propagation environment. In this paper we analyzed the performance of wireless networks by OPNET Modeler .In this paper we quantify the parameters such as throughput, packet received attenuation.

**Keywords:** Throughput, attenuation, opnet, radio propagation model, packet, Simulation**.**

## 1. Introduction:

Wireless communication technologies are undergoing very rapid advancements. In the past few years researcher have experienced a steep growth in the area of wireless networks in wireless domain. The attractiveness of wireless networks, in general, is attributed to their characteristics/features such as ability for infrastructure-less setup, minimal or no reliance on network planning and the ability of the nodes to self-organize and self-configure without the involvement of a centralized network manager, router, access point or a switch. These features help to set up a network fast in situations where there is no existing network setup or in times when setting up a fixed infrastructure network is considered infeasible, for example, in times of emergency or during relief operations. Even though wireless networks have emerged to be attractive and they hold great promises for our future, there are several challenges that need to be addressed. Some of the well-known challenges are attributed to issues relating to scalability, quality-of-service, energy efficiency and security. Currently the field of wirelesses communication systems is one of the fastest growing segments of the communications industry. Wireless communication systems, such as cellular, cordless and satellite phones as well as wireless networks have found widespread use and have become an essential tool in everyday life both professional and personal. Radio channels are more complicated to model than wired channels. Their characteristics may change rapidly and

randomly and they are dependent on their surroundings. The radio propagation models used in common wireless networks simulator is a free line of sight communication between the different devices assuming obstacle free area. As a result this range is nothing but a circle assuming that the devices residing within this circle receive the transmitted frames without errors. It is assumed that radio signals are completely blocked by obstacles. This approach poorly reflects radio wave propagation in a typical outdoor scenario, like a city center in which buildings significantly affect communication between nodes. Most of the publications investigating wireless networks behavior consider simple models. There exists a lot of work using NS2 but very few in OPNET platform [6] . A limitation in NS2 regarding two ray ground is that sender and receiver have to be in the same height [2,3,4,5]. The earlier work was carried out in open space with random mobility and idealized signal propagation model. In modeling authors investigate the behavior by randomly placing building environments. Secondly a scenario consists of several zones. Zones are either movement zones or obstacles[2,3,4]. Such environments are modeled not accurately. In this paper we have used CADRG/CIB (Compressed Arc Digitized Raster Graphics / Controlled Image Base) maps and terrain modeling module to achieve the realistic results by creating parameters sets of frequently used combinations of parameter values such as open terrain in dry weather, open terrain in rainy season and terrain with heavy vegetation by varying surface refractivity, relative permittivity, ground conductivity and resolution**.** Using opnet TMM (Terrain modeling module) we have simulated the radio signals being distributed over the varying terrain and observed the changes in signal strength. The signal strength is observed as the receiver moves over pre-defined path that goes through many elevation changes. TMM enhances the accuracy of the result by taking into account signal loss due to the effect of the terrain. Incorporating TMM we can determine whether the sender will be able to communicate with the receiver due to the terrain. It gives more accurate Propagation loss, signal strength and noise results.

In this paper we have shown the performance of wireless networks by integrating realistic models. We also observed how the models affect the output (i.e. Simulation results). In this paper we use OPNET Modeler 14.5. Here we integrate more realistic radio propagation models. Besides the model itself, we consider the geography data of the simulation area. In our case we have taken it from digital map vendors. The ionosphere affects radio signals in different ways depending on their frequencies (Figure 1), which range from extremely low (ELF) to extremely high (EHF). On frequencies below about 30 MHz the ionosphere may act as an efficient reflector, allowing radio communication to distances of many thousands of kilometers. Radio signals on frequencies above 30 MHz usually penetrate the ionosphere and, therefore are useful for ground-to-space communications. The ionosphere occasionally becomes disturbed as it reacts to certain types of solar activity. Solar flares are an example; these disturbances can affect radio communication in all latitudes. Frequencies between 2 MHz and 30 MHz are adversely affected by increased absorption, whereas on higher frequencies (e.g., 30–100 MHz) unexpected radio reflections can result in radio interference. Scattering of radio power by ionospheric irregularities produces fluctuating signals (scintillation), and propagation may take unexpected paths. TV and FM (on VHF) radio stations are affected little by solar activity, whereas HF ground-to-air, ship-to-shore, Voice of America, Radio Free Europe, and amateur radio are affected frequently. Figure 2 illustrates various ionospheric radio wave propagation effects.

Some satellite systems, which employ linear polarization on frequencies up to 1 GHz, are affected by Faraday rotation of the plane of polarization.

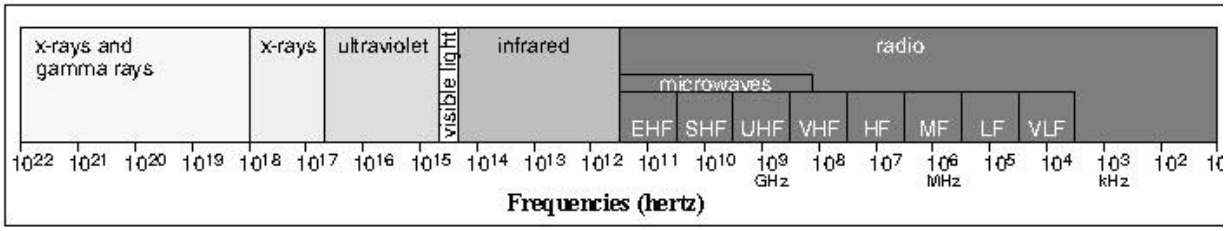


**Figure 1** : The Electromagnatic Spectrum

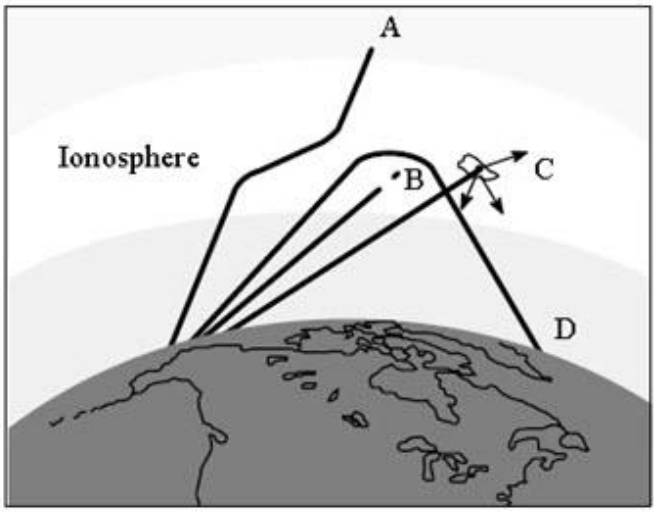


A. *Wave penetrates the ionospheric layer.*
B. *Wave is absorbed by the layer.*
C. *Wave is scattered in random directions by irregularities in the layer.*
D. *Wave is reflected normally by the layer.*

**Figure 2**: Radio Waves In Ionosphere

## 2 Preliminaries

**Free Space Model:** The Free Space model represents by equation (1) a signal propagating through open space, with no environmental effects. It has one parameter, called "lineofsight". With this parameter off, terrain has no effect on propagation. With it on, the model uses terrain data solely to determine if a line-of-sight (LOS) exists between the transmitting and receiving antennas. If there is no LOS, the signal is blocked entirely and no communication takes place.

$$\mathrm{P}_r = \frac{P_t G_t G_r \lambda^2}{(4\pi)^2 d^2 L} \quad \text{---------- (1)}$$

Where $P_r$ the received signal is power (in Watt), $P_t$ is the transmitted signal power, $G_r$ and $G_t$ are the gains of the receiving and the transmitting antennas respectively. $\lambda$ is the wave length , L is the system loss, and d is the distance between the transmitter and the receiver. According to [8], a single direct path between the communicating partners exists seldom at larger distances

**Two Ray Ground Model:** The two ground model equation (2) assumes that the received energy is the sum of the direct line of sight path and the path including one reflection on the ground between the sender and the receiver. The received power becomes independent of the frequency of the transmitted signal but depends on the height of the transmitter $h_t$ and the receiver $h_r$ , $G_r$ and $G_t$ are the gains of the receiving and the transmitting antennas respectively, d is the distance between the transmitter and the receiver.

$$\mathrm{P}_r = \frac{P_t G_t G_r h_t h_r}{d^4} \quad \text{---------- (2)}$$

### 2.1 Total Path loss:

The total path loss $L_t$ in db is defined as

$$L_t = L_o + L_l + L_{md} + L_r \quad \text{---------- (3)}$$

$L_o$ , $L_l$ and $L_{md}$ are the losses due to free space propagation, local screen ( building) in the vicinity of the mobile node and multiple diffractions caused by the building respectively. $L_r$ is the loss caused by the reflection of the diffracted electric fields from the walls of the building next to mobile.

### 2.2 Line of sight (Los) propagation model:

When the mobile node is located in the vehicle over the flat terrain, Los propagation using 2-ray model .The received power can be expressed as-

$$\frac{P_r}{P_t} = \left\{ \frac{\lambda}{4\pi} \right\}^2 \frac{1}{r_1} \exp(-jkr_1) + R \frac{1}{r_2} \exp(-jkr_2)^2 \text{ ---------- (4)}$$

Where $P_t$ and $P_r$ denote the base station or transmitter power and power received by the receiver mobile node. R is the reflection coefficient and $r_1$ , $r_2$ represents the path length of the direct ray and the path length due to ground reflected ray, k is constant.

### 2.3 Troposcatter loss model:

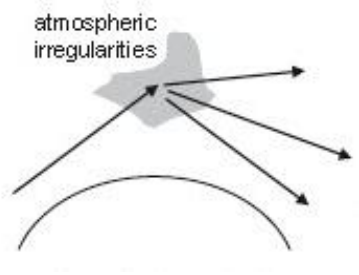


**Figure 3:** Troposphere Scattering

Air is not uniform, there are eddies, thermals, turbulence etc. where the air has slightly different pressure and hence a different refractive index. Scattering from refractive index irregularities in the high atmosphere (the troposphere) with sufficiently directive antennas and high transmitter powers is called *troposcattering* shown by figure-3

The median loss is given by
L = M + 30log(f) + 10log(d) + 30log(θ) + LN+ LC - Gt – Gr ----------(5)
This is an empirical model, with M is typically 19-40 dB depending on climate.
Where θ is the scatter angle (milliradians), LN is the height of the common volume, LC is the aperture-medium coupling loss and Gt , Gr are the gains of the antennas.

### 2.4 Diffraction loss:

If the direct line –of-sight is obstructed by a single knife-edge type of obstacle, with height $h_m$ via –figure Where $T_x$ and $R_x$ are the transmitter and receiver at the points B and C. |BE| = $d_T$ ,

|CE|= $d_R$ , |DE|= $h_m$

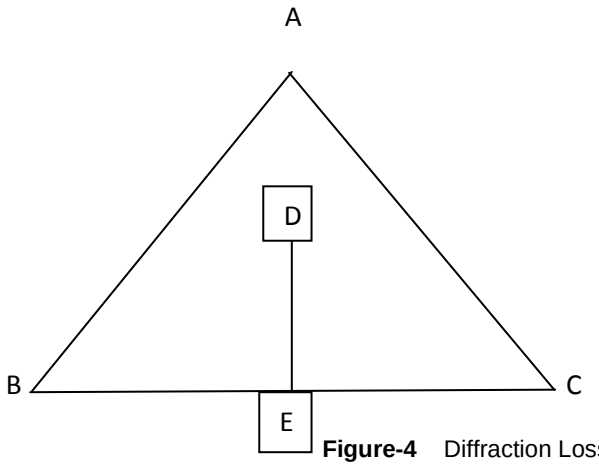


**Figure-4** Diffraction Loss

diffraction parameter $v$ can be expressed as,

$$v = h_m \left\{ \frac{2}{\lambda} \sqrt{\left(\frac{1}{d_T} + \frac{1}{d_R}\right)} \right\} \quad \text{----------(6)}$$

The diffraction loss additional to free space loss and express in dB can be closely approximated by

$A_D = 0$ if $v < 0$

$A_D = 6 + 9v + 1.27v^2$ if $0 < v < 2.4$

$A_D = 13 + 20 \log v$ if $v > 2.4$

The attenuation over rounded obstacles higher than $A_D$ in the above formula

### 2.5 Rician Fading Model :

Rician fading is a stochastic model for radio propagation anomaly caused by partial cancellation of a radio signal by itself. The signal arrives at the receiver by two different paths( hence exhibiting multipath interference), and at least one of the paths is changing( lengthening or shortening). Rician fading occurs when one of the paths, typically a line of sight signal is much stronger than the others. In Rician fading ( via fig -3)a strong dominant component is present. Similar to the case of Rayleigh fading, the in-phase and quadrature phase component of the received signal are i.i.d. jointly Gaussian random variables. However, in Rician fading the mean value of (at least) one component is non-zero due to a deterministic strong wave.

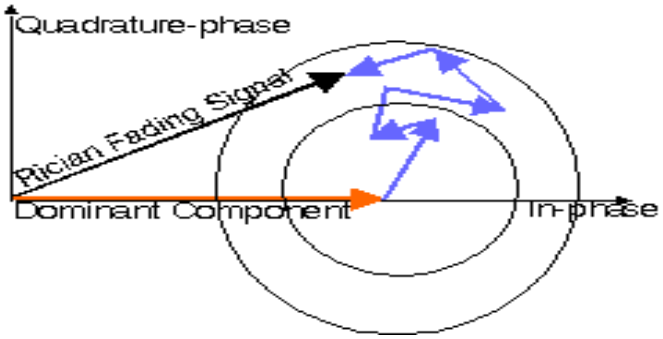


**Figure 3**: Rician Fading Model

The amplitude gain at the receiver is characterized by a Rician distribution.

The Rician amplitude r with parameter K can be defined as

$$r = \sqrt{(\sigma x_1 + A)^2 + \sigma x_2^2} \quad \text{---------- (7)}$$

Where $x_1$ and $x_2$ are quadrature components and $A^2/(2\sigma^2) \cong K$, $\sigma x_i$ is a random variable with variance $\sigma^2$. The mean-squared value of the Rician distribution is given by

$$A^2 + 2\sigma^2 = 2\sigma^2(K+1) \quad \text{---------- (8)}$$

and we get the normalized power envelop from (7) and (8) is

$$\frac{r^2}{P} = \frac{1}{2(K+1)}\left[(x_1 + \sqrt{2K})^2 + x_2^2\right] \quad \text{----------(9)}$$

Where P is the large scale model expression for the power in the dominant path. This power envelop can be used to modulate the output of a large scale propagation model. The above description assumes that the mean squared value of the envelop is the power predicted by the large scale model. Specifically, in the Rician model, this power contains the power in the dominant path and the multipath power. With certain propagation models, it may be more appropriate for the large scale power calculation to represent only the value in the dominant path. In the equation (7) after divided by the factor $A^2 = 2\sigma^2 K$. The normalized power envelop then takes the form

$$\frac{r^2}{P} = \frac{1}{2K}\left[(x_1 + \sqrt{2K})^2 + x_2^2\right] \quad \text{----------(10)}$$

Where P is the large scale model expression for the power in the dominant path.

### 2.6 Longley Rice Model :

The Longley-Rice model predicts long-term median transmission loss over irregular terrain relative to free-space transmission loss. The model was designed for frequencies between 20 MHz and 40 GHz and for path lengths between 1 km and 2000 km. This model considers environmental condition along the signal path. Here we can create parameters sets to hold frequently used combination of parameters values such as .

| | Relative Permittivity | Conductivity (Siemens per meter) |
|---|---|---|
| Average ground | 15 | 0.005 |
| Poor ground | 4 | 0.001 |
| Good ground | 25 | 0.020 |
| Fresh water | 81 | 0.010 |
| Sea water | 81 | 5.000 |

**TABLE 1** : Longley Rice Parameters

**2.7 TIREM :**

The Terrain-Integrated Rough Earth Model is a computer software library that calculates basic median propagation loss(path loss) of radio wave over irregular earth terrain. The method was develop revived improved and evolved into a TIREM software version for use by the Department of Defense (DoD). The TIREM used for radio frequencies in the range of 1 through 20,000 MHz over terrain elevations which are specified by a set of discrete points between the great circle path of the transmitting antenna and receiving antenna. The earth terrain information can be provided by the digital terrain elevation data(DTED). TIREM provides more accuracy in the radio propagation model than the FSPL model by taking into account the transmitting medium (surface refractivity and humidity), antenna properties (height, frequency, and polarization), conductivity, and terrain elevations). The calculation of path loss is also determined by effects of free space spreading, reflection, surface wave propagation, diffraction, tropospheric scatter propagation, and atmospheric absorption but not ducting phenomena, fading, ionospheric effect, or absorption due to rain or foliage.

| Variable | Description | Valid Range |
|---|---|---|
| CONDUC | Conductivity of earth surface | 0.00001 to 100 S/m |
| EXTNSN | Profile indicator flag :<br>.TRUE –profile is an extension of the last path along a radial<br>.FALSE -new profile | .TRUE or .FALSE |
| HPRFL | Array of profile terrain heights above mean sea level. | -450 to 9000 m |
| HUMID | Surface humidity at the transmitter site | 0 to 50 $g/m^3$ |
| NPRFL | Total number of profile points for the entire path | $\geq 3$ |

| | | |
|---|---|---|
| PERMIT | Relative Permittivity | 1 to 100 |
| POLARZ | Transmitter antenna polarization : 'V' –Vertical 'H'-Horizontal | 'V' or 'H' |
| PROPFQ | Transmitter frequency | 1 to 20000MHz |
| RANTHT | Receiver structural antenna height | >0 to 30000m |
| REFRAC | Surface refractivity | 200 to 450 N-units |
| TANTHT | Transmitter structural antenna height | >0 to 30000 m |
| XPRFL | Array of great-circle distance from the beginning of the profile<br>Point to each profile point | $\geq$ 0 m |

**TABLE 2:** TIREM Parameters Ranges

To develop the Algorithm for the TIREM we consider the equations (3) ,(4),(5) and (6)

---

**Algorithm for the TIREM**

Step-1 : Input the parameters from the set of parameters

Step-2: Extract the key parameters

Step-3: If (line of sight) == True

Step-4: compute line of sight loss

Step-5: go to step- 10

Step-6: If (line of sight) == False

Step-7: compute diffraction loss

Step -8: compute Troposcatter loss

Step-9: combine diffraction loss and Troposcatter loss

Step-10: compute mode and total path loss

Step-11: output

---

## 3. Simulation Model:

OPNET used to build the simulation model. All the operations are done by using OPNET kernel procedures. This is Baseline simulation. Till now we had been using default radio pipeline of OPNET figure - 4. The radio pipeline stages model the flow of data from a transmitter to a receiver. There are stages like transmission delay pipeline stage, SNR stage, BER stage etc. To realize the Rician fading stage 7 (receiver power ) of the Radio Pipeline stage *figure-4* has been modified. This stage uses by default free space propagation model. The purpose of this stage is to compute the receive power of the arriving packet's signal (watts). For packets that are classified is valid, the received power result is the key factor in determining the ability of the receiver to correctly to capture the information in the packets .Packets are classified as valid , invalid , or ignored by the stage -3 via-figure-4. In general, the calculation of received power is based on factors such as the power of the transmitter , the distances separating the transmitter and the receiver , the transmission frequency ,and transmitter and receiver antenna gain. The simulation kernel requires that the received power stage procedure accept a packet address as its sole argument. The antenna pattern and the power parameters have been defined at the runtime of the simulation.

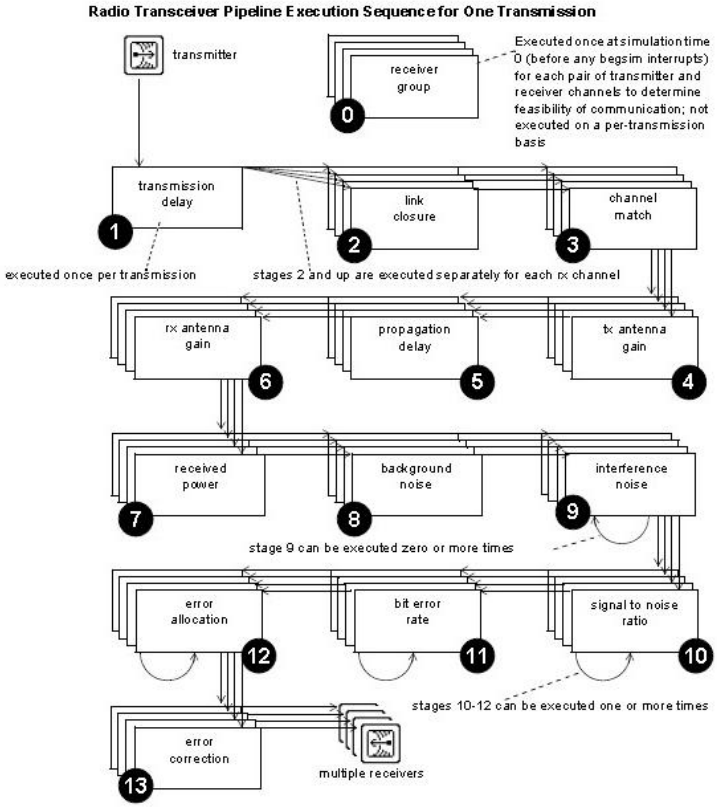


**FIGURE 4:** Radio Pipeline Stages

So for realizing the Rician fading we used the Rician Fading Power Module as via figure 4.

### 3.1 Node model

**3.1.1 Transmitter :** The transmitter composed of three modules via figure -5

1) Simple source i.e. packet generator.
2) Radio transmitter module. This module transmits the packets to the antenna at 1024 bits/sec using 100 percent of its channel bandwidth .

3) Antenna module. This module transmits signals.

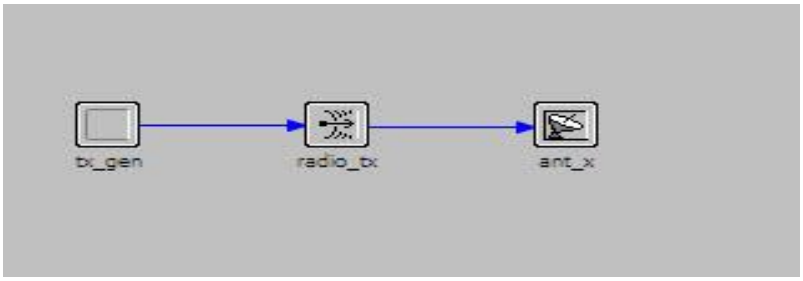


**FIGURE – 5** Transmitter

Fig: 6 represent Transmitter ($T_x$) Node Model .The parameters which are shown below in the table -2 have been used for Transmitter which is shown in figure – 6

| | |
|---|---|
| Packet Format | None |
| Packet Inter arrival Time | constant1.0 |
| Packet Size | Constant 1024 |
| Start Time | 10 |

**TABLE -3** : Simulation parameters for Transmitter

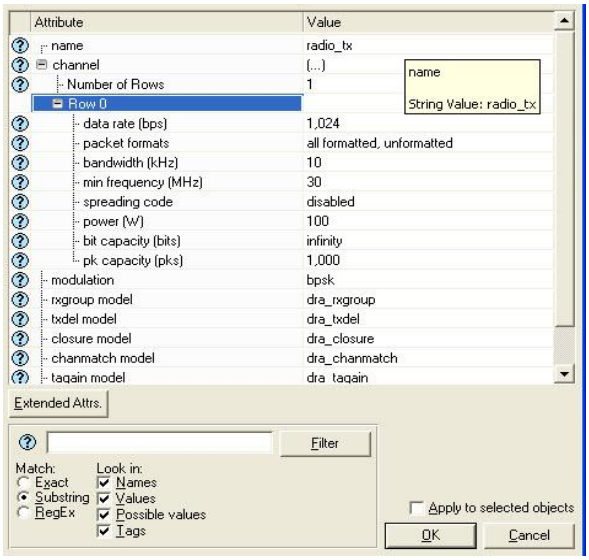

**FIGURE 6:** Transmitter $T_x$ attributes

This $T_x$ module is used for the all propagation models .

### 3.1.2 Receiver:

The receiver composed of three modules via figure- 7

1) Antenna module.
2) Radio receiver module: The radio receiver module consider several properties for each arrival of packets to determine ,if the packet's average bit error rate (BER) is less than a specified threshold . If the BER is low enough the packet is sent to the sink and destroyed. This module defines the gain which will be adjusted at run time.
3) Sink processor module: This module store the received packets.
4) Processor module ( $R_x$ ) which calculates the information that the antenna needs to point at a target : latitude , longitude and altitude coordinates the processor makes this calculation by using a kernel procedure that convert a node position in a subnet ( described by the X and Y position attributes) into the global coordinates that the antenna required .

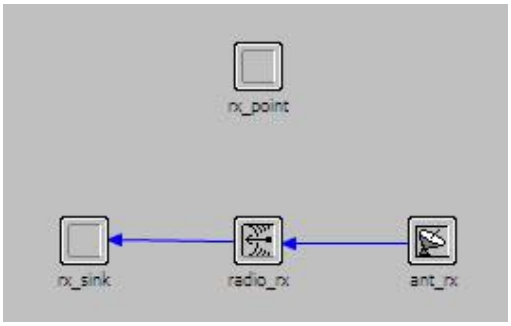


**FIGURE 7:** Receiver Antenna

The parameters which are shown below in the table - 2 have been used for the Receiver $R_x$ for Free Space Model, Hata Large City, Longley Rice and Risen Model

| Network Scale | Enterprise |
|---|---|
| Size | 8 X 5 Km |
| Packet Interarrival Time | Constant 1.0 |
| Packet Size | Constant 1024 |
| Start Time | 10 |
| Data rate(bps) | 1,000,000 |
| Bandwidth(KHz) | 20,000 |
| Minimum Frequency(MHz) | 905 |
| Spreading Code | Disabled |
| Modulation | bpsk |
| Power | promoted |

**TABLE 2:** Simulation Parameters For Receiver

Figure-8 is the $R_x$ attributes used in for Free Space Model, Hata Large City and Longley Rice models

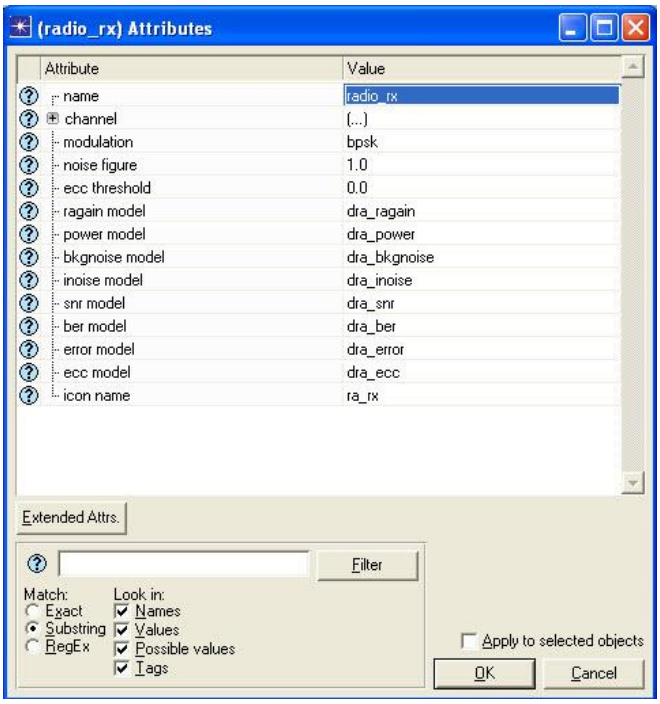


**Figure 8:** $R_x$ Attributes

Figure-9 is the $R_x$ attributes used in Rician models **.**The parameters which are shown below in the table - 3 have been used for the Receiver $R_x$ for Rician Model

| **Attribute** | **Value for Rx** |
|---|---|
| Altitude | 0.003 |
| Radio .rx Max Velocity | 1.0 |
| Radio rx Table Offset | 0 |
| Radio_ rx. Rician K Factor | 0.5 |
| Radio _rx .Use Two Ray | 1 |

**TABLE 3:** Simulation Parameters For Risen Propagation Model

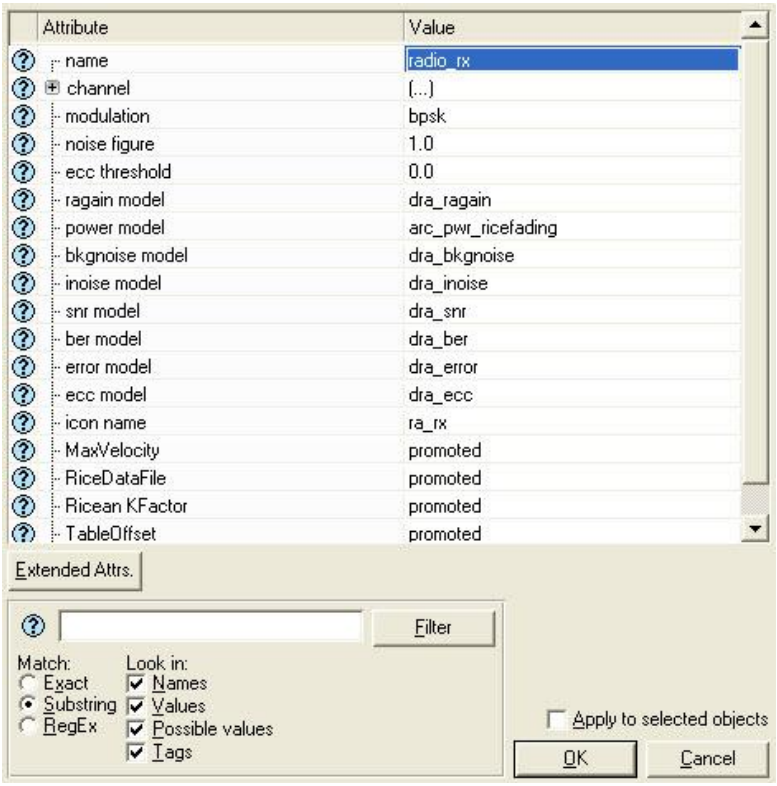


**FIGURE 9:** Attributes For Rician Propagation Model

## 4. Results and Discussion:

The following graphs via fig -10.1, 10.2, and 10.3 represents the Attenuation vs Distance. The graph are corresponding to the different propagation models free space ,Longley Rice model and TIREM model respectively. The transmitter and receiver are vertically polarized at the height of 25m (fig-10.1). We see further that the receiver, from the transmitter attenuation increases. From the fig-10.1 we observe the free space model shows linearity between the distance and the attenuation. Since the Longley Rice and TIREM takes terrain effect into consideration attenuation is much higher and realistic.

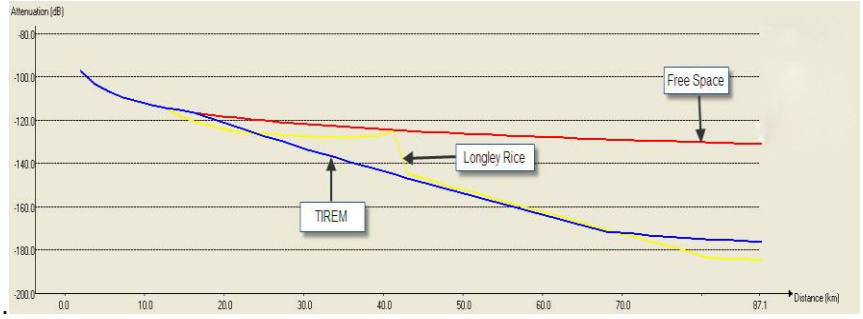


**FIGURE -10.1** Free space (Attenuation Vs Distance)

Antenna Height – 25 M

In the fig-10.2 and 10.3 the transmitter antenna height was raised to 75m and 100m respectively. By raising the height shows a consideriable change in signal strength .The attenuation in Longley Rice model is almost same as the free space model till 60Km (approx) after which it start separating and is same as TIREM model. So we see an elevation change affects signal strength.

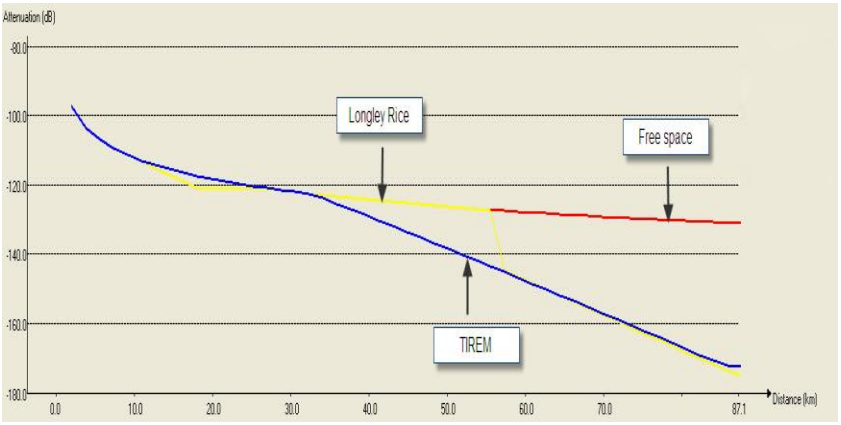


**FIGURE-10.2** Longley Rice (Attenuation Vs Distance)

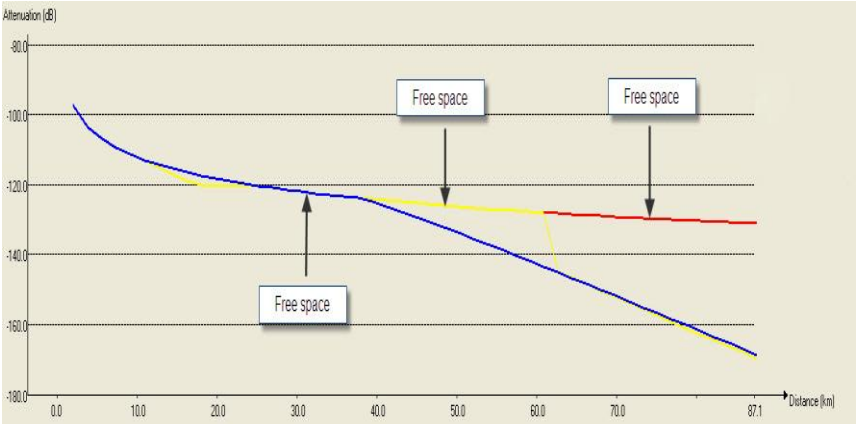


**FIGURE-10.3** TIREM (Attenuation Vs Distance)

Figure -11 shows the traffic received at the receiver end .We observe diferent types of graph depending on the propogation model used.In the free space we notice not much change in the packet received. This is because that model assumes ideal propogation enveriomeent. The other two models (Longley Rice and TIREM models) are realstic model so we see changes in the graph. We observe packets get drop because of lower height of transmitter antenna.

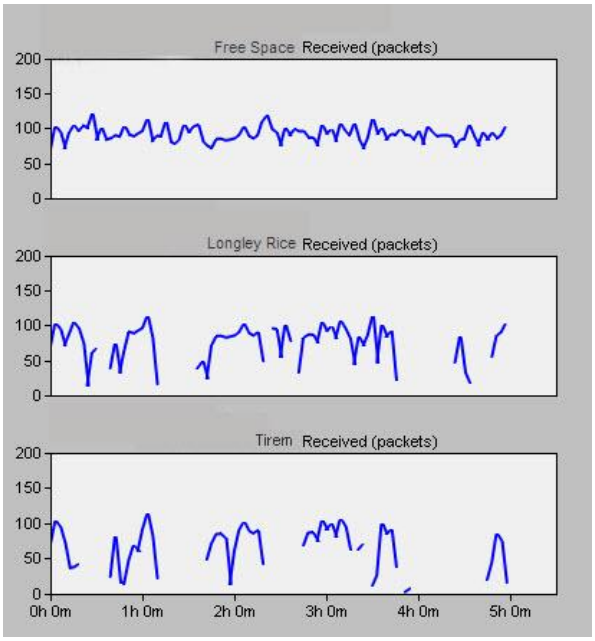


**FIGURE -11** Packet Received

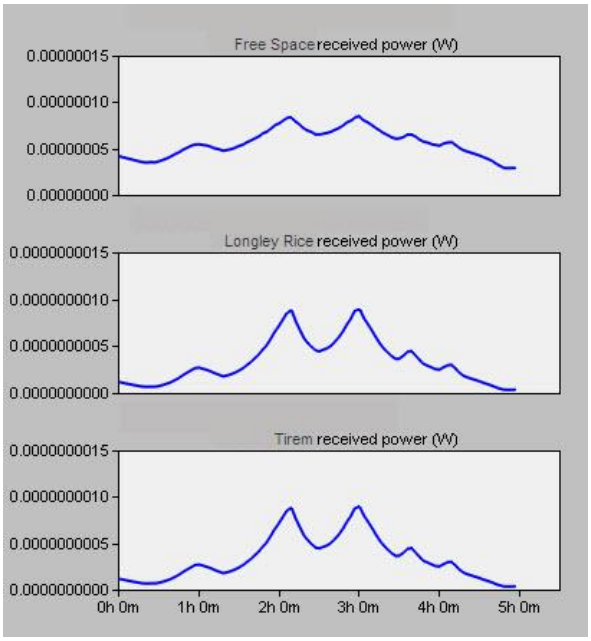


**Figure 12:** Received Power

The received power is only dependent on the transmitted power, the antenna's gain and on the distance between the sender and the receiver. It accounts manly for the facts that a radio signal which moves away from the sender has to cover in large area.So the received power decreasese with the square of the distance. Since the free sapce propogation model assume the ideal propogation condtion that there is only one clear line –of-sight path between the transmitter and the receiver the graph for the free space does not show much variation (Fig-12). In free space, the power radiated by an ***isotropic antenna*** is spread uniformly and without loss over the surface of a sphere surrounding the antenna. There is a considerable change in the received power for Longlay Rice and The TIREM

models as it takes in to account the system loss (Fig-12). The path loss and the statistical characteristics of the received signal envelope are the most inportant for the coverage planing application.

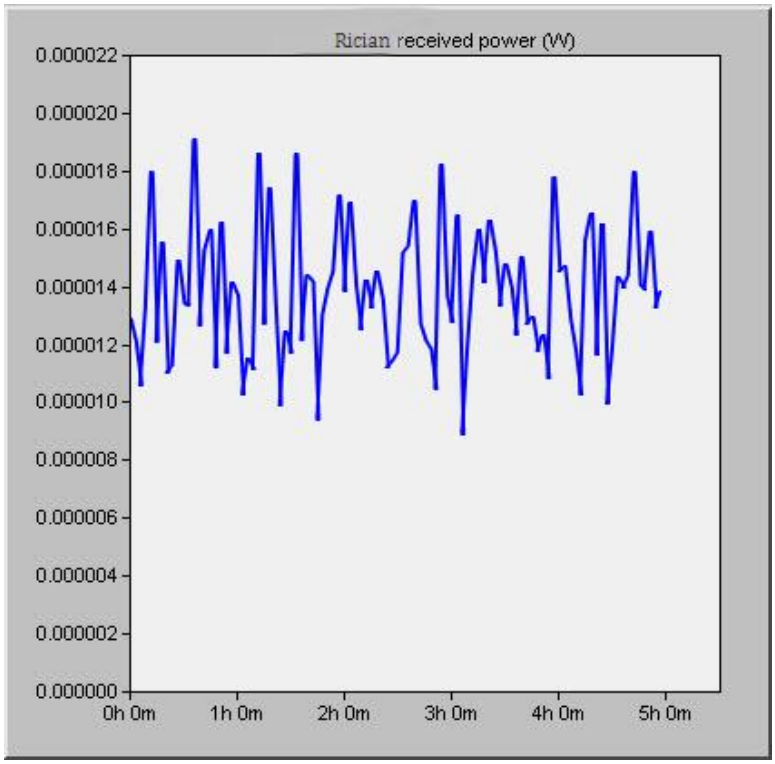


**FIGURE 13:** Power Level Of Received Packet

Figure-13 shows the power levels of the received packets of Rician fading model. Here we observe the realistic Rician fading power envelope at the receiver. This envelope is time correlated as its obeys the Risen distribution. Fading is mostly coused by the the multipath propogation of the radion signals. Rician fading occurs if there is one dominant( Line of Sight) path and multiple indirect signals . The above graph represent by the the expression

$$Y(t) = \sum_{n=0}^{N-1} \rho_n e^{j\varphi_n} \delta(t - \tau_n) \quad \text{----------(11)}$$

Where N is the number of received signals (correspond to the number of electromagnetic paths and very large). $\tau_n$ is the time delay of the generic $n^{th}$ impulse and $\rho_n e^{j\varphi_n}$ represent the complex amplitude (i.e. magnitude and phase) of the generic received pulse. As a consequence $y(t)$ represents the impulse response of multipath correspond to the signal received by the receiver in Watt and x axis represent the time axis.

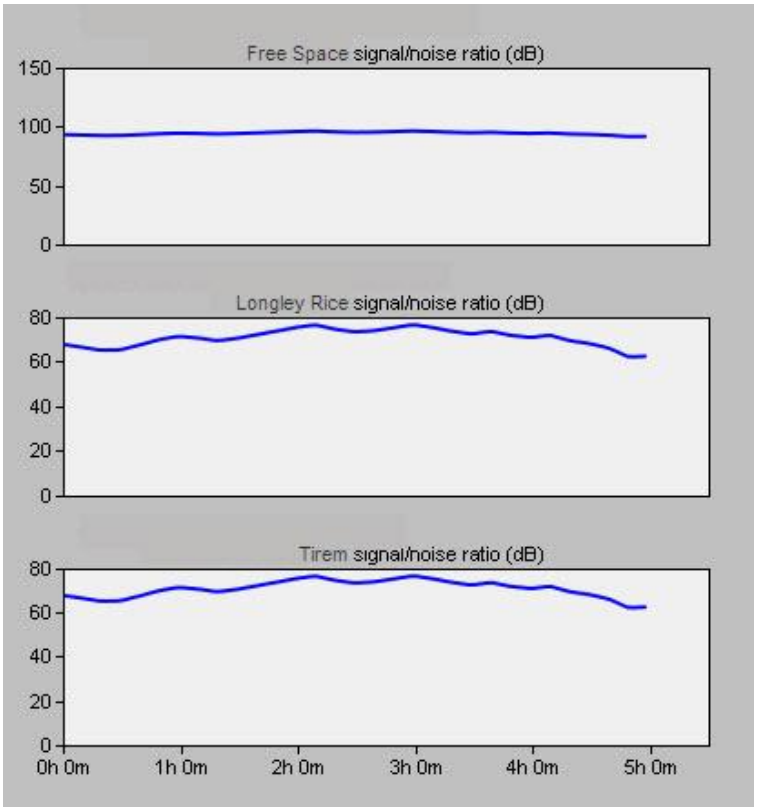


**FIGURE 14 :** Signal To Noise Ratio

The signal to noise ratio is important in the transmission of data because it set the upper bound on the achievable data rates .This is an important characteristic to show the performance of the wireless networks. There is a significant difference in the path loss between free space and the other two models ( fig 14). This difference is because Longley Rice and TIREM takes into account the real environment and the path loss calculation of each model. So with the change in terrain, SNR varies.

## 5.Concluding Remarks:

In this work we have shown the effect on the signal strength as the receiver moves over the varying terrain ( using *Compressed Arc Digitized Raster Graphics / Controlled Image* Base maps). This results give realistic result on propagation loss, signal strength and noise. We have also shown the effect on radio signal strength due to change in antenna height, elevation change and the distance between transmitter and receiver. In this work we observe Rician fading best characterizes a situation where there is a direct LOS path in addition to a number of indirect multiple singles. The Rician model is often applicable in an indoor environment. The Rician model also becomes more applicable in smaller cells or in more open outdoor environments. The channels can be characterized by a parameter K, can be express as the ratio of the (power in the dominant path) to the (power in the scattered paths). When K =0 the fading occurs when there are multiple indirect paths between transmitter and receiver and no distinct dominant path, such as an LOS path . Changing Max Velocity parameters will cause Rician fading envelope to fade faster or slower.

As further work more detailed simulation scenarios will be created by different performance evaluation by compare the radio propagation models, performance variety of metrics, Packets sent, throughput, dropped packets, packet Delivery Ratio and packet routing overhead. The more accurate movement and communication patterns could give

hints where existing protocols still have drawbacks and what has to be changed in order to overcome these problems. Especially when QoS – aware algorithms.

## References :

[1] Arne Schmitz, Martin Wenig "The Effect of the Radio Wave Propagation Model in mobile Wireless Networks" MSWiM 2006 ACM

[2] Illya Stepanov, Kurt Rothermel ,On the impact of a more realistic physical layer on MANET simulation results ScienceDirect Wireless Networks 6 (2008) 61-78

[3] Gianni A. Di caro, Fredrick Ducatelle, and Luca m. Gambardella "A Simulation study of routing performance in realistic urban scenarios for MANETS "– Proceedings of ANTS - 2008

[4]. Ibrahim khider , Furong Wang, WeiHua Yin,Sacko " The impact of different radio propagation models for MANET in urban area environment" Vol -5 .2009 PP 45-52 World Journal of Modelling and Simulation

[5] Illya Stepanov, Daniel Herrscher,Kurt Rothermel On the impact of radio propogation Model on MANET Simulation .

[6] Agustin Zaballos, Guiomar Corral, Albert Carne, Joan Lluis Pijoan " Modeling new indoor and outdoor propagation models for WLAN"

[7] Ratish J. Punnose,Pavel V. Nikitin, and Daniel D. Stancil " Efficent Simulation of Rician Fading with in a Packet Simulator". IEEE Vehicular Technology Conference, Sept 2000.

[8] Wireless Communications & Networks By William Stallings -Second Edition

[9] Models for Realistic Mobility and radio wave propagation for Wireless Networks Simulation By Mesut Gunes and Martin Wenig Chapter -11 "Guide to Wireless Wireless Network" Springer -2009.

[10] Soumen Kanrar , Mohammad Siraj "Automated Position Syatem Implementation over Vehicular Ad Hoc Networks in 2D Space" JCS 6(2) PP 126-132 – 2010

[11] Soumen Kanrar , Mohammad Siraj " Enhanced Antenna Position Implementation over Vehicular Ad Hoc Network(VNET) in 3D Space . IJWMN Vol-2 No-1, 2010

[12] Opnet Technologies Inc. http://www.Opnet.com